Single-Particle Levels of Nonspherical Nuclei In The Region $150 < A < 190$*

W. OGLE† AND S. WAHLBORN†
Los Alamos Scientific University, University of California, Los Alamos, New Mexico 87544
R. PIEPENBRING‡
Département de Physique Nucléaire Théorique, Centre de Recherches Nucléaires, Strasbourg-Cronenbourg, France
S. FREDRIKSSON
Division of Theoretical Physics, Royal Institute of Technology, Stockholm 70, Sweden

The application of the single-particle model to nonspherical nuclei is reviewed. The band-head ($I=K$) energy data for intrinsic states of predominantly one-quasiparticle character are compiled for odd-A nuclides in the region $150< A <190$. The data are analyzed in two steps: first, the rotational and vibrational contributions to the energies are subtracted to give quasiparticle excitation energies; second, single-particle level schemes are fitted to the quasiparticle energies by BCS blocking calculations. The resulting schemes are presented graphically. The single-particle energies and the pairing calculation parameters are made available so that they can be utilized for various purposes in nuclear structure work. As a result of the analysis, we find indications that the zero-point rotational contributions to the band-head energies may have appreciable variations. The level systematics is compared with various single-particle model calculations, assuming local, axially symmetric potentials, and the potential and shape parameters entering are discussed. The potentials used offer satisfactory interpretation of the relevant features of the systematics. The use of a diffuse potential well with proper parameter choices is of significance, particularly for the single-neutron levels. The values of the deformation parameters ϵ_2 and ϵ_4 (or β_2 and β_4) preferred by the level systematics are compatible with other evidence concerning the nuclear surface shapes.

CONTENTS

I. INTRODUCTION

Since the advent of the nuclear shell model about 20 years ago, the interpretation of spectra from nuclei with odd mass-numbers in terms of the motion of the odd particle has been highly successful (Bohr and Mottelson, 1969, Chap. 2 and 3). The extension of the single-particle[1] model approach to nonspherical[2] nuclei—

* Work supported by the U.S. Atomic Energy Commission, the Swedish Atomic Research Council, and the French National Center for Scientific Research.

† Present address: Division of Theoretical Physics, Royal Institute of Technology, Stockholm 70, and Research Institute for Physics, Stockholm 50, Sweden.

‡ Present address: Institut des Sciences Nucléaires, Cedex No. 257, 38-Grenoble-Gare, France.

[1] The "single-particle model" concept of the nucleus generally refers to a description where the nucleons move independently in a common average field. The Hamiltonian for the system then consists of a sum of individual terms for all the particles. Each term contains the spatial and spin coordinates of one particle, and consists of a kinetic and a single-particle potential energy contribution.

[2] We prefer to use the term "nonspherical" for nuclei where the equilibrium shape of the mass distribution deviates from spherical symmetry. This is synonymous to the term "deformed", frequently used in the literature. We often use the term "deformation" for the deviation from spherical symmetry, and occasionally the term "distortion" for the deviation from any defined shape.

characterized by the presence of rotational bands[3] in their level structure—was made in the pioneering work by Nilsson (1955). Reviews of the relationship between the models and the data have been given by Mottelson and Nilsson (1959), and by Nathan and Nilsson (1965). A careful analysis of the present experimental situation for intrinsic[4] states of odd-A nuclides in the rare-earth region is presented in the preceding review by Bunker and Reich (1971).

In our conception, the single-particle model is essentially phenomenological. Its validity depends on its usefulness in interpreting the data and predicting systematic trends. It contains parameters which are effective quantities and not necessarily predictable by any "fundamental" theory. The interest in this model is based on its stability, i.e., the smooth variation of the parameters with changing nucleon numbers.

In the present review, we use the single-particle model as a basis for interpreting the band-head[3] energy level data, which are attributable to one-quasiparticle[5] excitations of odd-A nuclides in the region $150<A<190$. This interpretation has two main objectives: to derive from an analysis of the data semiempirical single-particle level schemes which can be applied in various nuclear-structure considerations; and to discuss the relevant features of these schemes in terms of potential model calculations, whereby one may learn about the appropriate potential and shape parameters.[6]

We envisage many possible uses of the information contained in this review. Both the theoretical and experimental aspects should be of interest to the specialist. The semiempirical single-particle level schemes can be utilized in several ways: for more detailed nuclear-structure calculations; for comparison with other theoretical approaches;[7] as a guide in the experimental search for new intrinsic states; etc. Furthermore, we have attempted to make the presentation readable for as large an audience as possible, including, for instance, graduate students in other fields of physics. The sections of the article are relatively independent of each other. Background and technical materials are presented in Appendices.

The single-particle model with a local potential, adapted for nonspherical nuclei with axial symmetry, is described in Sec. II. In Sec. III, we discuss the relation between the band-head[3] energy data and the single-particle levels. The analysis of the data involves the application of corrections due to collective[8] effects, and fitting of the resulting quasiparticle energies by BCS blocking[9] calculations. The compilation of data and the single-particle level schemes obtained from the analysis are presented in Sec. IV. The level systematics and the potential model calculations are compared and discussed in Sec. V. The conclusions are summarized in Sec. VI. The five Appendices contain the following material: (a) Presentation of the simple rotor-plus-particle model; (b) Details on models with axially symmetric potentials; (c) Brief account of quasiparticles and their interactions (within the framework of the BCS[9] and RPA[10] theories); (d) Bibliography for experimental level data; (e) The odd-mass ytterbium isotopes as a case study.

II. THE SINGLE-PARTICLE MODEL FOR NONSPHERICAL NUCLEI

As stated in the Introduction, the single-particle[1] model furnishes a basis for the description of intrinsic[4] states in nuclei. Since the single-particle potential is

[3] A quantum-mechanical system having a nonspherical, axially symmetric, static mass distribution exhibits rotational motion associated with level sequences of the type

$$E(I, K)=\text{const.}+A_0 I(I+1),$$

where I is the total angular momentum, and the difference $(I-K)$ takes nonnegative integer values. Such a sequence is called a "rotational band," and the member with minimum angular momentum, $I=K$, is called the "band head".

[4] Excitations related to the motion of particles relative to the rotating core are called "intrinsic" (this terminology should not be taken to imply that the two degrees of freedom can be strictly separated). The intrinsic coordinates (x, y, z) refer to a system fixed in the nucleus [these coordinates are frequently denoted by (x_1, x_2, x_3) in the literature]. We assume the nuclei of interest here to have axial symmetry with respect to the z axis, and reflection symmetry with respect to the xy plane. The coordinates (ξ, η, ζ) refer to a space-fixed system.

[5] The concept of "quasiparticle" state generalizes the concept of "particle" or "hole" state by including the effects of the diffuse Fermi surface due to the presence of pairing correlations. Since these correlations conserve "seniority" (the number of particles not occupying pairs of time-reversed orbitals), the classification of the one-quasiparticle states remains the same as that of the single-particle orbitals. See further Appendix C.1 and Sec. III.A.1.

[6] The "potential parameters" are such quantities as, e.g., the depth and the average radius of the potential, which remain well defined independent of the surface shape of the nucleus. The "shape parameters" characterize the deformation of the nuclear surface and are assumed to vanish in the spherical limit.

[7] It should be noted that the single-particle level schemes discussed in this review, whether calculated from a potential model or derived from experimental information, cannot be directly compared with results of Hartree-Fock or other self-consistent theories. Such theories necessarily lead to nonlocal potentials, and the residual interactions are defined in a different framework. Also the rearrangement energies complicate the comparison with experimental levels.

[8] By "collective" motion, we mean both the rotational and the vibrational motion of a nucleus (the vibrational motion, being intrinsic, consists of dynamic oscillations around the static equilibrium shape). The "collective" and "quasiparticle" degrees of freedom are not in reality distinct.

[9] The initials BCS stand for Bardeen, Cooper, and Schrieffer (1957), who introduced a scheme for treating the pairing correlation effect in superconductors. This scheme provides a useful approximation in nuclear-structure theory. By "blocking," we mean, in brief, that the nuclear pairing correlation problem is solved for each quasiparticle excitation separately, omitting from the single-particle spectrum the level or levels occupied by the unpaired particles. (The physical significance of this procedure is discussed in Secs. III.A and III.C.)

[10] The abbreviation RPA stands for "random-phase approximation." This provides a general theoretical scheme for the microscopic description of harmonic vibrations in many-fermion systems. The main features consist of linearizing the equations of motion, including the "field-producing" interactions, and of accounting for the seniority-nonconserving ground-state correlations, in addition to those of the pairing type.

expected to vary in a smooth way with the nucleon numbers, it should also furnish a natural framework for analyzing and systematizing data on such states. In the present review we base our analysis and discussion of the quasiparticle[5] level data on the single-particle model, assuming a local, axially symmetric potential. In this Section we outline the main features of this model and its use for various calculations. We restrict ourselves to such static potential wells as are of interest for the region of nuclides considered in this review.

In Appendix A we indicate how the particle and rotational[3] motion enter into the description of spectra of nonspherical[2] nuclei, using the simplified case of the rotor-plus-particle model. Further details about axially symmetric potential models are presented in Appendix B. For more information about the single-particle model for nonspherical nuclei and its applications we refer the reader to the original article by Nilsson (1955) and to the following books and review articles: Moszkowski, 1957, pp. 497–516; Kerman, 1959, pp. 467–477; Nemirovskiĭ, 1963, pp. 115–127; Preston, 1963, pp. 261–278; Nathan and Nilsson, 1965, pp. 659–673; Rogers, 1965, pp. 257–280; and Davidson, 1968, pp. 66–78 and pp. 183–224.

A. The Hamiltonian and the Shape Parameters

The single-particle Hamiltonian with a static average field can be written

$$H_{\rm sp}=-(\hbar^2/2m)\Delta_r+V(\mathbf{r})+V_{\rm so}(\mathbf{r};\,\text{spin})+(\tfrac{1}{2})(1+\tau_3)V_{\rm Coul}(\mathbf{r}), \quad (2.1)$$

where the intrinsic[4] coordinates $\mathbf{r}=(x,y,z)$, and the Laplacian Δ_r refer to the motion of the particle relative to the core. We assume m to be the actual nucleon mass.[11] The potential terms represent the average interaction between the particle and the core (cf. Appendix A). The term $V(\mathbf{r})$ is the nuclear potential well. The spin–orbit term is assumed to have the invariant form[12]

$$V_{\rm so}(\mathbf{r};\,\text{spin})=-\kappa_{\rm so}\boldsymbol{\sigma}\cdot[\text{grad}\,U(\mathbf{r})\times\mathbf{p}/\hbar], \quad (2.2)$$

where $\kappa_{\rm so}$ is a constant, $U(\mathbf{r})$ is a potential well, $\boldsymbol{\sigma}=2\mathbf{s}$ is the Pauli spin vector, and $\mathbf{p}$ the momentum vector of the nucleon.[13] The Coulomb term, which vanishes for a neutron due to the factor[14] $(1+\tau_3)$, is obtained from an assumed charge distribution, $\rho_c(\mathbf{r})$, for the nucleus, giving

$$V_{\rm Coul}(\mathbf{r})=e\int\rho_c(\mathbf{r}')\,|\,\mathbf{r}-\mathbf{r}'\,|^{-1}\,d^3r'. \quad (2.3)$$

The volume integral of the density $\rho_c(\mathbf{r})$ equals the total nuclear charge Ze.

The nuclear potential well $V(\mathbf{r})$ is furnished by a generalization of the shell model potential, $V(r)$, for spherical nuclei to the case of nonspherical symmetry. This generalization is not unique, and there are various possible choices of the potential $V(r)$ to be generalized. In the Nilsson (1955) model, the potential $V(\mathbf{r})$ is taken to be an anisotropic harmonic-oscillator potential. In several approaches, use has been made of the Woods–Saxon potential form for $V(r)$ (Woods and Saxon, 1954), applying different methods for generalization to $V(\mathbf{r})$. In either approach, the formulation of $V(\mathbf{r})$ involves some kind of parameterization. We can suitably distinguish two types of parameters[6]—the potential parameters [related to the spherical well, $V(r)$], and the shape parameters (describing the nuclear surface shape). A general discussion of these matters is outside the scope of this review. Here we shall only briefly discuss some generalizations of the static Woods–Saxon potential to axially symmetric nonspherical shapes. Further details and comments on alternative approaches are given in Appendix B.

In the spherical case, the Woods–Saxon potential is defined by the Fermi function radial form function (cf. Appendix B.1),

$$V(r)=-V_0F(r;R_0,a_0), \quad (2.4)$$

$$F(r;R_0,a_0)=\{1+\exp[(r-R_0)/a_0]\}^{-1}, \quad (2.5)$$

where V_0 is the potential depth, R_0 is the "potential radius," and a_0 is the "surface diffuseness" parameter. There are various ways of parameterizing the nuclear surface shape for the nonspherical potential $V(\mathbf{r})$. For example, one may use either one of the following two types of expression for the equation of the nuclear surface (cf. Faessler and Sheline, 1966) (we assume here reflection symmetry with respect to the xy plane):[4]

(a) Introducing an angular-dependent nuclear radius $R(\theta)$ expressed in terms of a multipole expansion, describing the surface shape; this leads to an equation which may be written (it is conventional to use here spherical harmonics)

$$r=R(\theta)=b_0[1+\beta_0+\beta_2Y_{20}(\theta)+\beta_4Y_{40}(\theta)+\cdots]. \quad (2.6)$$

[11] One might introduce an "effective mass," m_*, instead of the regular mass, m, to represent, in a very crude approximation, the possible energy dependence of the potential. For excitations near the Fermi surface, one should then choose $m_*<m$. However, there is no apparent need for such a choice in connection with the potential models discussed here. For details on the "effective mass" approximation, see Preston (1963) Chap. 10, and Lemmer (1960).

[12] In the case of a central potential well with $U(r)=V(r)$, the invariant expression for the spin-orbit term reduces to the form

$$-\kappa_{\rm so}[V'(r)/r]\mathbf{l}\cdot\boldsymbol{\sigma},$$

which is analogous to the well-known Thomas term in atomic physics.

[13] The angular momentum vectors, e.g., $\boldsymbol{\sigma}=2\mathbf{s}$, $\mathbf{l}$, $\mathbf{R}$, $\mathbf{j}=\mathbf{l}+\mathbf{s}$, $\mathbf{I}=\mathbf{J}+\mathbf{R}$, are throughout expressed in units of $\hbar$. The linear momentum vector, $\mathbf{p}$, however, has its proper dimension, so that $\hbar\mathbf{l}=\mathbf{r}\times\mathbf{p}$ holds.

[14] We define the third component of isospin in such a way that $\tau_3=+1$ corresponds to a proton, and $\tau_3=-1$ corresponds to a neutron.

(b) Substituting for the square of the radial coordinate an expression $r^2S(\theta)$, the shape function $S(\theta)$ containing the angular dependence; this leads to an equation which may be written (it is conventional to use here Legendre polynomials)

$$r^2S(\theta)=r^2[1+\eta_0-\eta_2P_2(\cos\theta)+\eta_4P_4(\cos\theta)+\cdots]=c_0^2. \tag{2.7}$$

The constants b_0 and/or β_0 in case (a), and c_0 and/or η_0 in case (b), may be used to make the surface described by Eq. (2.6) or (2.7) enclose a given volume, $(4\pi/3)R_0^3$. The further parameters β_L or η_L, with $L=2, 4, \cdots$, evidently describe the deviation from spherical symmetry. For finite deviations, the shapes described by Eqs. (2.6) and (2.7) are quite different if only one term (e.g., $L=2$), or a few terms, are included in the functions $R(\theta)$ and $S(\theta)$. Thus, in practical cases, there is no exact one-to-one correspondence[15] between the parameterizations expressed by Eqs. (2.6) and (2.7). We emphasize this by using a distinctive terminology to classify the shapes of interest.[16]

The parameterization of the type (a), Eq. (2.6), has been most frequently represented in the literature, e.g., in the work by Faessler and Sheline (1966), Nemirovskiĭ and Chepurnov (1966), Gareev *et al.* (1967, 1968, 1969), and Ford, Hoffman, and Rost (1970). The type (b) implies a simultaneous generalization of the Nilsson and Woods–Saxon potentials. The parameters η_2 and η_4 are closely related[15] to the parameters ϵ_2 and ϵ_4 used in recent years in Nilsson model calculations (see Appendix B and Gustafson *et al.*, 1967; Lamm, 1969; and Nilsson, 1969). Woods–Saxon potential calculations with this parameterization have been performed, e.g., by Chasman (1969), and Ehrling and Wahlborn (1970, 1971).

Due to the imprecise nature of the concept of "nuclear surface," the procedure described—assuming Eqs. (2.4), (2.5), and (2.6) or (2.7)—still leaves a certain ambiguity in the definition of the potential $V(\mathbf{r})$. A unique definition involves, in principle, a prescription for all the equipotential surfaces, $V(\mathbf{r})=\text{const}$, and a precise formulation of the volume conservation criterion adopted. However, these details are mainly of technical nature and hardly affect the essential physical features already expressed above. A brief discussion of these questions is given in Appendix B.

B. The Potential Parameters

For definiteness we continue to discuss the Woods–Saxon potential. In its generalizations, the potential parameters, V_0, R_0, and a_0, are customarily chosen in the same way as for spherical nuclei. Although theoretical estimates of these parameters are available (see e.g., Myers, 1970), semiempirical values are used as a rule. The information on the size and depth of the potential well, and the strength of the spin–orbit coupling, is derived primarily from optical-model analysis of elastic nucleon-scattering data (see Elton, 1961; and Collard, Elton, and Hofstadter, 1967). For nuclei in the heavy-mass region ($A\gtrsim100$), this information is known to be consistent with the shell-model interpretation of bound state data, using the static potential obtained from the energy-dependent real part of the optical-model potential in the zero-energy limit. These matters are discussed in some detail by Bohr and Mottelson (1969), paragraph 2-4 (see also Blomqvist and Wahlborn, 1960). For the energy-independent potential depth, V_0, the findings can be summarized by the phenomenological expression[14,17]

$$V_0(\tau_3; Z, N)=V_1+\tau_3V_2(N-Z)/A, \tag{2.8}$$

where the constants V_1 and V_2 have the approximate values[17]

$$V_1\approx52\text{ MeV}, \qquad V_2\approx33\text{ MeV}. \tag{2.9}$$

The potential radius and diffuseness parameters have roughly the values[17]

$$R_0=r_0A^{1/3}, \qquad r_0\approx1.25\text{ fm}, \qquad a_0\approx0.65\text{ fm}. \tag{2.10}$$

In the expression for the spin–orbit term, Eq. (2.2), the potential well $U(\mathbf{r})$ is also determined on the basis of evidence from spherical nuclei. In principle, $U(\mathbf{r})$ might be different from $V(\mathbf{r})$. On the other hand, there is no decisive evidence against setting them equal

$$U(\mathbf{r})=V(\mathbf{r}), \tag{2.11}$$

which has the desirable property of concentrating the spin–orbit coupling effect in the surface region. Actual optical-model fits, as well as results of shell-model calculations, indicate the near equality of the two wells

---

[15] For small or moderate deformations, an approximate relation holds between the two main sets of deformation parameters used in the literature (cf. Gareev, Ivanova, and Pashkevitch, 1969),

$$\beta_2\approx1.06\epsilon_2+0.20\epsilon_2^2-1.8\epsilon_2\epsilon_4,$$

$$\beta_4\approx-1.18\epsilon_4+0.27\epsilon_2^2-1.2\epsilon_2\epsilon_4,$$

where ϵ_2 and ϵ_4 are the Nilsson model parameters,

$$\epsilon_2\approx3\eta_2/4, \qquad \epsilon_4\approx\eta_4/2.$$

For the Bohr and Mottelson (1953a) distortion parameter, $\beta_{BM}\approx0.9\beta_2$ holds.

[16] With the multipole expansion, Eq. (2.6), the deformations associated with β_2, β_4, etc., are called, respectively, "quadrupole," "hexadecapole," etc. With the substitution, Eq. (2.7), the parameter η_2 (or ϵ_2) evidently describes "spheroidal" deformations. For the distortion introduced by finite η_4 (or ϵ_4), we suggest the term "tetroidal". In either type of parameterization, the surface shapes associated with positive β_2, ϵ_2, or η_2 are called "prolate," while negative β_2, ϵ_2, or η_2 describe "oblate" shapes.

[17] The suitable unit of length for nuclear physics is the "femtometer", 1 fm$=10^{-13}$ cm. A natural unit is provided by the reduced Compton wavelength of the proton, $\hbar^2/m_pc=0.2103$ fm. The energy units used most frequently are keV and MeV; 1 MeV$=10^3$ keV$=10^6$ eV. Other standard notations in nuclear physics are: Z=proton number=atomic number; N=neutron number; $A=Z+N$=mass number.

(Bohr and Mottelson, 1969, pp. 233–240). In terms of the dimensionless parameter λ_{so}, the phenomenological strength of the spin–orbit term is[17]

$$\lambda_{so} \equiv (2mc/\hbar)^2 \kappa_{so} \approx (90 \text{ fm}^{-2}) \kappa_{so} \approx 35, \quad (2.12)$$

to within ± 5. The variations of λ_{so} should compensate in an approximate way for the possibly inadequate representation of the spin–orbit term by Eqs. (2.2) and (2.11).

In the Coulomb term, Eq. (2.3), one could use a charge distribution in accordance with experimental measurements such as the electron scattering data. From spherical nuclei it is known that these data can be fitted with Fermi functions, i.e., $\rho_c(r) \sim F(r; R_c, a_c)$ [Eq. (2.5)], where the charge radius, R_c, and diffuseness, a_c, are both smaller than the corresponding potential parameters, R_0 and a_0 (see e.g., Bohr and Mottelson, 1969, pp. 158–165). One might, therefore, obtain the nonspherical distribution $\rho_c(\mathbf{r})$ by a generalization analogous to that leading to $V(\mathbf{r})$. However, the results of single-particle bound state calculations are not very sensitive to the details of the charge distribution. A good approximation results from inserting into Eq. (2.3) a uniform charge distribution, which has the value

$$\rho_c^{\text{uniform}} = (3/4\pi) Ze R_0^{-3}, \quad (2.13)$$

and is bounded by the actual—spherical or nonspherical—nuclear surface, Eq. (2.6) or (2.7), which encloses the conserved volume.

The single-particle level schemes of nonspherical nuclei depend both on the potential parameters, the choice of which we have just discussed, and the shape parameters, as introduced e.g., in Eq. (2.6) or (2.7). The shape parameters—primarily β_2, η_2, or ϵ_2—have a major influence on the levels. Illustrations of this dependence are given in Sec. II.D. There are theoretical predictions of the values of shape parameters from equilibrium deformation calculations (cf., Sec. V). It is one of the main objectives of this review to relate significant features of the empirical systematics of single-particle levels to possible effects of both shape and potential parameters via potential model calculations. These matters are discussed in Sec. V.

C. The Single-Particle Eigenstates

The single-particle eigenstates are obtained from the solution of the Schrödinger eigenvalue problem,[18]

$$H_{\text{sp}} \psi_K = \epsilon_K \psi_K, \quad (2.14)$$

where the boundary conditions require $|\psi_K|^2$ to approach zero for $r \to \infty$, and to stay finite or approach zero for $r \to 0$, in all directions $\hat{\mathbf{r}}$. Among all the possible methods of solving this problem, one of the most efficient ways consists of diagonalizing the Hamiltonian, Eq. (2.1), in a suitably chosen representation.

The use of the three-dimensional harmonic-oscillator wave functions as a set of basis functions offers several advantages (see Appendix B). We consider here the following two possible expansions of the eigenstates ψ_K in such a basis, assuming H_{sp} to have axial symmetry (z axis), and reflection symmetry (xy plane):[4]

(a) Spherical harmonic-oscillator representation

$$|\psi_K\rangle = \sum_{n,l,j} S_K(n,l,j) \, |K^\pi; n, l, j\rangle_{\text{sph}}. \quad (2.15)$$

(b) Cylindrical harmonic-oscillator representation

$$|\psi_K\rangle = \sum_{\mu,\nu,\Lambda} C_K(\mu, \nu, \Lambda) \, |K^\pi; \mu, \nu, \Lambda\rangle_{\text{cyl}}. \quad (2.16)$$

Details on the form of the basis eigenstates are given in Appendix B.2, where the transformation between the two representations is also discussed. The numbers (n, l, j) give the usual classification of the spherical shell-model states [functions of (r, θ, ϕ) and spin], the angular and spin parts being coupled[19] to an angular momentum eigenstate ($\mathbf{j} = \mathbf{l} + \mathbf{s}$), and n being the radial quantum number. We have the rules[18]

$$j = l \pm \tfrac{1}{2}, \qquad j \geq K, \qquad \pi = (-1)^l, \quad (2.17)$$

$$n = 1, 2, 3, \cdots. \quad (2.18)$$

The numbers (μ, ν, Λ) characterize the cylindrical eigenstate, which is a product of functions of each of the coordinates (ρ, ϕ, z) and the spin; μ and ν being the number of oscillator quanta, and Λ being the magnitude of the orbital angular momentum component (l_z) eigenvalue. We have the rules[18] (Appendix B.2)

$$\mu \equiv n_\perp = 0, 1, 2, \cdots, \qquad \nu \equiv n_z = 0, 1, 2, \cdots, \quad (2.19)$$

$$\pi = (-1)^{\mu+\nu}, \qquad \mu - \Lambda = \text{even number} \geq 0, \quad (2.20)$$

$$\Lambda = K - \Sigma, \qquad \Sigma = \pm \tfrac{1}{2}. \quad (2.21)$$

The first published works with the representations (2.15) and (2.16) were done with the Nilsson model: by Chi (1966), using the expansion (2.15) [Nilsson (1955) utilized the "uncoupled" components[19]], and by Rassey (1958), using the expansion (2.16).

For the classification of the component states it is practical to introduce the total number of oscillator

[18] Since we assume axial symmetry with respect to the z axis, the intrinsic angular momentum component, j_z, is a constant of motion for H_{sp}. The absolute magnitude of the eigenvalue is denoted by K, which is a good quantum number in the single-particle model. Since we assume reflection symmetry with respect to the xy plane, parity ($\pi = \pm 1$) is also a good quantum number. We occasionally use the notation K^π or just K to label an eigenstate of H_{sp}.

[19] The "coupled" angular momentum eigenstates, $X_{ljm}(\hat{r}; \text{spin})$, are expressed in terms of the "uncoupled" product states $Y_{lm'}(\hat{r})\chi_{m''}(\text{spin})$ according to the relation

$$X_{ljm}(\hat{r}; \text{spin}) = \sum_{m'} (l, m', \tfrac{1}{2}, m - m' \,|\, j, m) \, Y_{lm'}(\hat{r}) \chi_{m-m'}(\text{spin}).$$

Thus, the orthogonal matrix of Clebsch-Gordan coefficients (see, e.g., Rose, 1957; and Edmonds, 1968) transforms between the "coupled" and "uncoupled" spherical representations.

quanta,[20] N_0, which for the two representations (2.15) and (2.16) is given by the relations

$$N_0=2(n-1)+l, \tag{2.22}$$

$$N_0=\mu+\nu\equiv n_\perp+n_z, \tag{2.23}$$

respectively. We have the rules[18]

$$N_0=0, 1, 2, \cdots, \qquad \pi=(-1)^{N_0}. \tag{2.24}$$

The eigenstate ψ_K is in general a mixture of components with different even values of N_0, or with different odd values of N_0. However, components with different N_0 values ($|\Delta N_0|\geq 2$) have large energy differences in the spherical limit—more than 5 MeV in the region under consideration—and their mutual matrix elements of $H_{\rm sp}$ normally have reduced magnitude compared to those which are diagonal in N_0. Consequently, the eigenstates ψ_K are as a rule markedly pure in N_0. The possible exceptions occur when two or more different single-particle states, having the same parity and the same value of K, come together at some finite deformation[2] close enough in energy to interact significantly. Appreciable mixtures of two or more N_0 values may then occur.

For many applications it is suitable to express the eigenstates in spherical components,[21] Eq. (2.15). However, in the case of finite deformations, the expansion in cylindrical components, Eq. (2.16), can be made to converge better, and the use of this representation therefore furnishes in general a more efficient method of solution (see e.g., Damgaard *et al.*, 1969). This matter is discussed in Appendix B, where we also show that one component (μ, ν, Λ) usually dominates the expansion in deformation regions between quasi-intersections,[22] particularly for large prolate[16] distortions. Since well-established quasiintersections occur only in a couple of cases for the distortions considered in this work, we can take the numbers (μ, ν, Λ) for the dominating component at large distortion to classify each single-particle eigenstate. This has in fact been done in earlier literature—on the basis of the Nilsson (1955) model—whereby usually N_0 is given instead of μ. (See Moszkowski, 1957; Rassey, 1958; Kerman, 1959; and Mottelson and Nilsson, 1959.) Setting $\nu\equiv n_z$, and using bars to indicate the "average" quantum numbers dominating the "asymptotic" component, we define the *cylindrical classification*[23] by the conventional set of numbers

$$\{K^\pi; \bar{N}_0, \bar{n}_z, \bar{\Lambda}\}. \tag{2.25}$$

These numbers can be defined in a more general way than done here, and they play an important role beyond mere classification. These matters are briefly discussed in Appendix B.1 and Sec. II.D (see also Bunker and Reich, 1971). In cases of quasi-intersection,[22] two or more states, classified according to Eq. (2.25), are strongly mixed.[24]

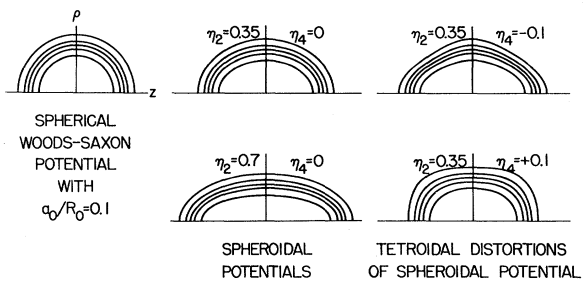

FIG. 1. Equipotential contour curves for a Woods-Saxon potential well with spherical and various deformed[15,16] shapes. The curves correspond to 0.1, 0.3, 0.5, 0.7, and 0.9 of the potential depth. (For further details see Sec. II.D, and Appendix B.3.)

D. Illustrations and Applications

For illustration we present results of calculations with a Woods–Saxon type of potential, generalized to nonspherical shapes with a parameterization according to Eq. (2.7). We utilize a scheme developed by Ehrling and Wahlborn (1970) for the formulation of the potential $V(\mathbf{r})$ and the solution of the Schrödinger equation. The details are briefly described in Appendix B. The kinds of equipotential surfaces describing the potential well $V(\mathbf{r})$, for several choices of η_2 and η_4, are illustrated graphically in Fig. 1, showing the contour curves $\rho(z)$ for several values of v, characterizing equipotential surfaces by the equation

$$V(\mathbf{r})=-vV_0=\text{const.} \tag{2.26}$$

The cases with $\eta_2=0.7$ or $|\eta_4|=0.1$ represent fairly

[20] We use the notation N_0 for the total number of oscillator quanta in an eigenstate of a three-dimensional harmonic-oscillator potential (the notation N is reserved for the neutron number).

[21] The spherical representation is usually preferable if multipole expansions are involved. For some applications, however, the cylindrical representation may be more advantageous—e.g., in the calculation of two-body matrix elements with certain types of nucleon-nucleon interactions (see Chasman and Wahlborn, 1967).

[22] Unless the matrix of the Hamiltonian $H_{\rm sp}$ for given K^π reduces further due to some accidental symmetry (which in practice does not occur), all the eigenvalues from the diagonalization of this matrix are strictly nondegenerate, except for the fundamental degeneracy due to time reversal invariance. From this follows the famous "noncrossing rule": single-particle levels having the same K^π and considered as functions of the deformation parameters, "normally" never cross each other in any part of the parameter space. They may approach to within a closest energy distance at which they are strongly mixed with each other. We refer to this situation as a "quasi-intersection". The crossings occurring in the usual Nilsson model schemes are a spurious effect, arising from neglecting the interaction between N_0 shells (cf. Appendix B).

[23] We prefer to use the term "cylindrical" instead of the somewhat misleading word "asymptotic" for the quantum numbers and classification according to Eq. (2.25). It should be noted that the cylindrical classification actually diagonalizes the Nilsson (1955) model Hamiltonian in the limit of vanishing spin-orbit term ($\kappa_{\rm so}=0$).

[24] In a situation where two states with the same K^π and with $|\Delta N_0|=2$ may actually be strongly mixed (close to a quasi-intersection), we set the cylindrical classification $(\bar{N}_0, \bar{n}_z, \bar{\Lambda})$ within parentheses, e.g., $3/2^+$ (402).

large distortions which rarely occur in the region under consideration.

The eigenvalue problem, Eq. (2.14), is solved by diagonalization of the Hamiltonian matrix in the cylindrical representation (2.16). The result of this procedure is illustrated in Figs. 2 (proton) and 3 (neutron) for a somewhat schematic case, where we have assumed $A=176$ and $Z=70$, and used the following potential parameter values[17]:

$$V_0(\text{proton})=60\text{ MeV}, \qquad V_0(\text{neutron})=45\text{ MeV},$$
$$r_0=1.25\text{ fm}, \qquad a_0=0.70\text{ fm}, \qquad \lambda_{so}=32. \quad (2.27)$$

The diagrams show the single-particle levels as functions of η_2, with $\eta_4=0$. It should be noted that in the region under consideration, η_2 has its maximum, not exceeding ≈ 0.4, roughly at $A=170$, where we expect η_4 to be ≈ 0 (cf. Sec. V). For each assignment according to the cylindrical classification (2.25), we indicate, by an arrow, the "trajectory" along which the classification is valid. At points of quasi-intersection,[22] the levels (considered as functions of η_2) exchange character within an interval of η_2 where they mix. The diagrams in Figs. 2 and 3 illustrate several of the main features of single-particle level schemes entering in the discussions throughout this review.

There are many applications of single-particle model schemes for nonspherical nuclei, such as that described here. In deriving information from experiment, the analysis of the data may involve model calculations. For the low-lying intrinsic states (quasiparticle excitations)[4,5] of odd-A nuclei, the data available in the presently considered region can essentially be divided into the following types:

(a) Information on energies, spins, and parities of levels, particularly the band heads.[3] Such information can be obtained from various kinds of experiments.

(b) Spectroscopic data on the rates of beta- and gamma-ray transitions (branching ratio and lifetime measurements; internal conversion studies).

(c) Cross-section data from one-nucleon transfer experiments, particularly measurements of intensities and angular distributions in reactions leading to several members of rotational bands.[3]

The band-head energy information of type (a) is discussed in this review [see particularly Sec. IV and also the review article by Bunker and Reich (1971)]. Data of type (b)—e.g., measurements of gamma-ray branching ratios between and within rotational bands, and lifetime measurements of retarded multipole transitions—have so far played a great role in deriving detailed information on intrinsic states.[4] In particular, the use of approximate selection rules, based on the cylindrical classification,[23] often makes it possible to determine the quantum numbers, Eq. (2.25) (see, e.g., Alaga, 1955, 1957; Chasman and Rasmussen, 1956; and Mottelson and Nilsson, 1959). In recent years, "in-beam" experiments—especially at beams of heavy ions or high-energy protons—have given a wealth of new information of type (a) as well as (b).

The data of type (c) have turned out to be perhaps the most important source of detailed information on the structure of quasiparticle states in nuclei in general. With the availability of beams of deuterons, tritons, ^{3}He particles and alpha particles of sufficient intensities and energies, it is nowadays possible to perform stripping and pickup reactions, with transfer of proton as well as neutron, in the region of A and Z considered here. For a discussion of the nucleon transfer reaction data for nuclides in this region, we refer the reader to the review article by Bunker and Reich (1971). The angular distributions give information on the angular momentum and parity of the transferred nucleon and hence of the final state, and the intensity pattern[25] for the excitation of several members of a rotational band depends sensitively on the structure of the quasiparticle wave function (see Satchler, 1958; and Elbek and Tjøm, 1969). To first approximation, the intensity for a member $I \geq K$ is proportional to the weight, P_{lj}, of the spherical components (n,l,j) with given $j=I$ and $l=j\pm\frac{1}{2}$ (determined by parity) in the single-particle wave function ψ_K. From the coupled spherical representation,[19] Eq. (2.15), this weight can be evaluated by the equation

$$P_{lj}=\sum_n S_K(n,l,j)^2. \quad (2.28)$$

Such calculations—and similar ones for the analysis of various data—furnish important applications of the single-particle model for nonspherical nuclei.

III. RELATION BETWEEN BAND-HEAD ENERGIES AND SINGLE-PARTICLE LEVELS

The extraction of information on single-particle[1] states from experimental data is not a straightforward procedure. In general, considerable care is needed to take into account correlations and other possible effects of residual interactions. For nonspherical[2] nuclei, the

[25] The relative intensity pattern for the excitation of the various members of a rotational band in a one-nucleon transfer reaction on an even-even nucleus is often referred to as the "finger prints." If the transferred angular momentum, l, is known, the I value of the populated state also fixes j and thus selects the "active" spherical component of the intrinsic state [this is the basis of Eq. (2.28)]. In addition, the spectroscopic factor (Elbek and Tjøm, 1969) contains the BCS population amplitudes u_K and v_K (Appendix C). In general, stripping reactions lead preferentially to particle excitations, and pick-up reactions lead preferentially to hole excitations (see further Bunker and Reich, 1971). Together with the Q values (or nucleon separation energies), which can be obtained from the reactions as well, the u and v factors give information on the "Fermi surface," specifically on the BCS parameters λ_* and Δ_* (also indirectly on ϵ_F). The use of one-nucleon transfer reactions for the study of nuclear structure is described by Satchler (1958), and in the book by Tobocman (1961).

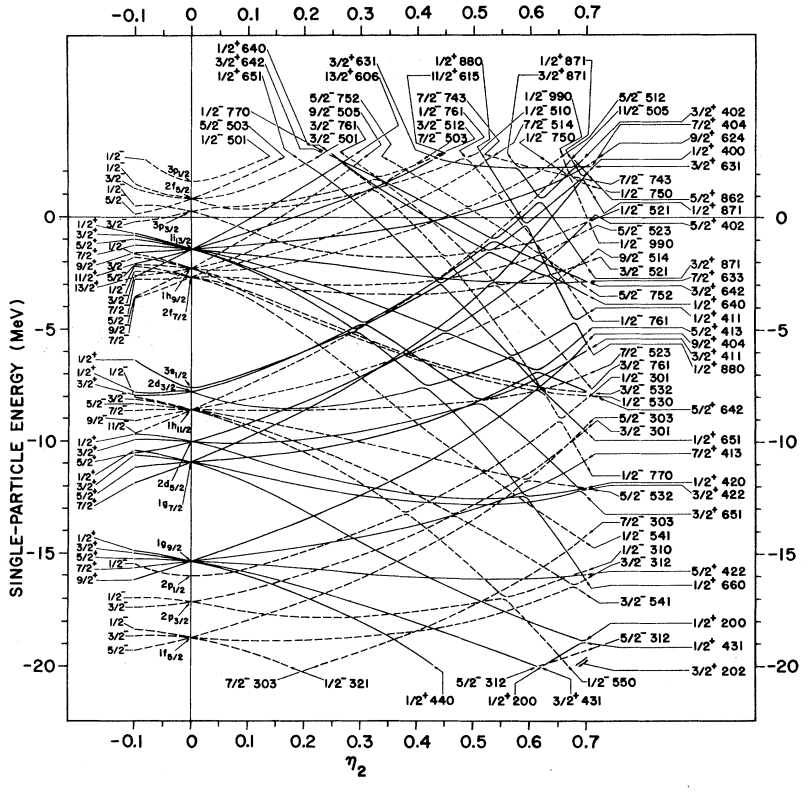

FIG. 2. Illustrative graph of single-proton levels from a deformed Woods-Saxon potential field as functions of the spheroidal[15,16] deformation parameter η_2 (with $\eta_4=0$; for further details see Secs. II.B and II.D and Appendix B.3).

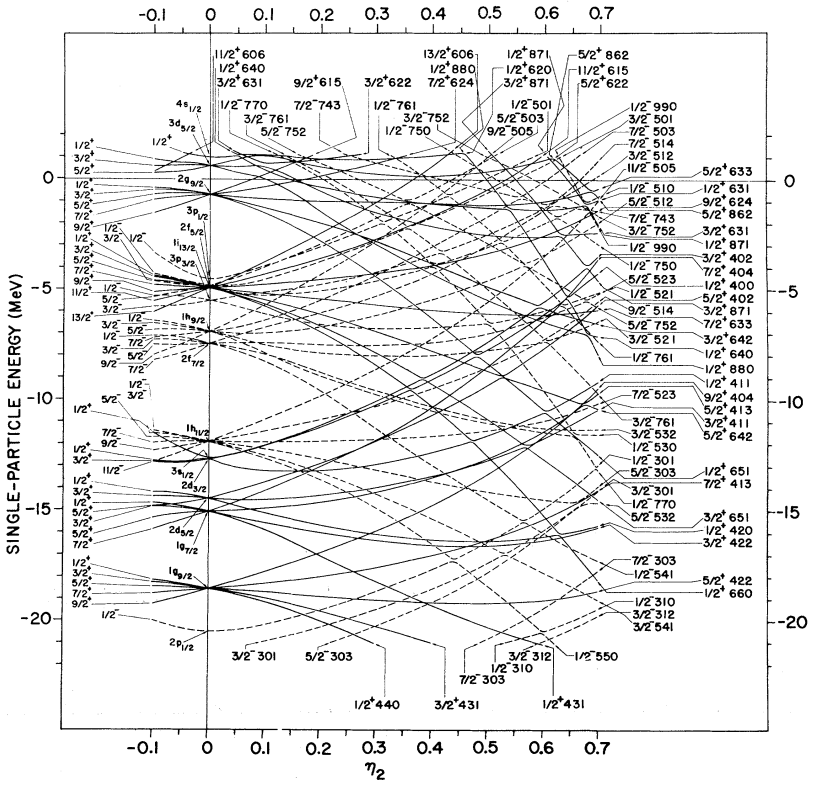

FIG. 3. Illustrative graph of single-neutron levels from a deformed Woods-Saxon potential field as functions of the spheroidal[15,16] deformation parameter η_2 (with $\eta_4=0$; for further details see Secs. II.B and II.D and Appendix B.3).

TABLE I. Standard scheme of 39 single-proton levels (MeV)[29,30] for the region $150<A<190$.

Fixed[a]		Varied[b]		Fixed[a]	
[1/2⁻ 310]	−6.7	3/2⁻ 541	(≈0.5)	1/2⁻ 530[c]	7.2
[1/2⁺ 440]	−6.5	5/2⁺ 413	(1.5±0.5)	11/2⁻ 505[c]	7.2
[3/2⁺ 431]	−6.1	5/2⁻ 532	(1.5±0.5)	[3/2⁺ (mix)][d]	7.8
[5/2⁻ 303]	−5.3	3/2⁺ 411	(≈2)	[1/2⁺ (mix)][e]	7.8
[5/2⁺ 422]	−5.1	7/2⁻ 523	(≈2.5)	[5/2⁺ 642]	8.2
[3/2⁻ 301]	−3.7	1/2⁺ 411	(≈3)	[3/2⁻ 521]	8.7
[7/2⁺ 413]	−3.5	7/2⁺ 404	(3.5±0.5)	[5/2⁻ 523]	8.8
[1/2⁺ 431]	−3.0	9/2⁻ 514	(4±0.5)	[7/2⁺ 633]	9.3
[1/2⁻ 301]	−2.8	5/2⁺ 402	(4.5±0.5)	[9/2⁺ 624]	10.8
[3/2⁺ 422]	−1.7	1/2⁻ 541	(5±1)	[5/2⁻ 512]	11.0
[9/2⁺ 404]	−1.0	3/2⁻ 532	(6±0.5)	[7/2⁻ 514]	11.8
1/2⁺ 420[c]	−0.4	1/2⁺ (mix)[e]	(7±1)	[1/2⁻ 521]	12.5
1/2⁻ 550[c]	−0.1	3/2⁺ (mix)[d]	(7.5±1)	[1/2⁻ 770]	13.5

[a] The cylindrical classification in brackets is irrelevant for the present purposes.
[b] The energy values in parentheses indicate roughly the variation allowed for each level.
[c] Expected to appear in this mass region, but not yet observed.
[d] In the middle of the region, the mixed single-proton levels 3/2⁺ (651) and 3/2⁺ (402) are expected to be located relatively close together, with 3/2⁺ (651) probably being the lower. At the ends of the region 3/2⁺ (651) is expected to be higher than 3/2⁺ (402).
[e] In the middle of the region, the mixed single-proton levels 1/2⁺ (660) and 1/2⁺ (400) are expected to be located relatively close together, with 1/2⁺ (660) probably being the lower. At the ends of the region 1/2⁺ (660) is expected to be higher than 1/2⁺ (400).

rotational[3] motion, and also its coupling[26] to the intrinsic[4] motion, must be taken into account. We present in Sec. III.A the theoretical basis for the relation between the observed band-head[3] energies and the model-dependent single-particle levels. The discussion is appropriate to the region of nonspherical nuclei considered here.

In the present review we have undertaken a fairly elaborate analysis of the band-head energy data to derive semiempirical, single-particle level schemes. We have not systematically taken other spectroscopic data into account, but have used such information when needed for the energy analysis. For a more complete discussion of this subject we refer the reader to the review article by Bunker and Reich (1971). Since the single-particle level schemes furnish the main result of our analysis, and because of the large role they play for our discussion, we describe the methods applied in some detail in Secs. III.B and III.C. The reliability of the results is discussed in Sec. III.D.

The approach we utilize is based on a phenomenological model for quasiparticles[5] and their interactions. In Appendix C we give a brief account of the theory (BCS and RPA)[9,10] and furnish references for background reading. For the rotational effects, we use in essence the description presented schematically in Appendix A, assuming axial symmetry.

[26] The motion is called "adiabatic" if the rotation is slow enough that the intrinsic motion can be considered to be independent of the rotational motion at every moment. The two degrees of freedom can then be separated. Effects which couple them and make them no longer independent are called "nonadiabatic." The coupling affects mainly close-lying levels (I, K) and (I, K') of bands with the same parity and $|K\pm K'|=1$. For band heads, the energy contribution is in most cases insignificant.

A. Theoretical Background of Energy Relations and Analysis

1. *Description of the Physical Effects*

The gross, qualitative resemblance between the predictions of single-particle models[1] and the experimental band-head[3] properties in odd-A nonspherical[2] nuclei was early an established fact (see Mottelson and Nilsson, 1959). Specifically, such agreement is found, as a rule, for the ground state assignments, as well as the approximate order of the observed excited states. However, there is much evidence showing that a detailed, direct, quantitative comparison between the measured energies and the single-particle levels is hardly meaningful. If the simple model of independent particles moving in the average single-particle field were valid, the excitations associated with the motion of the odd particle would simply have the energies given by[27,28] $|\epsilon_K-\epsilon_F|$. With reasonable model assumptions, the comparison with experiment shows this not to be true, not even for the average excitation energies. There

[27] As a rule, we use the lower case k (or κ) to label a set of arbitrary single-particle levels, including states in the continuum, while capital K denotes a definite, bound, single-particle level with energy eigenvalue ϵ_K (see Sec. II). The symbol $s=\pm1$ (or $\sigma=\pm1$) is used to distinguish, if needed, the two time-reversed orbitals having the same energy, ϵ_k (or ϵ_κ). The eigenvalue of j_z in the state (sk) or (sK) is denoted by M_k or M_K, respectively (note that $K=|M_K|$).

[28] The Fermi level, ϵ_F, is the highest occupied single-particle level in the ground state of the uncorrelated many-fermion system. In the BCS approximation for pairing correlations, the solution without blocking gives the relevant parameters λ_*—the "Fermi-energy parameter", which is on the average approximately equal to ϵ_F [it is also related to the "chemical potential," $\tilde{\lambda}$; see Belyaev (1959)]—and Δ_*—the "gap parameter," characterizing the diffuseness of the Fermi surface. For further notations related to BCS theory, see Sec. III.C and Appendix C.1.

are important energy contributions arising both from the rotational[3] motion and from correlations in the intrinsic[4] motion. We must consider both types of effects, starting here with the latter.

From several kinds of evidence, primarily the existence of an energy gap in the excitation spectra of noncollective[8] states in even–even nuclei (see, e.g., Belyaev, 1959; Soloviev, 1963; Nathan and Nilsson, 1965; and Bès and Sorensen, 1969), we know that the pairing correlations are important. These are associated with the comparatively strong interaction between particles which occupy pairs of time-reversed orbitals[27] ($\pm sk$). The gap is formed since the pairing correlations are much more effective in the ground state of the even system than in the excited states which require the breaking of pairs. [The largest part of the energy gap, or about 1 MeV, is caused by the nondiagonal correlation effects in the ground state, and the smaller, remaining part is due to the diagonal energy contribution associated with the breaking of a pair; cf. Wahlborn (1966)].

Now consider the odd system with only one unpaired particle. The effect of the pairing correlations is then reduced since the "blocked" level cannot be occupied by a pair. The energy depression, associated with the gap (see above), is therefore diminished. This effect is particularly strong when a level close to the diffuse Fermi surface is blocked, and usually strongest for the ground state, i.e., when ϵ_F is blocked.[28] In general, the effect decreases with increasing excitation energy. As a consequence, the low-lying excited states appear to be "compressed", their energies being smaller than expected from the expression $|\epsilon_K-\epsilon_F|$. From data, one can estimate the compression effect to be roughly a factor of 1.5 to 2 for the first few excited states, in agreement with estimates based on pairing-correlation calculations (Wahlborn, 1962, 1966). We refer to the excitations of an odd particle in the surrounding "sea" of correlated pairs as "one-quasiparticle excitations".[5] Detailed pairing-correlation calculations are needed to properly take into account the effects of blocking on the excitation energies.

Vibrational states (collective, nonrotational excitations) are known to be present in all nuclei (see, e.g., Bohr and Mottelson, 1953a; Nathan, 1964; Nathan and Nilsson, 1965; and Davidson, 1968), their presence usually being most obvious in even–even nuclei. In odd-A nuclei, there is significant coupling between the quasiparticle motion and the vibrational modes. This "particle–phonon" interaction often makes a considerable contribution to the energy. For nonspherical nuclei in the region considered here, the quadrupole gamma vibrations, intrinsically characterized by $\Omega^\pi=2^+$, are particularly important. Therefore, any members of fairly low-lying pairs of quasiparticle states having the same parity and $|K\pm K'|=2$ may be appreciably affected. In particular, this is often true if one of the affected states is the ground state, K_0. The observed band heads with $K=|K_0-2|$ located below or about 0.7 MeV usually have lower energies than the pure quasiparticle excitations would have. These shifts occasionally may amount to a few hundred keV, and it is necessary to take them into account in a comparison between predictions and data.

In addition to the intrinsic effects, there are contributions due to the rotational motion. The rotation, of course, is responsible for the band structure[3] observed in the energy spectra of nonspherical nuclei [see, e.g., Bohr (1952), Bohr and Mottelson (1953a, b), Nathan and Nilsson (1965), and Davidson (1968)]. For the band heads, the main effect comes from the "rotational" energy, which is proportional to $I(I+1)$ and therefore does not vanish for $I=K$ in an odd-A nucleus. This effect is modified due to the presence of an intrinsic $\mathbf{J}^2$ term [arising from the expansion of $\mathbf{R}^2=(\mathbf{I}-\mathbf{J})^2$]. However, there remains a term linear in K, and a less well known positive correction, $\gamma(K)$, which takes the precession into account (see Sec. III.B.1). In certain situations, the rotational energy contribution is crucial and should be taken into account (shifts of a few hundred keV may occur, e.g., in the neighborhood of the $K=11/2$ neutron states). Another, usually less important effect for band-head energies, arises from the nonadiabatic[26] (Coriolis) coupling between the intrinsic and the rotational motions. It is straightforward to also take this effect into account, if it is needed.

In Sec. III.A.2, we present a somewhat simplified theoretical model which includes, at least qualitatively, the main physical effects discussed here. In Sec. III.A.3, the analysis, in terms of single-particle level schemes, of experimental band-head energy data is outlined.

2. *A Simplified Phenomenological Model*

The total model Hamiltonian can be schematically written

$$H_{\text{model}}=H_{\text{intr}}+H_{\text{rot}}+H_{\text{rpc}}, \tag{3.1}$$

$$H_{\text{intr}}=H_{\text{ip}}+H_{\text{res}}, \tag{3.2}$$

where H_{intr} is the Hamiltonian of the intrinsic (particle) motion,[4] H_{rot} describes the rotational motion, and H_{rpc} represents the nonadiabatic coupling[26] between the two degrees of freedom (see Appendix A). The intrinsic Hamiltonian consists of an independent-particle part, H_{ip}, and the residual interactions, H_{res}. The main effects of the residual interactions are the correlations—pairing correlations and collective correlations. The remaining interaction effects are disregarded in our analysis.

The pairing correlations are approximately taken into account by transforming H_{intr} from an independent-particle basis to a quasiparticle basis.[5] The collective correlations, caused by the quasiparticle interactions, consist of vibrational motion and its coupling to the quasiparticle motion. Details of the approach are given in Appendix C in the framework of the BCS and RPA

theories.[9,10] In the simple phenomenological version of the model used here, we set

$$H_{\text{intr}} \approx H_0 + H_{\text{qp}} + H_{\text{vibr}} + H_{\text{pvc}}, \tag{3.3}$$

where H_0 is a constant, intrinsic contribution of the core (may be disregarded here), H_{qp} is the contribution from independent quasiparticles, H_{vibr} is the contribution from vibrational motion, and H_{pvc} is the particle-vibration coupling contribution. As shown in Appendix C, this Hamiltonian can be written in the form[27]

$$H_{\text{intr}} = H_0 + \sum_{sk} e_k \alpha_{sk}^{\dagger} \alpha_{sk} + \sum_{LM} \hbar\omega_{LM} O_{LM}^{\dagger} O_{LM} - \sum_{LM} \sum_{s'k',sk} \mathcal{K}_{s'k',sk}^{LM} [O_{LM}^{\dagger} + (-1)^M O_{L,-M}] \alpha_{sk}^{\dagger} \alpha_{s'k'}. \tag{3.4}$$

Here the "quasiparticle energy" given by

$$e_k = e_k(\lambda, \Delta) \equiv [(\epsilon_k - \lambda)^2 + \Delta^2]^{1/2}, \tag{3.5}$$

where λ and Δ are BCS parameters,[28] is known to be a poor approximation to the actual blocking calculation (see Sec. III.C).

The presentation here, Eq. (3.4), essentially follows Piepenbring (1966), and Monsonego and Piepenbring (1966, 1968). In Appendix C we explain the notations and discuss the structure of the intrinsic wave functions—i.e., the eigenstates of H_{intr}, Eq. (3.4), (see also Sec. III.B.2).

The rotational terms of the Hamiltonian, Eq. (3.1), can be written in the following way, for the case of an even-core rotor plus intrinsic motion with angular momentum **J**:

$$H_{\text{rot}} + H_{\text{rpc}} = (\hbar^2/2\mathfrak{I})[(\mathbf{I}^2 - J_z^2 + J_x^2 + J_y^2) - (I_+ J_- + I_- J_+)]. \tag{3.6}$$

The form of these terms is derived, and the notations are explained, in Appendix A.

The model presented by Eqs. (3.4) and (3.6) serves as a basis for the discussion given in the following parts of this Section. For the calculation of the total energy in an approximate eigenstate of the Hamiltonian, Eq. (3.1), we take the expectation value. This gives energy contributions which we identify according to the various effects described in Sec. III.A.1.

3. *Basis and Outline of the Energy Analysis*

Applying the model, defined by Eqs. (3.1) and (3.3), to the band-head[3] energy $E(K)$, we can decompose this approximately in the following way:

$$E(K) \approx E_K^{\text{intr}} + E_K^{\text{rot}} + E_K^{\text{rpc}}, \tag{3.7}$$

$$E_K^{\text{intr}} \approx E_K^{\text{qp}} + E_K^{\text{vibr}} + E_K^{\text{pvc}}. \tag{3.8}$$

Since we do not consider vibrational states, the "phonon" contribution [E_K^{vibr} in Eq. (3.8)] enters only in admixed vibrational components. Our analysis is based on the assumption that the experimental and theoretical excitation energies can be compared by the relation

$$E(K) - E(K_0) \approx E_{\text{expt}}(K), \tag{3.9}$$

where K_0 denotes the ground state. Due to the fact that the single-particle energies, ϵ_k, enter into the expression for $E(K)$, we can obtain information on single-particle spectra. This procedure is briefly described below.

The collective energy contribution,[8]

$$E_K^{\text{coll}} \equiv E_K^{\text{pvc}} + E_K^{\text{rot}} + E_K^{\text{rpc}}, \tag{3.10}$$

can be estimated in such a way that the result does not depend sensitively on the single-particle energies used [cf. Eqs. (3.13) and (3.18)]. We can, therefore, calculate it initially, and subtract its effect from the experimental energy, $E_{\text{expt}}(K)$. This correction gives an "empirical" (extracted from experimental data) quasiparticle[5] excitation energy, $E_{\text{qp}}^{\text{emp}}(K)$, which in our treatment is model dependent. The method of separation is described in Sec. III.B. We then make the second assumption that the excitation energy, calculated with the BCS method of "blocking,"[9] can be compared with the empirical value,

$$E_{\text{qp}}^{\text{BCS}}(K) \approx E_{\text{qp}}^{\text{emp}}(K). \tag{3.11}$$

Since the theoretical quasiparticle energy expression depends crucially on the single-particle energies—primarily on ϵ_K—Eq. (3.11) can be used for the determination of single-particle levels from data.

The second stage, i.e., the procedure based on Eq. (3.11), is the most difficult part of the analysis. The primary parameters of the theory are the single-particle levels, and there are many more of these than there are available empirical quasiparticle energies. One might formulate the problem in a more definite way by considering several nuclides simultaneously, and perhaps also using other experimental data, such as spectroscopic factors from one-nucleon transfer reactions, which may depend (though not so sensitively) on the single-particle states. However, in that way we might lose some of the information on detailed level variation, which we consider significant (see discussion in Sec. V).

Our approach consists in using "standard" schemes of single-particle levels, chosen to represent in an average way the possible single-particle spectra according to general theoretical predictions for the region considered (cf. Sec. II). The "peripheral" parts of these spectra, i.e., the levels far from the Fermi energies encountered, are kept fixed throughout the analysis. The levels belonging to the "central" parts, on the other hand, are treated in three different ways depending on the available information[27,28]:

(a) Whenever the value of $E_{\text{qp}}^{\text{emp}}(K)$ is known, the corresponding single-particle energy ϵ_K is determined

TABLE II. Standard scheme of 49 single-neutron levels (MeV)[29,30] for the region $150<A<190$.

Fixed[a]		Varied[b]		Fixed[a]	
[3/2+ 422]	−6.0	1/2+ (400)[c]	(1.5±1)	1/2+ 651[d]	9.9
[1/2+ 420]	−5.4	3/2+ (402)[c]	(1.5±1.5)	[5/2− 503]	10.9
[9/2+ 404]	−5.4	1/2− 530	(2±0.5)	[7/2− 743]	10.9
[5/2+ 413]	−4.0	3/2− 532	(2.5±0.5)	[3/2− 761]	11.0
[1/2− 550]	−3.7	11/2− 505	(2.5±1)	[5/2− 752]	12.3
[3/2+ 411]	−3.4	1/2+ (660)[c]	(3±1)	[1/2− (501)]	12.7
[3/2− 541]	−3.1	3/2+ (651)[c]	(3.5±1)	[3/2+ 642]	12.8
[5/2− 532]	−2.7	3/2− 521	(≈3.5)	[1/2− 770]	13.0
[1/2+ 411]	−2.2	5/2− 523	(≈3.5)	[9/2− 734]	13.2
[7/2− 523]	−1.7	5/2+ 642	(4±0.5)	[5/2+ 633]	13.2
[7/2+ 404]	−1.0	1/2− 521	(≈4.5)	[1/2+ 640]	13.7
[5/2+ 402]	−0.7	7/2+ 633	(5±0.5)	[3/2+ 631]	13.8
[9/2− 514]	−0.2	5/2− 512	(5±1)	[5/2+ 622]	15.4
1/2− 541[d]	0.6	7/2− 514	(5.5±0.5)		
		9/2+ 624	(≈6)		
		1/2− 510	(6.5±0.5)		
		3/2− 512	(7±0.5)		
		7/2− 503	(7±1)		
		11/2+ 615	(7.5±1)		
		9/2− 505	(8.5±1)		
		3/2− (501)	(9±1)		
		13/2+ 606	(9.5±1.5)[e]		

[a] The cylindrical classification in brackets is irrelevant for the present purposes.
[b] The energy values in parentheses indicate roughly the variation allowed for each level.
[c] The expected cylindrical classification of these single-neutron levels throughout the region.
[d] Expected to appear in this mass region, but not yet observed.
[e] Fixed at 10.3 MeV in Version I.

by Eq. (3.11) through a BCS blocking calculation (the Fermi level, ϵ_F, is considered fixed).

(b) If $E_{\rm qp}^{\rm emp}(K)$ is known in some, but not all, members of a sequence of odd-Z isotopes or odd-N isotones, the unfitted levels ϵ_K are roughly fixed by interpolation or extrapolation.

(c) If neither situation (a) nor (b) applies, the level ϵ_k may be kept fixed or varied smoothly with nucleon numbers, whichever appears compatible with model expectations.

Details of the steps in the procedure outlined here are described in Sec. III.C.

For orientation purposes and for further discussion we present in Table I (proton) and Table II (neutron) the standard single-particle level schemes[29,30] used in our analysis. For the peripheral (fixed) levels, only the positions enter. For the central (varied) levels, we indicate the tentative ranges of variation—the actual positions are to be determined along the lines outlined above.

B. The Collective Contributions to Band-Head Energies

The collective[8] contribution to the band-head[3] energy, Eq. (3.7), is given by Eq. (3.10). The corresponding correction, applied to the excitation energy, is calculated in two steps. First, we subtract from all the energies $E_{\rm expt}(K)$ [cf. Eq. (3.9)] and the ground state, the rotational contributions, $E_K^{\rm rpc}$ and $E_K^{\rm rot}$, estimated as described in Sec. III.B.1. This gives us the differences in intrinsic[4] energy, $E_K^{\rm intr}$ [Eq. (3.8)]. Second, we subtract from $E_K^{\rm intr}$ the particle–vibration coupling contribution, $E_K^{\rm pvc}$, estimated as described in Sec. III.B.2. This leaves us with the quasiparticle[5] excitation energies to be analyzed further according to Eq. (3.11) (see Sec. III.C). It should be noted that the order of the two steps described above cannot in principle be reversed (the evaluation of $E_K^{\rm pvc}$ depends on $E_K^{\rm intr}$—see Sec. III.B.2). In fact, the various effects on the band-head energies are not strictly additive, as written schematically in Eqs. (3.7), (3.8), and (3.10).

[29] In fixing the positions of the "peripheral" levels and indicating the ranges of the "central" levels in Tables I and II, we have consulted the schemes by Gareev *et al.* (1967) and by Gustafson *et al.* (1967) [see also Figs. 2 and 3], considering the appropriate deformation variations.

[30] The zero of the energy scale in Tables I and II as well as in Figs. 7-11 has been arbitrarily chosen in such a way that the sum of the single-particle energies for the occupied orbitals in the ground states is approximately zero on the average over the region of nuclides considered.

1. *The Effects of the Rotational Motion*

The main features of the rotational motion are described in Appendix A. The correlations in the intrinsic motion have certain effects—indirectly on the rotational parameter $\hbar^2/2\Im$, and more directly on the matrix elements of the operators $\mathbf{J}^2$ and $J_\pm$ which are not constants of motion. We present here the expressions used for estimating the rotational corrections, from Eq. (3.6).

In principle, we should first apply the correction due to the nonadiabatic effect, $E_K{}^{\rm rpc}$. If we assume that the Coriolis coupling in the band-head ($I=K$) admixes significantly only one state having $K'=K-1$, $\pi'=\pi$ (there is no such effect if $K=\frac{1}{2}$), and that the perturbation approximation is valid, we find

$$E_K{}^{\rm rpc}\approx\langle K, K' \mid H_{\rm rpc} \mid K, K\rangle^2[E_{\rm expt}(K)-E_{\rm expt}(K')]^{-1}. \tag{3.12}$$

Because of the correlations, the matrix element is reduced here compared to the single-particle value (cf. Appendix A). Usually the shifts due to $E_K{}^{\rm rpc}$ are insignificant, as known from the studies of ^{183}W by Kerman (1956), Rowe (1965), and Brockmeier *et al.* (1965). Non-negligible shifts are expected in a few cases, particularly for $N_0=6$ levels,[20] and some of these have been taken into account. (See further comments in the text and Tables of Sec. IV.)

The zero-point rotational energy is written in the form

$$E_K{}^{\rm rot}=(\hbar^2/2\Im)[K+\gamma(K)-\delta_{K,1/2}a], \tag{3.13}$$

where the decoupling factor, a, now includes correlation effects (cf. discussion in Sec. III.B.2). The quantity $\gamma(K)$ is defined as the contribution of the precession effect, i.e., of the operator $J_x{}^2+J_y{}^2$. To a good approximation, we can set

$$\gamma(K)\approx(\langle K \mid \mathbf{j}^2 \mid K\rangle-K^2) +2\sum_k{}' v_{K;k}{}^2(\langle k \mid \mathbf{j}^2 \mid k\rangle-M_k{}^2), \tag{3.14}$$

where we assume that the blocking effects[9] are included through $v_{K;k}$ (see Sec. III.C.1 and Appendix C.1). The single-particle matrix elements of $\mathbf{j}^2$ have appreciable variations (see Appendix A).

For a simple discussion, we may consider the variation of the approximate expression $[j(j+1)-K^2]$, and disregard the pairing effects. The most relevant cases are those which have a large value of j, and where K can be either equally large or much smaller. A particularly interesting instance occurs when the Fermi level[28] has $K_F=j_F\gg1$, whereas a hole state has $j=j_F$, and $K\ll j$. Then $\gamma(K)$ for the ground state is larger than that for the hole excitation by $K_F{}^2$. If, e.g., $(\hbar^2/2\Im)=20$ keV, and $K_F=11/2$, the difference in zero-point energy would amount to 600 keV. In practice, we do not expect such large values, since correlations and realistic values of $\langle\mathbf{j}^2\rangle$ tend to level out the variations.[31]

The situation described above is encountered in a fairly clear-cut way in the odd-neutron nuclides where a $K=11/2$ level is found at low excitation energy. In such a case, it is conceivable that the single-particle state $K=11/2$ is actually the Fermi level, whereas, e.g., the lowest hole excitation becomes the ground state, due to its much smaller value of $\gamma(K)$, Eq. (3.14). The data do not exclude the occurrence of this type of situation in actual nuclei. The zero-point rotational energy would then furnish at least part of the explanation why the $K=11/2$ levels have not been found as ground states.

In the present analysis we discuss two versions,

$$\gamma(K)=0, \qquad \text{"Version I"},$$
$$\gamma(K)\approx0.5K^2, \qquad \text{"Version II."} \tag{3.15}$$

Version I is the conventional form [cf. Nathan and Nilsson (1965), Eq. (4.2.2)]. We have analyzed all the data in this version. Version II involves a very rough and fairly extreme estimate of $\gamma(K)$ (see the preceding discussion). For the region considered, the coefficient of K^2 in Eq. (3.15) cannot be chosen much larger than ≈0.5 without destroying the general qualitative agreement between model predictions and quasiparticle level systematics. We have applied Version II only to the isotones with $N=91$, 109, and 111, and the results should be considered quite tentative. Discussion is given in Secs. IV.C and V.D.

The rotational parameter $\hbar^2/2\Im$ encountered in the region considered usually amounts to 10–20 keV. The values of this quantity, as well as of the decoupling factor [see Eq. (3.13)], are taken from an analysis of the band structure (cf. Bunker and Reich, 1971), or in some cases estimated from the empirical systematics.

2. *The Particle–Vibration Coupling*

We use the simple phenomenological model, formulated by Eq. (3.4), to estimate the contribution of $E_K{}^{\rm pvc}$ to the collective correction.[8] The nature of the wave functions is discussed in Appendix C. The description follows closely Piepenbring (1966) and Monsonego and Piepenbring (1966, 1968), and is based on the version of RPA [10] applied by Soloviev and collaborators

---

[31] With $\mathbf{J}=\Sigma_m\,\mathbf{j}_m$ (m=particle index), the precession effect is represented by the following operator:

$$J_x{}^2+J_y{}^2=\sum_m(\mathbf{j}_m{}^2-j_{mz}{}^2)+\sum_{m\neq m'}j_{m+}j_{m'-}.$$

In Eq. (3.13), $\gamma(K)$ is approximately the expectation value of this operator. In the absence of correlation effects, we find[27]

$$\langle J_x{}^2+J_y{}^2\rangle_{\rm ip}=\sum_{sk}(\langle sk \mid \mathbf{j}^2 \mid sk\rangle-M_k{}^2)-(\tfrac{1}{2})\sum_{sk,s'k'}|\langle s'k' \mid j_+ \mid sk\rangle|^2,$$

where the sums of the single-particle matrix elements are over occupied orbitals only. The second sum is generally much smaller than the first one. The same is true in the presence of pairing correlations, but the expression is then modified.

(Soloviev and Vogel, 1967; Soloviev, Vogel, and Jungklaussen, 1967).

The eigenstates considered can be written schematically in the following form (the "one-phonon approximation"; $\tilde{\Psi}_0$ denotes the correlated ground state):

$$|\Psi_{sk}\rangle = S_0\alpha_{sk}^\dagger|\tilde{\Psi}_0\rangle + \sum_{LM}\sum_{s'k'} S_{kk'}{}^{LM}O_{LM}^\dagger\alpha_{s'k'}^\dagger|\tilde{\Psi}_0\rangle. \quad (3.16)$$

In each term of the sum we assume that the projection quantum numbers add to $K=|M_k|$, and that only the lowest possible L modes ($L\geq 2$) compatible with parity conservation are included. Furthermore, for each LM mode we use the lowest, vibrational eigensolution of the RPA equations, having phonon energy $\hbar\omega_{LM}$. In practice, we include only the $L=2$ and $L=3$ modes, i.e., the beta, gamma, and octupole vibrations, for which there is some experimental information at low excitations (cf. Nathan, 1964; and Nathan and Nilsson, 1965, paragraph 4).

If we assume the amplitudes S_0, $S_{kk'}{}^{LM}$, and the eigenvalue, $E_k{}^{\rm intr}$, to be given and use the eigenvalue equation for $H_{\rm intr}$, we can eliminate the coupling coefficients, $\mathcal{K}_{s'k',sk}{}^{LM}$ [see Eq. (3.4)]. In addition, in the expression for $E_K{}^{\rm intr}$, Eq. (3.8), we use the rough approximation

$$E_k{}^{\rm qp}\approx e_k(\lambda,\Delta)-e_0(\lambda,\Delta), \quad (3.17)$$

where e_k is defined by Eq. (3.5), and e_0 is obtained with $\epsilon_k=\epsilon_F$. We can then solve for the particle–vibration coupling contribution to the band-head energy,[3]

$$E_k{}^{\rm pvc}\approx\sum_{LMk'}[E_k{}^{\rm intr}-\hbar\omega_{LM}-e_{k'}(\lambda,\Delta)](S_{kk'}{}^{LM}/S_0)^2. \quad (3.18)$$

This expression has the essential features qualitatively correct, and can be considered to give order-of-magnitude estimates of the effects involved.

In Eq. (3.18), $E_k{}^{\rm intr}$ has the value derived from the data (see Sec. III.B.1). For the remaining quantities, one can use experimental and/or theoretical information, either of which is, in most cases, available in the literature. In general, we have taken the phonon energies, $\hbar\omega_{LM}$, from the systematics of vibrational states in even–even nuclei. Information on the admixture amplitudes, $S_{kk'}{}^{LM}$ and S_0, may in some cases be extracted from transition rates or decoupling factors (Monsonego and Piepenbring, 1968), and from transfer reaction or inelastic scattering data. However, for most cases, a consistent evaluation of the admixture amplitudes is furnished by the calculations of Soloviev and Vogel (1967), Soloviev, Vogel, and Jungklaussen (1967), Kalpazhiu and Vogel (1966), and Malov, Soloviev and Fainer (1968), in which the force constants and single-particle energies are chosen to fit the vibrational energies in even–even nuclei. (See also Bés *et al.*, 1963, 1965, 1966, 1969). With this approach, the admixture amplitudes do not depend sensitively on the single-particle level schemes used. In several cases we have made use of the detailed discussion of these questions by Bunker and Reich (1971), particularly in cases where the available predictions contradict experimental data. For further quantitative details, such as values of $\hbar\omega_{LM}$, the reader is referred to the literature quoted above.

In most cases, the estimated vibrational shifts, $-E_k{}^{\rm pvc}$, are small, but in a few cases they may amount to as much as 0.5 MeV. The estimates are usually not accurate to better than $\pm 30\%$. States which are found to be mainly of vibrational character have as a rule not been included in our analysis.

C. The Blocking Calculations and the Fitting Procedure

The empirical quasiparticle[5] excitation energies, $E_{\rm qp}{}^{\rm emp}(K)$, extracted from level data as described in Sec. III.B, are analyzed in terms of single-particle spectra as outlined in Sec. III.A.3. The basic relation assumed is Eq. (3.11), where we take the theoretical energy, $E_{\rm qp}{}^{\rm BCS}(K)$, to be evaluated with the BCS method for blocking.[9] The significance of this method consists in the fact that it allows us to evaluate, in a quantitatively satisfactory way, the "compression" effect, discussed in Sec. III.A.1 (see Wahlborn, 1962, 1966). We shall first, in Sec. III.C.1, show how the BCS problem is solved and the energy calculated, and then, in Sec. III.C.2, describe how this method is used for fitting the energy data. A brief description of the basic BCS theory is given in Appendix C.1.

1. *The BCS Method*

In our version of the BCS method (Wahlborn, 1966) the following set of equations is solved for each quasiparticle state, obtained by blocking the single-particle level[27] ϵ_k:

$$n_0=\sum_{k'}\left(1-\frac{\epsilon_{k'}-\lambda_k}{e_{k'}(\lambda_k,\Delta_k-x_{k;k'})}\right); \quad (3.19)$$

$$2\Delta_k/G=\sum_{k'}[(\Delta_k-x_{k;k'})/e_{k'}(\lambda_k,\Delta_k-x_{k;k'})]; \quad (3.20)$$

$$x_{k;k'}=Gu_{k;k'}v_{k;k'}; \quad (3.21)$$

$$\left.\begin{matrix}u_{k;k'}\\ v_{k;k'}\end{matrix}\right\}=\frac{1}{\sqrt{2}}\left(1\pm\frac{\epsilon_{k'}-\lambda_k}{e_{k'}(\lambda_k,\Delta_k-x_{k;k'})}\right)^{1/2}; \quad (3.22)$$

$$e_{k'}(\lambda_k,\Delta_k-x_{k;k'})\equiv[(\lambda_k-\epsilon_{k'})^2+(\Delta_k-x_{k;k'})^2]^{1/2}. \quad (3.23)$$

This intricate system can only be solved by means of iterations (Ogle and Wahlborn, 1969). The solution consists of values of the BCS parameters λ_k and Δ_k, and the sets of amplitude parameters $u_{k;k'}$, $v_{k;k'}$. From

this result we can compute the energy expression

$$E_k^{\mathrm{BCS}}=\epsilon_k+2\sum_{k'}\epsilon_{k'}v_{k;k'}{}^2-G\sum_{k'}v_{k;k'}{}^4-(\Delta_k{}^2/G). \quad (3.24)$$

In Eqs. (3.19)–(3.24), the condition $k'\neq k$ holds, and all the sums therefore exclude the blocked level. The presence of the quantity (3.21) results from the variation of the term $-G\sum_{k'}v_{k;k'}{}^4$ in the basic BCS energy expression.

The number of paired particles, n_0, is fixed by the requirement that the system considered in Eqs. (3.19)–(3.24) has the correct Fermi level,[28] ϵ_F. In the BCS calculation without blocking[9] (here occasionally referred to as "NBCS") one solves Eqs. (3.19) and (3.20) without the condition $k'\neq k$, and with n_0 being the actual odd number of particles. (We also set $x_{k;k'}=0$.) The resulting quantities[28] are the "Fermi energy parameter," λ_*, and the "gap parameter," Δ_*. For an odd-Z nucleus, this solution furnishes an interpolation between the ground-state BCS solutions for the adjacent even–even nuclei with proton number $Z\pm1$, and correspondingly for neutrons. For the appropriately defined odd-even mass difference P, pertaining to an odd-A nucleus, it can be shown that the approximate relation

$$\Delta_*\approx P \quad (3.25)$$

is valid. Since Δ_* depends fairly sensitively on the pairing-force constant G, Eq. (3.25) furnishes a criterion for the choice of G, provided P has been derived from data. This procedure has been applied and justified in the literature (see Nilsson and Prior, 1961; Bang, Krumlinde, and Nilsson, 1965; and Prior, Boehm, and Nilsson, 1968). In the present analysis, G is chosen for each nuclide so that Eq. (3.25) is fulfilled.

The remaining quantities needed for the BCS solution are the single-particle energies themselves. We see from Eq. (3.24) that the quasiparticle[5] energy depends most sensitively on the blocked level ϵ_k—as we, of course, expect. This observation together with Eq. (3.11) furnishes the basis of the "fitting" procedure which we describe in Sec. III.C.2. Some questions about uncertainties and ambiguities are discussed in Sec. III.D.

2. *The Procedure of Energy Fitting*

The main ideas behind the procedure of determining single-particle level schemes from the quasiparticle level data are outlined in Sec. III.A, and our theoretical expressions for computing the quasiparticle energies are presented in Sec. III.C.1. It is obvious from Eqs. (3.19)–(3.24) that using the regular (blocking) BCS solution in every step of a procedure for fitting all the data would be prohibitively lengthy. We, therefore, need an approximation to the BCS energy [Eq. (3.24)] having a simple enough form that it can be inverted to give ϵ_k, but still being considerably more accurate than, e.g., Eq. (3.17). We apply this energy approximation to determine single-particle energies (relative to ϵ_F)[28] which are then used in the regular BCS calculation, where the final adjustments are made.

For the approximation, we utilize the observation by Wahlborn (1962) that the BCS energies [from Eq. (3.24)], calculated for several blocked states and plotted against ϵ_k, generally follow a hyperbolalike dependence intermediate between Eq. (3.5) and $|\epsilon_k-\epsilon_F|$. In fact, this behavior has also been found from results of pairing calculations with more accurate methods than BCS (Wahlborn, 1966). The "compression" effect for the energies of such low-lying excitations as we consider here can be approximated by the following expression:

$$E_{\mathrm{qp}}{}^{\mathrm{RBCS}}\approx[(\epsilon_k-\lambda_*)^2+(\Delta_*-D^{-1})^2]^{1/2}-[(\epsilon_F-\lambda_*)^2+(\Delta_*-D^{-1})^2]^{1/2}. \quad (3.26)$$

It can be shown (Wahlborn, 1962) that Eq. (3.26) on the average (i.e., for $\epsilon_F=\lambda_*$) reproduces the proper BCS excitation energies up to second derivatives in ϵ_k, if D is set equal to the average single-particle level density (this is a general estimate and is used here). We refer occasionally to the "reduced-delta" energy approximation, Eq. (3.26), as the RBCS method.

The BCS fit to the known (empirical) quasiparticle energies $E_{\mathrm{qp}}{}^{\mathrm{emp}}$, of an individual nucleus [see Sec. III.A.3(a)] proceeds in steps as follows:

(1) With an assumed scheme of single-particle levels [cf. Sec. III.A.3, and Tables I and II], the NBCS solution λ_*, Δ_* is derived.[28] This solution is repeated as needed with different G values until the condition (3.25) is fulfilled.

(2) The solutions ϵ_k are obtained from the inverse of the RBCS equation (3.26) with each $E_{\mathrm{qp}}{}^{\mathrm{emp}}$ inserted for $E_{\mathrm{qp}}{}^{\mathrm{RBCS}}$, giving a "new" single-particle spectrum.

(3) If necessary, the steps (1) and (2) are repeated until both the levels ϵ_k and the G values fulfill the conditions imposed.

(4) With the G value and the "new" single-particle spectrum thus obtained, the regular BCS solution is derived, and the energies $E_{\mathrm{qp}}{}^{\mathrm{BCS}}$ computed from Eqs. (3.19)–(3.24).

(5) If Eq. (3.11) is not found to be fulfilled to within an accepted tolerance (see Sec. III.D), suitable changes are made in the single-particle spectrum, and the steps (1)–(4) are repeated.

In most cases we need to perform the steps (1)–(4) only once. The calculated BCS and RBCS energies are found to agree remarkably well, for fitted as well as unfitted levels. Computer programs for automatizing part of the procedure have been utilized (Ogle and Wahlborn, 1969; Fredriksson, 1969).

The strategy formulated by points (b) and (c) in Sec. III.A.3 is difficult to put down in quantitative terms. The results presented in Sec. IV will best express what we have actually done with the unfitted levels.

These results are the end product of three series of fits for the entire region—in addition, several cases have been refitted once or more. In all likelihood, an independent repetition of the whole process would produce a different result. Yet, from our own experience we are confident that the relative positions of the *fitted* levels would not turn out to be substantially different from our results, assuming the same data for $E_{\mathrm{qp}}{}^{\mathrm{emp}}$. This is not to say that one could change some of the unfitted levels in our schemes even moderately without affecting the fit. Particularly when the level density is high near the Fermi surface, shifting a single-particle level in that region by, say, 100 keV may put the quasiparticle energy fits for adjacent levels off by comparable or larger amounts. However, if another fit is then made, the "new" single-particle levels may differ much less than 100 keV from their original positions. In conclusion, we have found the fits to be generally much more stable than one might expect off-hand by merely inspecting, e.g., Eqs. (3.19)–(3.24). This feature is no doubt related to the validity of the single-particle model as a basis for describing those nuclear excitations which we call quasiparticle states.[5]

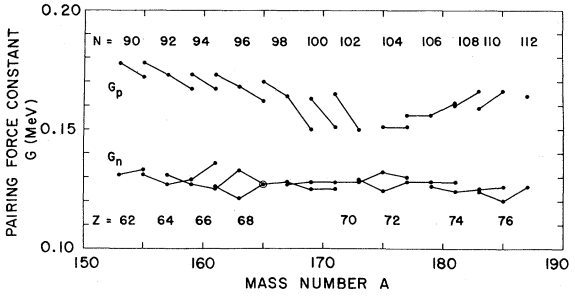

FIG. 4. Values of the pairing force constant, G, used in the present BCS calculations for odd-proton (G_p) and odd-neutron (G_n) nuclides (Version I analysis only).

We note, from Eq. (3.26), that the position of the Fermi level,[28] ϵ_F, is itself not uniquely determined by our procedure as it has been described here. In principle, equally good fits could be obtained from either of two initial choices of position for ϵ_F, one leading to $\epsilon_F > \lambda_*$, and the other to $\epsilon_F < \lambda_*$. In most cases the spectroscopic data are not sufficiently detailed to help determine the choice from experiment. However, we have found that uniformity considerations and systematics, where sequences of isotopes or isotones are compared, make the choice fairly unambiguous in practice.

In several cases, the calculated quasiparticle excitation energies turn out to be appreciably reduced compared to the corresponding single-particle energy spacing—more than expected from the average "compression" effect. Such reduction occurs particularly when the single-particle level scheme is nonuniform near ϵ_F, and the difference $|\epsilon_F - \lambda_*|$ is large. The opposite is true in some other cases—i.e., the excitation energies may turn out to be only slightly smaller than $|\epsilon_K - \epsilon_F|$. (See Sec. IV.B.)

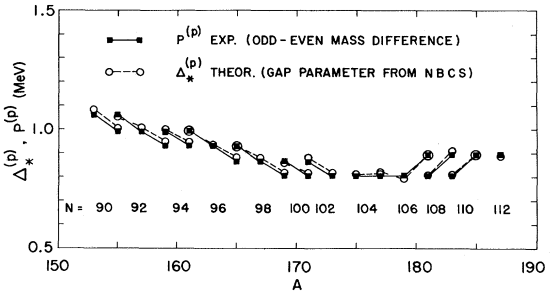

FIG. 5. Values of the gap parameter[28] $\Delta_*{}^{(p)}$, obtained from the NBCS solutions, and the experimental odd-even mass differences, $P^{(p)}$, for odd-proton nuclides (Version I analysis only).

D. Ambiguities, Uncertainties, and Tolerances

We summarize here the various elements entering into our analysis with a view to a critical evaluation of the relevant assumptions and approximations made. There are obvious ambiguities in the procedure we take, and there are uncertainties involved in the calculations. Consequently, we also need to discuss the tolerances in the fit to the data and in the determination of the single-particle energies.

The ambiguities involved in the results arise both from the methods used and the lack of experimental information. The prime ambiguity is probably introduced by the treatment of the zero-point rotational energy, Eq. (3.13). Problems are especially encountered in regions where $N_0 = 6$ states and $K = 11/2$ levels occur at low energies, since the precession contribution[31] may vary appreciably there. This is why we have chosen two relatively extreme estimates of the term $\gamma(K)$: Versions I and II [Eq. (3.15)]. In Version I, the rotational shifts are relatively small, while in

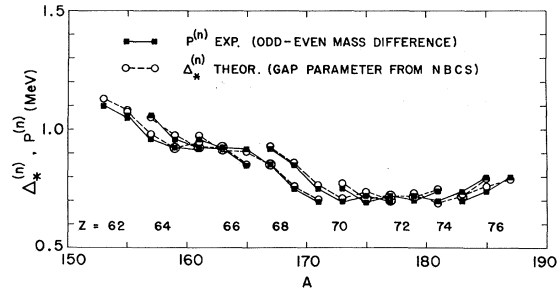

FIG. 6. Values of the gap parameter[28] $\Delta_*{}^{(n)}$, obtained from the NBCS solutions, and the experimental odd-even mass differences, $P^{(n)}$, for odd-neutron nuclides (Version I analysis only).

TABLE III. Energy data on quasiparticle excitations in odd-proton nuclides with $63 \leq Z \leq 69$.[aa]

	Assigned quasiparticle state					
		Energy (keV)				
Nuclide	Assignment	E_{expt}	E_{qp}^{emp}	E_{qp}^{BCS}	References and comments	
$^{153}_{63}$Eu	$3/2^-$ 541	(−712)	(−720)	−697	a, b	(*R*)
	$5/2^-$ 532	−98	−110	−124	a, c, d	
	$5/2^+$ 413	0	0	0	a, c, d	
	$3/2^+$ 411	103	110	101	a, c, d	(*R*)
	$5/2^+$ 402	(706)	(720)		b, c, e	(*R*)
$^{155}_{63}$Eu	$3/2^-$ 541	(−1100)	(−1110)	−1110	b, c, f	
	$5/2^-$ 532	−104	−110	−115	d, c, f	
	$5/2^+$ 413	0	0	0	d, c, f	
	$3/2^+$ 411	246	260	238	d, c, f	
$^{155}_{65}$Tb[ac]	$5/2^+$ 413	(−271)	(−260)	−267	g, h, i	(*R*)
	$5/2^-$ 532	−227	−230	−231	g, i	(*R*)
	$3/2^+$ 411	0	0	0	g, i	
$^{157}_{65}$Tb	$5/2^-$ 532	−326	−320	−326	i, j	(*R*)
	$5/2^+$ 413	(−300)	(−290)	−295	b, k	(*R*)
	$3/2^+$ 411	0	0	0	i, j	
	$7/2^-$ 523	(357)	(340)	347	b, i, j	(*R*)
	$1/2^+$ 411	597	[900]	913	i, j	*V*
$^{159}_{65}$Tb	$5/2^-$ 532	−363	−360	−335	l	(*R*)
	$5/2^+$ 413	−348	−360	−331	l	(*R*)
	$3/2^+$ 411	0	0	0	l	
	$1/2^+$ 411	(580)	[1000]	970	h, l	*V*
$^{161}_{65}$Tb	$5/2^-$ 532	−480	−480	−491	m	(*R*)
	$5/2^+$ 413	−315	−300	−306	m	(*R*)
	$3/2^+$ 411	0	0	0	m	
	$7/2^-$ 523	417	400	412	m	
$^{159}_{67}$Ho	$7/2^-$ 523	0	0	0	n, o	
	$1/2^+$ 411	206	230	231	n, o	*R*, (*V*)
$^{161}_{67}$Ho	$5/2^-$ 532	−827	−840	−845	p	(*R*)
	$7/2^-$ 523	0	0	0	p	
	$1/2^+$ 411	211	240	232	p	*R*, (*V*)
$^{165}_{67}$Ho	$5/2^-$ 532	(−1056)	(−1070)	−1099	h, s	(*R*)
	$5/2^+$ 413	−995	[−1000]	−1053	s, t	*R*, (*V*)
	$3/2^+$ 411	−362	−380	−356	s	*R*
	$7/2^-$ 523	0	0	0	s	*U*
	$1/2^+$ 411	429	460	443	s	*R*, (*V*)
	$7/2^+$ 404	715	710	694	s, u	*R*
$^{165}_{69}$Tm	$7/2^-$ 523	(−150)	(−130)	−99	h, u	*R*
	$1/2^+$ 411	0	(0)	0	u	ab
	$7/2^+$ 404	(69)	(50)	56	h, u	*R*, ab
$^{167}_{69}$Tm	$7/2^-$ 523	−293	−270	−256	v	(*R*)
	$1/2^+$ 411	0	(0)	0	v	ab
	$7/2^+$ 404	179	140	130	v	*R*, ab
$^{163}_{67}$Ho	$5/2^+$ 413	(−876)	(−880)	−879	b, q	(*R*)
	$7/2^-$ 523	0	0	0	q	
	$1/2^+$ 411	298	320	342	n, q, r	*R*, (*V*)
	$7/2^+$ 404	440	430	456	q	(*R*)

TABLE III (*Continued*)

Nuclide	Assigned quasiparticle state: Assignment	Energy (keV): E_{expt}	E_{qp}^{emp}	E_{qp}^{BCS}	References and comments	
$^{169}_{69}$Tm	(5/2+ 413)	(−1189)	(−1550)	−1603	w	Vibr.
	3/2+ 411	−570	−600	−616	h, l	*V*
	7/2− 523	−379	−360	−371	l, x	*R*
	1/2+ 411	0	0	0	l, x	*U*
	7/2+ 404	316	290	299	l, x	*R*
$^{171}_{69}$Tm	3/2+ 411	−676	−700	−700	y, z	*R, V*
	7/2− 523	−425	−410	−443	y, z	*R*
	1/2+ 411	0	0	0	y, z	*U*
	7/2+ 404	635	610	632	r, y, z	*R*
	5/2+ 402	913	890	902	r, y, z	(*R*)

[a] Reference [66Bl06].
[b] Not well established.
[c] Reference [66Fu11].
[d] Reference [69Un04].
[e] Not fitted.
[f] Reference [68Ke].
[g] Reference [64Pe13].
[h] Identification probable.
[i] Reference [67Bl12].
[j] Reference [66Fu06].
[k] Reference [66Gn].
[l] Reference [63Di09].
[m] Reference [66Zy02].
[n] Reference [66Bo02].
[o] Reference [64Ab03].
[p] Reference [65Gr35].
[q] Reference [66Fu04].
[r] See Bunker and Reich (1971).
[s] Reference [68Bu].
[t] Vibrational shift not evaluated.
[u] Reference [69Ar23].
[v] References [64Lö04, 70Wi09].
[w] Reference [65De05].
[x] Reference [65Bo08].
[y] Reference [68Me02].
[z] Reference [68Gr].
[aa] Notations and symbols are explained in the text (Sec. III.A.3 and IV.A).
[ab] These two single-particle levels could change order (see discussion in text).
[ac] The 7/2− 523 level in ^{155}Tb has been established at 250 keV [J. Jursik, V. Hnatowicz, and J. Zvolsky, Czech. J. Phys. **19B**, 870 (1969)].

Version II, the rotational shifts may be large, and may cause substantial rearrangement of the level order in certain cases. The results are compared in Sec. IV (see also Sec. V).

For the single-particle level schemes, derived according to the fitting procedure described in Sec. III.C.2, there are, admittedly, an infinity of choices which fit the data. However, there are constraints imposed on the position and variations of the levels (cf. Figs. 2 and 3, Tables I and II, and the discussion in Sec. III.A). We have attempted to keep with such general considerations. Judging from our own experience, we hardly expect any serious ambiguity to be involved in the relative determination of the *fitted* levels. Also the possible effect of the duality in the position of the Fermi level is limited.

There are evidently several computational uncertainties involved in the analysis. Appreciable errors should in general be attached to the vibrational shifts, particularly to the large shifts applied in some cases (see Sec. III.B.2). Also the estimate of the rotational correction—in either Version I or II—involves uncertainties. We never quote the empirical quasiparticle energies,[5] E_{qp}^{emp}, to better than 10 keV, and in several cases not to better than 50 or 100 keV.

The energy uncertainty inherent in the BCS method for blocking, due primarily to the particle-number fluctuations (see Appendix C.1), has been subject to previous examinations (see, e.g., Wahlborn, 1966). The error is found to be roughly constant for the quasiparticle excitations in a given nucleus, and therefore the uncertainties of the calculated excitation energies are relatively small. Pessimistic estimates for low-lying excited states indicate a possible error of ± 100 keV, which should include the worst cases. In some cases, we have not been able to find an iterative solution to the BCS Eqs. (3.19)–(3.22), despite attempts to vary the conditions (e.g., the G value) slightly. We interpret this lack of convergence as the absence of a solution with $\Delta_k \neq 0$, and therefore set $\Delta_k = 0$ in such a case. This may lead to increased uncertainty.

Including the effects of all possible ambiguities and uncertainties, we consider ± 100 keV to be an acceptable tolerance in the fit of individual quasiparticle energies, as well as in the relative determination of each single-particle level from a fit. Usually excitation energies below 100 keV are fitted to much better than this value. If the uncertainty is for any reason estimated to be appreciably larger than 200 keV, we usually do not perform a fit or include the information on the level.[32]

[32] For the purposes of this review, we may characterize the quality of a fit or determination involving an energy level in the following way, the precision being given in terms of the estimated energy error: better than 50 keV—good; better than 100 keV—acceptable; better than 200 keV—tolerable; worse than 200 keV—bad.

TABLE IV. Energy data on quasiparticle excitations in odd-proton nuclides with $71 \leq Z \leq 75$.[aa]

Nuclide	Assigned quasiparticle state: Assignment	Energy (keV): E_{expt}	E_{qp}^{emp}	E_{qp}^{BCS}	References and comments	
$^{169}_{71}$Lu	$7/2^-$ 523	(−493)	(−490)	−494	a, b	
	$7/2^+$ 404	0	0	0	c, d	
	$1/2^-$ 541	29	120	116	c, d	*R*
$^{171}_{71}$Lu	$7/2^-$ 523	−662	−670	−681	e	
	$1/2^+$ 411	−208	−240	−250	e	*R*, (*V*)
	$7/2^+$ 404	0	0	0	e, f	
	$1/2^-$ 541	71	160	165	e, f	*R*
	$5/2^+$ 402	296	310	321	e, f	(*R*)
	$9/2^-$ 514	470	450	473	e	(*R*)
$^{173}_{71}$Lu	$1/2^+$ 411	−425	−450	−462	g	*R*, (*V*)
	$7/2^+$ 404	0	0	0	g	
	$1/2^-$ 541	128	210	228	g	*R*
	$5/2^+$ 402	357	370	391	g	(*R*)
	$3/2^-$ 532	(888)	(920)	952	b, g	*R*
$^{175}_{71}$Lu	$7/2^+$ 404	0	0	0	h, i	
	$5/2^+$ 402	343	360	349	h, i	(*R*)
	$1/2^-$ 541	358	440	426	h, i	*R*
	$9/2^-$ 514	396	380	374	j	(*R*)
$^{177}_{71}$Lu	$1/2^+$ 411	−570	−600	−621	k	*R*, (*V*)
	$7/2^+$ 404	0	0	0	k, l	*U*
	$9/2^-$ 514	150	140	154	k, l	(*R*)
	$5/2^+$ 402	458	470	489	k, l	(*R*)
$^{177}_{73}$Ta	$1/2^+$ 411	(−488)	(−520)	−504	b, m	*R*
	$9/2^-$ 514	−74	−60	−53	m, n	*R*, ab
	$7/2^+$ 404	0	(0)	0	m, n	ab
	$5/2^+$ 402	71	90	100	m, n	(*R*)
	$1/2^-$ 541	217	340	349	m, n	*R*
$^{179}_{73}$Ta	$1/2^+$ 411	−520	−550	−557	o	*R*
	$9/2^-$ 514	−31	−20	−21	o, p	*R*, ab
	$7/2^+$ 404	0	(0)	0	o, p	ab
	$5/2^+$ 402	239	250	222	o	*R*
	$1/2^-$ 541	750	870	849	o	*R*
$^{181}_{73}$Ta	$1/2^+$ 411	−615	−650	−683	q	*R*
	$9/2^-$ 514	−6	(+)3	−10	q	*U*, *R*, ab
	$7/2^+$ 404	0	(0)	0	q	*U*, ab
	$5/2^+$ 402	482	500	531	q	*R*
$^{183}_{73}$Ta	$9/2^-$ 514	−73	−80	−80	r, s	*U*, *R*, ab
	$7/2^+$ 404	0	(0)	0	r, s	*U*, ab
	$5/2^+$ 402	459	470	468	r, s	*R*
$^{181}_{75}$Re	$1/2^+$ 411	−826	−850	−840	t	*R*
	$9/2^-$ 514	−262	−240	−255	u	*R*
	$5/2^+$ 402	0	0	0	t, u	
	$1/2^-$ 541	432	520	480	t	*R*
$^{183}_{75}$Re[ac]	$1/2^+$ 411	−1102	−1130	−1094	t	*R*
	$7/2^+$ 404	−851	−830	−816	t	*R*
	$9/2^-$ 514	−496	[−500]	−457	u	*R*
	$5/2^+$ 402	0	0	0	t, u	*U*
	$3/2^+$ (402)	1035	>1300		t, v	*R*, *V*

TABLE IV (*Continued*)

Nuclide	Assigned quasiparticle state: Assignment	Energy (keV): E_{expt}	E_{qp}^{emp}	E_{qp}^{BCS}	References and comments	
$^{185}_{75}Re$[ac]	$1/2^+$ 411	−880	−910	−930	t, w, x	*R*
	$9/2^-$ 514	−387	[−400]	−424	y	*R*
	$5/2^+$ 402	0	0	0	t, w, x	*U*
	$1/2^+$ (400)	646	[900]	1007	t, w, x	*R, V*
$^{187}_{75}Re$[ac]	$(3/2^+$ 411)	−865	−(>2000)		w, z	Vibr.
	$1/2^+$ 411	−625	−720	−723	w, z	*R, V*
	$9/2^-$ 514	−206	−190	−195	w, z	*R*
	$5/2^+$ 402	0	0	0	w, z	*U*
	$1/2^+$ (400)	511	760	738	w, z	*V*
	$(3/2^+$ (402))	773	(>2000)		w, z	Vibr.

[a] Reference [69Ar23].
[b] Identification probable.
[c] Reference [61Me5].
[d] References [65Bj01, 68Sk].
[e] Reference [70Gi].
[f] Reference [66Ha23].
[g] Reference [62Va6].
[h] Reference [69Ha10].
[i] Reference [69Jo16].
[j] Reference [62Ba32].
[k] Reference [65He06].
[l] Reference [65Ma18].
[m] Reference [69Ad].
[n] References [70Sk04, 70Ba46].
[o] Reference [69Ko18].
[p] Reference [63Va28].
[q] References [70Ro, 66Al05].
[r] Reference [67Mo13].
[s] Reference [69Mc08].
[t] Reference [68Ha39].
[u] Reference [69Hj01].
[v] Not fitted.
[w] Reference [67Bi10].
[x] Reference [69Co16].
[y] Reference [68Al].
[z] Reference [65Bi07].
[aa] Notations and symbols are explained in the text (Sec. III.A.3 and IV.A).
[ab] The order of these two states might be reversed (see comments in text).
[ac] The $1/2^-$ 541 level has been identified at 702 keV in ^{183}Re, and at 1045 keV in ^{185}Re. The $11/2^-$ 505 level has been identified at 1309 keV in ^{183}Re, at 1303 keV in ^{185}Re, and tentatively at 1208 keV in ^{187}Re. [See Bunker and Reich (1971) quoting information from M. T. Lu and W. P. Alford (1970).]

IV. LEVEL DATA AND SEMIEMPIRICAL SINGLE-PARTICLE LEVEL SCHEMES

The main result of the analysis described in Sec. III consists of the central portions of the single-particle level schemes which have been subject to variation. Before presenting this result graphically in Sec. IV.B, we tabulate in Sec. IV.A the compilation of the level data used. Brief comments on certain details of the data and the results are given in Sec. IV.C.

The pairing force constant, G, and the NBCS parameters[28], Δ_*, λ_*, have been determined and calculated as described in Sec. III.C. The values of G which we have obtained according to the rough criterion Eq. (3.25), using the resulting single-particle levels (Sec. IV.B), are shown in Fig. 4. We note that the behavior of our G_n and G_p values, within the region considered, does not agree with the usually adopted $(1/A)$ dependence. It also appears that no simple isospin dependence of G is substantiated [cf. Nilsson *et al.* (1969)]. It would be of little interest here to fit the points shown in Fig. 4 by an expression[14,17] containing τ_3 and powers of $A^{-1/3}$ and $(N-Z)/A$. It should also be noted that a comparison between our G values and those used for somewhat different purposes by other authors, e.g., by Nilsson *et al.* (1969), Lamm (1969), and Nilsson (1969), is obscured because of the different single-particle level schemes used; ours containing a bias through the built-in variations with the nucleon numbers.

The precision to which we fulfill Eq. (3.25) is illustrated by Fig. 5 (odd-proton cases) and Fig. 6 (odd-neutron cases). The experimental odd–even mass differences, $P^{(p)}$ and $P^{(n)}$, have been taken from Prior, Boehm, and Nilsson (1968) (supplemented by Lamm, 1969), and the "gap parameters",[28] $\Delta_*{}^{(p)}$ and $\Delta_*{}^{(n)}$, have been calculated with the G values of Fig. 4. Naturally, the approximate nature of the relationship between Δ_* and P makes a precise fit pointless.

A. The Band-Head Level Data

We have compiled the available band-head energy[3] data for excitations of primarily one-quasiparticle[5] type in the region $150<A<190$. We have restricted ourselves to a selection of such levels where the cylindrical classification,[23] Eq. (2.25), appropriate to eigenstates of the single-particle model for nonspherical nuclei, is considered established or probable for the predominant component of the state. It should be pointed out that the classification of one-quasiparticle states is exactly the same as for the single-particle states (see Appendix C), and that the admixtures discussed in Sec. III.B do not violate the classification. Details on how the classification is made from the data in individual cases are discussed by Bunker and Reich (1971), whom we

TABLE V. Energy data on quasiparticle excitations in odd-neutron nuclides with $91 \leq N \leq 95$[aa]

	Assigned quasiparticle state					
		Energy (keV)				
Nuclide	Assignment	E_{expt}	E_{qp}^{emp}	E_{qp}^{BCS}	References and comments	
$^{153}Sm_{91}$	$1/2^+$ (400)	−415	[−400]	−390	a, b	*C*, (*V*)
	$3/2^+$ (402)	−321	[−300]	−289	a, b	*C*, (*V*)
	$3/2^-$ 532	−127	−120	−107	b	
	$11/2^-$ 505	−98	[−40]	−35	a	*R*, ab
	$3/2^+$ (651)	0	(0)	0	a, b, c	ab
	$3/2^-$ 521	36	30	50	b	ab
	$1/2^-$ 521	696	[900]	883	a, b, c	*V*
$^{155}Gd_{91}$	$1/2^-$ 530	−423	[−700]	−640	d	*V*
	$1/2^+$ (400)	−368	[−800]	−826	d, e	*V*
	$3/2^+$ (402)	−269	[−700]	−657	d, e	*V*
	$11/2^-$ 505	−122	[−70]	−64	d, f	*R*, ab
	$3/2^-$ 521	0	(0)	0	d, f	ab
	$3/2^+$ (651)	105	120	120	d, f, g	ab
	$5/2^+$ 642	(267)	(220)	215	e, h	
	$5/2^-$ 523	(321)	(320)	316	d, h	
	$1/2^-$ 521	556	[1000]	946	d	*V*
$^{157}Dy_{91}$	$11/2^-$ 505	−199	[−150]	−144	i, j	*R*, ab
	$3/2^-$ 521	0	(0)	0	i, j	ab
	$5/2^-$ 523	344	330	338	i	(*R*)
$^{155}Sm_{93}$	$3/2^-$ 521	0	0	0	a, c	
	$5/2^+$ 642	≈18	≈20	34	a, k	
	$5/2^-$ 523	(427)	(420)	442	a	(*R*)
	$1/2^-$ 521	821	[1200]	1160	a, c	(vibr.)
$^{157}Gd_{93}$	$1/2^-$ 530	(−782)	(−800)	−780	d	
	$3/2^-$ 532	(−700)	(−700)	−673	d	
	$1/2^+$ (400)	(−684)	(−700)	−724	d, l	(*R*)
	$3/2^+$ (402)	(−475)	(−480)	−457	d, l	(*R*)
	$11/2^-$ 505	−426	[−400]	−378	d	*R*
	$3/2^-$ 521	0	0	0	d	
	$5/2^+$ 642	63	60	50	d	
	$5/2^-$ 523	435	420	374	d	(*R*)
	$1/2^-$ 521	704	[1200]	1069	d	(Vibr.)
$^{159}Dy_{93}$	$11/2^-$ 505	−354	[−300]	−329	i, m	*R*
	$3/2^-$ 521	0	0	0	i, m, n	
	$5/2^+$ 642	178	180	148	i, m, n	
	$5/2^-$ 523	310	300	302	i, n	(*R*)
	(1/2⁻ 521)	(538)	(1400)		i, o	Vibr.
$^{161}Er_{93}$	$1/2^+$ (660)	(≈−400)	(≈−550)	−591	p, q, r	
	$11/2^-$ 505	−396	[−350]	−370	p, q, r	*R*
	$3/2^-$ 521	0	0	0	p, q, r	
	$5/2^-$ 523	172	160	117	p, q, r	(*R*)
$^{159}Gd_{95}$	$1/2^-$ 530	(≈−1100)	(≈−1100)	−1079	d	*V*
	$3/2^-$ 532	(−1109)	(−1110)	−1107	d	
	$1/2^+$ (400)	(−973)	(−1000)	−987	d	(*R*), *V*
	$1/2^+$ (660)	−780	−920	−922	d	(*R*)
	$3/2^+$ (402)	−743	−740	−741	d, s	
	$11/2^-$ 505	−681	[−650]	−643	d	*R*
	$5/2^+$ 642	−68	−70	−76	d, s	
	$3/2^-$ 521	0	0	0	d, s	
	$5/2^-$ 523	146	130	152	d, s	
	$1/2^-$ 521	507	[1100]	1108	d	(Vibr.)
	$7/2^+$ 633	(733)	(720)	705	s	(*R*)
	$5/2^-$ 512	873	870	882	d, s	

TABLE V (*Continued*)

Nuclide	Assigned quasiparticle state: Assignment	Energy (keV): E_{expt}	E_{qp}^{emp}	E_{qp}^{BCS}	References and comments	
$^{161}Dy_{95}$	$3/2^+$ (651)	−551	−550	−555	i, t	(*R*)
	$3/2^-$ 521	−75	−70	−71	i, t	
	$5/2^+$ 642	0	0	0	i, t	
	$5/2^-$ 523	26	10	8	i, t	
	$1/2^-$ 521	367	[1100]	1083	i, t	*V*
	$5/2^-$ 512	799	786	816	i	
$^{163}Er_{95}$	$1/2^+$ (400)	(−541)	(−570)	−591	q	(*R*)
	$3/2^+$ (402)	(−463)	(−480)	−507	q	(*R*)
	$11/2^-$ 505	−444	[−400]	−424	q, r	*R*
	$3/2^-$ 521	−104	−120	−135	q, r	
	$5/2^-$ 523	0	0	0	q, r	
	$5/2^+$ 642	(69)	(90)	109	q, r	*C*
	$1/2^-$ 521	346	[800]	893	q	(*R*), *V*
	$5/2^-$ 512	609	610	658	q, u	
	$1/2^-$ 510	1074	[900]	965	q	(*R*), (Vibr.)

[a] Reference [69Tj].
[b] References [69Sm04, 68Sh].
[c] Reference [65Ke09].
[d] Reference [67Tj01].
[e] Reference [69Me].
[f] Reference [70Lφ].
[g] Complicated structure.
[h] Nature of state not well established.
[i] Reference [67Be].
[j] Reference [70Bo02].
[k] Extrapolated energy.
[l] Relative positions of $1/2^+$ and $3/2^+$ not established.
[m] Reference [68Bo18].
[n] Reference [66Gr25].
[o] Not fitted.
[p] Reference [69Ha12].
[q] Reference [69Tj01].
[r] Reference [70Hj].
[s] Reference [69Ke10].
[t] Reference [66Fu07].
[u] Reference [69Gr].
[aa] Notations and symbols are explained in the text (Sec. III.A.3 and IV.A). The extracted energies, E_{qp}^{emp}, in this table should be considered essentially qualitative (see Sec. IV.C.2).
[ab] These states could appear in different order (see Version II).

essentially follow in our selection of data. For further information we refer the reader to the bibliography for level data given in Appendix D.

The compilation is presented in Tables III and IV (odd-proton levels) and Tables V–VII (odd-neutron levels). In Columns 3–5, we give the following excitation energies (see definitions in Sec. III.A): the experimental band-head energies (E_{expt}); the extracted quasiparticle energies (E_{qp}^{emp}) in Version I [see Eq. (3.15)], evaluated from data as described in Sec. III.B; and the calculated quasiparticle energies (E_{qp}^{BCS}), obtained from the final BCS fit (Sec. III.C). In all three columns, the hole excitations are distinguished by a minus sign.

In Column 6, the lower case letters refer to the footnotes which contain certain comments and literature references. For each level there is given at least one reference for the experimental information, as listed in Appendix D (the notation for the references is explained there). As a rule, we have chosen to include the most recent and/or the most complete source of information known to us. More complete references for each case are furnished by Bunker and Reich (1971).

The capitalized comments in Column 6 refer to the various uncertainties which we estimate or anticipate.[32] By comparison of the Version I and Version II treatments [see Eq. (3.15)], we estimate the possible error of E_{qp}^{emp} due to the rotational term. The symbol (*R*) denotes an uncertainty roughly between 50 and 100 keV, while *R* denotes that it is larger than 100 keV. If the rotational correction is large enough to possibly reorder two or more levels, including the Fermi level (see discussion at the end of Sec. III.B.1), we indicate the affected levels by the Footnote ab, and set the quasiparticle ground state within parentheses in Column 4. The cases in which a vibrational correction has been estimated and applied, as described in Sec. III.B.2, are usually denoted by the letter *V*. If a small vibrational correction is expected, but is either not applied or considered very uncertain, the symbol (*V*) is used. The comment "(Vibr.)" means that we have included the state as if it were mainly of one-quasiparticle nature, although this might be in doubt. The comment "Vibr." means that the state is probably mainly vibrational (we then also set the entire assignment in Column 2 in parentheses). By the letter *U*, we indicate the cases where the BCS blocking solution fails to converge and we consequently set $\Delta_k=0$ (see Sec. III.D). In a few cases, we have used the letter *C* to indicate the possible presence of an appreciable, but unevaluated, correction due to Coriolis coupling (see Sec. III.B.1).

In Columns 3 and 4, the energy values in parentheses indicate that the identification of the state is not considered certain (footnotes may furnish further in-

TABLE VI. Energy data on quasiparticle excitations in odd-neutron nuclides with $97 \leq N \leq 103$.[aa]

Nuclide	Assigned quasiparticle state: Assignment	Energy (keV): E_{expt}	E_{qp}^{emp}	E_{qp}^{BCS}	References and comments	
$^{161}Gd_{97}$	3/2⁻ 521	−313	−320	−375	a	
	5/2⁻ 523	0	0	0	a	
	1/2⁻ 521	356	[800]	865	a	(*R*), *V*
	7/2⁺ 633	446	450	498	a, b	
	5/2⁻ 512	809	810	845	a	
	1/2⁻ 510	1309	[1200]	1231	a	*R*, (Vibr.)
	1/2⁺ 651	(1489)	(1510)		a, c	(*R*)
$^{163}Dy_{97}$	3/2⁺ (651)	−859	[−1100]	−1123	d	*V*
	3/2⁻ 521	−422	−430	−446	d	
	5/2⁺ 642	−251	−270	−288	d	
	5/2⁻ 523	0	0	0	d	
	1/2⁻ 521	351	[800]	800	d	(*R*), *V*
	5/2⁻ 512	719	720	712	d, e	
	1/2⁻ 510	(1159)	(1160)	1143	e, f	(*R*), *V*
$^{165}Er_{97}$	1/2⁺ (400)	(−746)	(−770)		c, g, h	*R*
	11/2⁻ 505	(−551)	(−520)		c, i	*R*
	3/2⁺ (402)	(−534)	(−550)		c, g	(*R*)
	1/2⁺ (660)	(−507)	(−500)		c, g, j	*C*, (*R*), *V*
	3/2⁻ 521	−243	−260	−251	g, h, i, j	
	5/2⁺ 642	−47	−60	−63	h, i, j	*C*
	5/2⁻ 523	0	0	0	g, h, i, j	
	1/2⁻ 521	297	[550]	511	g, h, j	(*R*), *V*
	5/2⁻ 512	478	490	437	b, g, h	
	1/2⁻ 510	920	[1100]	1028	g, j	*R*, (Vibr.)
$^{167}Yb_{97}$	3/2⁻ 521	−187	−200	−219	k	(*R*)
	5/2⁺ 642	−30	−40	−38	k, l	*C*
	5/2⁻ 523	0	0	0	k, l	
	1/2⁻ 521	212	[≈500]	509	k	(*R*), (Vibr.)
$^{165}Dy_{99}$	3/2⁻ 521	−574	−680	−647	m, n, o	(*R*), *V*
	5/2⁻ 523	−533	−540	−516	m, n, o	(*R*)
	7/2⁺ 633	0	0	0	m, n, o	
	1/2⁻ 521	108	140	155	m, n, o	*R*
	5/2⁻ 512	184	190	205	m, n, o	
	1/2⁻ 510	570	[1400]	1328	m, n, o	*R*, (Vibr.)
$^{167}Er_{99}$	1/2⁺ (400)	(−1135)	(−1140)		c, f, g	(*R*)
	3/2⁺ (402)	(−1086)	(−1090)		c, f, g	(*R*)
	5/2⁺ 642	−812	−800	−840	f, g	(*R*), (*V*)
	3/2⁻ 521	−753	−800	−786	g, p, q	(*R*), *V*
	5/2⁻ 523	−668	−670	−662	g, p, q	
	7/2⁺ 633	0	0	0	g, p, q	
	1/2⁻ 521	208	240	269	g, p, q	*R*
	5/2⁻ 512	346	350	350	g, p, q	
	1/2⁻ 510	763	[1200]	1245	g, q, r	*R*, (Vibr.)
	3/2⁻ 512	1384	[1400]	1530	g, q	(*R*), (*V*)
$^{169}Yb_{99}$	3/2⁻ 521	−660	−720	−709	k, s	(*R*), *V*
	5/2⁺ 642	−584	−860	−843	k	(*R*), *V*
	5/2⁻ 523	−570	≈−600	−568	k, s	(*V*)
	7/2⁺ 633	0	0	0	k, s	
	1/2⁻ 521	24	60	68	k, s	(*R*)
	5/2⁻ 512	191	190	191	k, s	
	1/2⁻ 510	813	[1400]	1412	s	*R*, (Vibr.)
	7/2⁻ 514	(960)	(950)	962	s	

TABLE VI (*Continued*)

Nuclide	Assigned quasiparticle state: Assignment	Energy (keV): E_{expt}	E_{qp}^{emp}	E_{qp}^{BCS}	References and comments	
$^{169}Er_{101}$	$5/2^-$ 523	−850	[−1600]	−1665	g, r, t	*R*, (Vibr.)
	$3/2^-$ 521	−714	[−900]	−970	g, t	(Vibr.)
	$7/2^+$ 633	−244	−210	−204	g, r, t	*R*
	$1/2^-$ 521	0	(0)	0	g, r, t	ab
	$5/2^-$ 512	92	60	80	g, r, t	(*R*), ab
	$1/2^-$ 510	562	[1200]	1241	g, t	*R*, (Vibr.)
	$7/2^-$ 514	(823)	(780)	822	g, t, u	*R*
	$(3/2^-$ 512)	1082	[1400]	1431	g, t	Vibr.
$^{171}Yb_{101}$[ac]	$(3/2^-$ 521)	−902	−(>2000)		c, k	Vibr.
	$7/2^+$ 633	−95	−60	−59	k, v	(*R*), ab
	$1/2^-$ 521	0	(0)	0	k, v	ab
	$5/2^-$ 512	122	90	127	k, v	(*R*)
	$7/2^-$ 514	835	790	771	k, v	*R*
	$1/2^-$ 510	≈945	[1300]	1282	k	(Vibr)
$^{173}Hf_{101}$	$7/2^+$ 633	−165	−140	−131	w	(*R*)
	$1/2^-$ 521	0	(0)	0	w	ab
	$5/2^-$ 512	107	70	113	w	(*R*), ab
$^{171}Er_{103}$	$1/2^-$ 521	−195	−230	−212	g, r	(*R*)
	$5/2^-$ 512	0	0	0	g, r	*U*
	$9/2^+$ 624	(378)	(370)	370	g, u	(*R*)
	$7/2^-$ 514	(531)	(510)	525	g, u	(*R*)
	$1/2^-$ 510	706	[900]	943	g, r	(*R*), (Vibr.)
	$3/2^-$ 512	(906)	(910)	916	g	(*R*)
$^{173}Yb_{103}$	$3/2^-$ 521	(−1224)	(−1200)	−1260	k, u	(*R*), (Vibr.)
	$1/2^-$ 521	−399	−430	−457	k	(*R*)
	$7/2^+$ 633	−351	−360	−363	k, x	
	$5/2^-$ 512	0	0	0	k, x	*U*
	$7/2^-$ 514	637	620	636	k, x	
	$1/2^-$ 510	1031	1170	1189	k	*V*
	$3/2^-$ 512	(1340)	(1330)	1350	k, u	(*R*)
$^{175}Hf_{103}$	$7/2^+$ 633	−207	−210	−178	y	(*R*)
	$1/2^-$ 521	−126	−160	−134	y	(*R*)
	$5/2^-$ 512	0	0	0	y	*U*
	$7/2^-$ 514	348	330	315	y	*R*

[a] Reference [67Tj01].
[b] Evaluated position.
[c] Not fitted.
[d] Reference [67Sc05].
[e] Reference [69Gr].
[f] Collective corrections not applied to this level.
[g] Reference [69Tj01].
[h] Reference [68Ku14].
[i] Reference [70Hj].
[j] Reference [68Ku02].
[k] Reference [66Bu16].
[l] Reference [65Gr20].
[m] Reference [67Du05].
[n] Reference [67Bo31].
[o] Reference [67Ma25].
[p] Reference [65Ko13].
[q] Reference [70Mi01].
[r] Reference [68Ha10].
[s] Reference [68Sh12].
[t] Reference [70Mu].
[u] Identification of level probable.
[v] Reference [69Ba38].
[w] Reference [68Ha39].
[x] Reference [59Bi11].
[y] Reference [60Ha18].
[aa] Notations and symbols are explained in the text (Sec. III.A.3 and IV.A).
[ab] The order of these two levels could be reversed (see discussion in text).
[ac] The level $9/2^+$ 624 in ^{171}Yb has been established at 935 keV. See [69Ba38].

formation). Uncertainties in the position of an experimental level—e.g., if members of a rotational band have been observed but not the band head[3]—are also pointed out. In Column 4 we set within brackets such values of E_{qp}^{emp} which for any reason are considered to have large uncertainties (especially in connection with *V* and *R* as mentioned above). This is done if the estimated uncertainty is larger than 200 keV, and also in a few other cases, such as, e.g., if there is expected to be a fairly large, but unknown, vibrational correction

TABLE VII. Energy data on quasiparticle excitations in odd-neutron nuclides with $105 \leq N \leq 111$.[aa]

Nuclide	Assigned quasiparticle state: Assignment	Energy (keV): E_{expt}	E_{qp}^{emp}	E_{qp}^{BCS}	References and comments	
$^{175}Yb_{105}$	$3/2^-$ 521	(−1620)	(−1650)	−1666	a, b	*R*, (Vibr.)
	$7/2^+$ 633	≈−1000	[≈−1000]	−1047	a	
	$1/2^-$ 521	−919	−960	−1001	a, b	*R*
	$5/2^-$ 512	−639	−650	−680	a, b	(*R*)
	$7/2^-$ 514	0	0	0	a, b	*U*
	$9/2^+$ 624	265	260	284	a, b	(*R*)
	$1/2^-$ 510	514	550	608	a, b	*R*
	($3/2^-$ 512)	811	[1400]	1466	a, b	*R*, Vibr.
$^{177}Hf_{105}$	$7/2^+$ 633	−746	−760	−744	c	(*R*)
	$1/2^-$ 521	−560	−600	−600	d	*R*
	$5/2^-$ 512	−509	−520	−520	c, d	(*R*)
	$7/2^-$ 514	0	0	0	c, d, e	*U*
	$9/2^+$ 624	321	320	337	c, d, e	
	$1/2^-$ 510	≈590	[≈700]	716	d, f	*R*, *V*
	($3/2^-$ 512)	804	[1200]	1135	d	*R*, Vibr.
	$7/2^-$ 503	1058	1050	1022	c, d	(*R*)
$^{179}W_{105}$	$7/2^+$ 633	−477	−490	−500	g	
	$5/2^-$ 512	−430	−440	−447	g, h	(*R*)
	$1/2^-$ 521	−222	−270	−244	g, h	*R*
	$7/2^-$ 514	0	0	0	g, h	
	$9/2^+$ 624	309	310	331	g, h	(*R*)
	$1/2^-$ 510	(≈630)	(≈700)	690	g, h, i	*R*
$^{177}Yb_{107}$	$7/2^-$ 514	−104	−110	−116	a, j	*R*
	$9/2^+$ 624	0	0	0	a, j	*U*
	$1/2^-$ 510	333	[400]	380	a, j	*R*
	$3/2^-$ 512	709	960	967	a, j	*R*, *V*
	$7/2^-$ 503	(1226)	(1220)	1222	a, j	(*R*)
	$3/2^-$ 501	(1365)	(1390)	1404	a, j	*R*
$^{179}Hf_{107}$	$1/2^-$ 521	−614	[−700]	−696	d, k	*R*
	$5/2^-$ 512	−518	−530	−563	d, k	*R*
	$7/2^-$ 514	−214	−220	−259	d, k	(*R*)
	$9/2^+$ 624	0	0	0	d, k	*U*
	$1/2^-$ 510	375	[400]	483	d, k	*R*
	$3/2^-$ 512	720	750	794	d, k	*R*
	$7/2^-$ 503	872	870	914	d, k	(*R*)
$^{181}W_{107}$	$1/2^+$ (660)	(−1364)	(−1360)		f, h, l, m	*R*
	$7/2^+$ 633	−953	[−950]	−961	h, l	
	$7/2^-$ 514	−409	−410	−428	h, n	*R*
	$1/2^-$ 521	−385	−400	−455	h, l	(*R*)
	$5/2^-$ 512	−365	−370	−393	h, n	*R*
	$9/2^+$ 624	0	0	0	h, n	*U*
	$1/2^-$ 510	458	[500]	511	h	*R*
	$7/2^-$ 503	662	660	669	h	(*R*)
	$3/2^-$ 512	726	750	777	h	*R*
$^{183}Os_{107}$	$9/2^+$ 624	0	0	0	o	(*R*)
	$1/2^-$ 510	171	[200]	234	o	*R*
$^{181}Hf_{109}$	$9/2^+$ 624	(−68)	(−30)	−25	d, p	*R*
	$1/2^-$ 510	0	0	0	d	
	$3/2^-$ 512	255	230	251	d	
	$7/2^-$ 503	670	620	605	d	*R*
	$3/2^-$ 501	(1063)	(1040)	1060	d	
	$13/2^+$ 606	(1729)	(≈1700)		d, q	*R*, *V*

TABLE VII (*Continued*)

Nuclide	Assigned quasiparticle state: Assignment	Energy (keV): E_{expt}	E_{qp}^{emp}	E_{qp}^{BCS}	References and comments	
$^{183}W_{109}$	1/2+ (660)	(−1794)	(−1800)		f, h, l, q	
	7/2− 514	−1072	[−1100]	−1044	h, l	*R*
	7/2+ 633	(−985)	(−1000)	−967	f, h, l	*R*
	1/2− 521	−936	[−900]	−904	h, l	
	5/2− 512	−906	[−900]	−840	h, l	(*R*)
	9/2+ 624	−623	[−600]	−587	h, r, s	*R*
	1/2− 510	0	(0)	0	h, r, s	*U*, ab
	3/2− 512	209	190	209	h, r, s	ab
	11/2+ 615	309	[200]	249	h, r, s	*R*, ab
	7/2− 503	453	400	426	h, r, s, t	*R*
	9/2− 505	(1390)	(1400)	1410	h, l	*R*
$^{185}Os_{109}$[ac]	1/2− 510	0	0	0	u	
	3/2− 512	128	110	111	u	
	7/2− 503	(352)	(300)	277	u, v	*R*
	11/2+ 615	717	[600]	579	u	*R*
$^{185}W_{111}$	1/2+ (660)	(−2059)	(−2100)		f, h, l, q	
	7/2− 514	−1058	[−1100]	−1031	h, l	*R*, (*V*)
	1/2− 521	≈−1010	[≈−1000]	−985	h, l	(*V*)
	7/2+ 633	(−966)	(−1000)	−939	f, h, l	(*R*)
	5/2− 512	−888	[−900]	−949	h, l	
	9/2+ 624	−716	[−700]	−713	h, l	*R*
	1/2− 510	−24	−30	−26	h, w, x	ab
	3/2− 512	0	(0)	0	h, s, w, x	ab
	11/2+ 615	198	[100]	112	h, w, x	*R*, ab
	7/2− 503	244	200	184	h, s, x	(*R*)
	9/2− 505	≈785	[800]	774	h, l	*R*
$^{187}Os_{111}$[ac]	3/2− 512	−10	−4	−3	y	ab
	1/2− 510	0	(0)	0	y	ab
	7/2− 503	100	60	74	u, y	*R*, ab
	11/2+ 615	257	[200]	190	u, y	*R*, ab

[a] Reference [66Bu16].
[b] Reference [67Bo19].
[c] Reference [61We11].
[d] Reference [68Ri07].
[e] Reference [64Al04].
[f] Evaluated position.
[g] Reference [68Ha39].
[h] Reference [70Ca].
[i] Energy from Ref. [70Ca] adopted.
[j] Reference [63Ve09].
[k] Reference [67Ma24].
[l] Collective corrections not applied to this level.
[m] Not fitted.
[n] Reference [60Ha18].
[o] Ref. [60Ne2].
[p] Identification doubtful.
[q] Fitted only in Version II.
[r] Reference [69Ku03].
[s] Reference [65Er03].
[t] Reference [67Ma28].
[u] Reference [69Fo].
[v] Identification of level probable.
[w] Reference [69Da01].
[x] References [69So, 69Ku07].
[y] Reference [62Ha24].
[aa] Notations and symbols are explained in the text (Sec. III.A.3 and IV.A).
[ab] The order of these single-particle levels can be exchanged (see Version II).
[ac] See also Bunker and Reich (1971).

to the level. Comparison between Columns 4 and 5 shows the actual precision of the BCS fit to the data for each case (cf. Sec. III.C).[32] Several uncertain cases have not been fitted, and other cases have only been fitted in Version II—see the comments and footnotes.

We have supplemented the level data compilation by a compilation of experimentally substantiated ground-state assignments in Tables VIII (odd-proton) and Table IX (odd-neutron). We include primarily cases where the ground-state spin has been measured. Tables VIII and IX cover a substantially larger set of nuclides than do Tables III–VII. By this extension, certain additional features of the level systematics, such as possible level crossings, which have a place in our discussion (see Secs. IV.C and V), are brought out.

B. The Single-Particle Level Schemes from Analysis of Data

The single-particle level schemes, obtained from the analysis of data as described in Secs. III.A, III.B, and

TABLE VIII. Experimental ground state assignments for odd-proton nuclides.

Z	Nuclide	Exp[a] I	Adopted[b] assignment	Footnote
63	^{147}Eu	(5/2)	$5/2^+$	
	^{149}Eu	(5/2)	$5/2^+$	
	^{151}Eu	5/2	$5/2^+$ 413	
	^{153}Eu	5/2	$5/2^+$ 413	
	^{155}Eu	(5/2)	$5/2^+$ 413	
65	^{151}Tb	1/2	1/2	c
	^{153}Tb	5/2	$5/2^-$ 532	c
	^{155}Tb	3/2	$3/2^+$ 411	c
	^{157}Tb	(3/2)	$3/2^+$ 411	
	^{159}Tb	3/2	$3/2^+$ 411	
	^{161}Tb	3/2	$3/2^+$ 411	
	^{163}Tb	(3/2)	$3/2^+$ 411	
67	^{155}Ho	5/2	$5/2^-$ 532 or $5/2^+$ 402	d
	^{157}Ho	7/2	$7/2^-$ 523 or $7/2^+$ 404	d
	^{159}Ho	7/2	$7/2^-$ 523	d
	^{161}Ho	7/2	$7/2^-$ 523	
	^{163}Ho	(7/2)	$7/2^-$ 523	
	^{165}Ho	7/2	$7/2^-$ 523	
	^{167}Ho	(7/2)	$7/2^-$ 523	
69	^{159}Tm	5/2	$5/2^+$ 402	c
	^{161}Tm	7/2	$7/2^+$ 404	c
	^{163}Tm	1/2	$1/2^+$ 411	
	^{165}Tm	1/2	$1/2^+$ 411	
	^{167}Tm	1/2	$1/2^+$ 411	
	^{169}Tm	1/2	$1/2^+$ 411	
	^{171}Tm	1/2	$1/2^+$ 411	
71	^{169}Lu	7/2	$7/2^+$ 404	
	^{171}Lu	7/2	$7/2^+$ 404	
	^{173}Lu	(7/2)	$7/2^+$ 404	
	^{175}Lu	7/2	$7/2^+$ 404	
	^{177}Lu	7/2	$7/2^+$ 404	
	^{179}Lu	(7/2)	$7/2^+$ 404	
73	^{175}Ta	(7/2)	$7/2^+$ 404	e
	^{177}Ta	(7/2)	$7/2^+$ 404	
	^{179}Ta	(7/2)	$7/2^+$ 404	
	^{181}Ta	7/2	$7/2^+$ 404	
	^{183}Ta	7/2	$7/2^+$ 404	
75	^{181}Re	(5/2)	$5/2^+$ 402	e
	^{183}Re	(5/2)	$5/2^+$ 402	
	^{185}Re	5/2	$5/2^+$ 402	
	^{187}Re	5/2	$5/2^+$ 402	
77	^{187}Ir	(3/2)	$3/2^+$	
	^{189}Ir	(3/2)	$3/2^+$	
	^{191}Ir	3/2	$3/2^+$	
	^{193}Ir	3/2	$3/2^+$	

[a] Measured ground-state spins are quoted from Fuller and Cohen (1969) unless otherwise noted. Values in parentheses have been inferred from spectroscopic data and are quoted from Lederer, Hollander, and Perlman (1967), or the references mentioned in Footnotes b and e.
[b] Where no reference is given, the adopted assignments are from the Nuclear Data Group (1959–1965, 1966), or from Bunker and Reich (1971).
[c] Reference [70Li].
[d] Reference [69Ek01].
[e] Reference [68Ha39].

III.C, are presented graphically in Figs. 7 and 8 (proton levels), and in Figs. 9 and 10 (neutron levels). These are all based on Version I of the assumed rotational contribution[31] (see Sec. III.B). We present also, in Fig. 11, the Version II results for the odd-neutron cases $N=91$, 109, and 111, where $K=11/2$ levels play an important role. In addition to setting $\gamma(K)\approx 0.5K^2$ in Eq. (3.13) for these cases, we have rounded off most of the adopted $E_{\rm qp}^{\rm emp}$ values to 50 or 100 keV before fitting. The Version II result should be considered highly tentative. The dashed line in Figs. 7–11 connects the values of λ_* obtained from the NBCS solution in each case (see Sec. III.C.1).[28] The medium width solid lines connect the single-particle energies in general, and indicate the levels (ϵ_k) not fitted to the data. The thick lines indicate fitted levels (ϵ_K). The Fermi levels are distinguished by a cross. We note, furthermore, that the zero of the energy scale has been fixed in an arbitrary way, compatible with Tables I and II.[30]

The symbols R, V, and U in Figs. 7–11 are defined in essentially the same way as for Tables III–VII (see Sec. IV.A). However, their quantitative meaning is here somewhat different since they are applied to the single-particle levels, not to the quasiparticle excitations. Generally, they indicate that the uncertainty in the position may be larger than 100 keV. If we estimate the probable uncertainty in the determination of ϵ_K to be larger than 200 keV, we set the level within brackets.[32] The parentheses, however, have exactly the same meaning as in Tables III–VII, i.e., the experimental identification of a level with this assignment is uncertain.

The principles concerning the variation and the fitting of the central portions of the standard level schemes (Tables I and II) have been briefly described in Secs. III.A and III.C. From Figs. 7–11 we can clearly see how these principles have actually been applied. We note that there are, in some cases, appreciable parallel shifts of several levels when we pass from one sequence of isotopes (for odd Z) or isotones (for odd N) to another. This is a consequence of our choice of position for the Fermi levels (see Sec. III.B) relative to the arbitrarily fixed energy scale (cf. Tables I and II), and has little significance for the result. We also note that a few levels for which data are scarce (e.g., the proton level $1/2^-$ 541) have been varied in a regular fashion across the region, in rough agreement with general model expectations. Such model features, arising from attempts to make our approach reasonably realistic, have negligible effects on the positions of the actually fitted single-particle levels.

For each nuclide, a BCS blocking calculation[9] (Sec. III.B.1) with the G value taken from Fig. 4, and with the single-particle levels taken from Figs. 7–10 (for the central levels) and from Tables I and II (for the peripheral[29] levels), will reproduce the quasiparticle energies, $E_{\rm qp}^{\rm BCS}$, given in Tables III–VII. For simpler calculations using NBCS, the values of Δ_* and

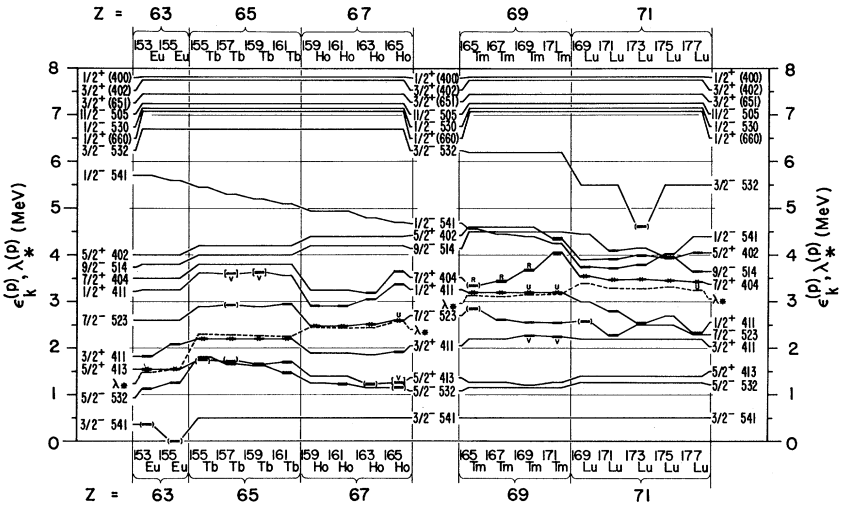

FIG. 7. The central portions of the single-proton level schemes, resulting from our analysis and BCS fit, for the region $63 \leq Z \leq 71$ (Version I analysis only). Values of the parameter[28] $\lambda_*^{(p)}$, resulting from the NBCS calculations are also included. (The zero for the energy scale[30] is the same as in Table I. Notations are explained in Sec. IV.B of the text.)

TABLE IX. Experimental ground-state assignments for odd-neutron nuclides.

N	Nuclide	Exp[a] I	Adopted[b] assignment	Footnote
87	^{147}Nd	5/2	$5/2^-$	
	^{149}Sm	7/2	$7/2^-$	
	^{151}Gd	(7/2)	$7/2^-$	
	^{153}Dy	7/2	$7/2^-$	c
89	^{149}Nd	5/2	$5/2^-$	
	^{151}Sm	(5/2, 7/2)	(5/2, 7/2)	
	^{153}Gd	3/2	$3/2^-$ 521	d
	^{155}Dy	3/2	$3/2^-$ 521 or $3/2^+$ 651	c
	^{157}Er	3/2	$3/2^-$ 521 or $3/2^+$ 651	e
91	^{153}Sm	3/2	$3/2^+$ 651	
	^{155}Gd	3/2	$3/2^-$ 521	
	^{157}Dy	3/2	$3/2^-$ 521	c
	^{159}Er	3/2	$3/2^-$ 521	e
93	^{155}Sm	3/2	$3/2^-$ 521	
	^{157}Gd	3/2	$3/2^-$ 521	
	^{159}Dy	3/2	$3/2^-$ 521	
	^{161}Er	3/2	$3/2^-$ 521	e
95	^{159}Gd	3/2	$3/2^-$ 521	
	^{161}Dy	5/2	$5/2^+$ 642	
	^{163}Er	5/2	$5/2^-$ 523	
97	^{161}Gd	(5/2)	$5/2^-$ 523	
	^{163}Dy	5/2	$5/2^-$ 523	
	^{165}Er	5/2	$5/2^-$ 523	
	^{167}Yb	(5/2)	$5/2^-$ 523	
99	^{165}Dy	7/2	$7/2^+$ 633	
	^{167}Er	7/2	$7/2^+$ 633	
	^{169}Yb	(7/2)	$7/2^+$ 633	
101	^{169}Er	1/2	$1/2^-$ 521	
	^{171}Yb	1/2	$1/2^-$ 521	
	^{173}Hf	(1/2)	$1/2^-$ 521	
103	^{171}Er	5/2	$5/2^-$ 512	
	^{173}Yb	5/2	$5/2^-$ 512	
	^{175}Hf	(5/2)	$5/2^-$ 512	
105	^{175}Yb	(7/2)	$7/2^-$ 514	
	^{177}Hf	7/2	$7/2^-$ 514	
	^{179}W	(7/2)	$7/2^-$ 514	
	^{181}Os	(7/2)	$7/2^-$ 514	f
107	^{177}Yb	(9/2)	$9/2^+$ 624	
	^{179}Hf	9/2	$9/2^+$ 624	
	^{181}W	(9/2)	$9/2^+$ 624	
	^{183}Os	(9/2)	$9/2^+$ 624	
109	^{181}Hf	(1/2)	$1/2^-$ 510	
	^{183}W	1/2	$1/2^-$ 510	
	^{185}Os	(1/2)	$1/2^-$ 510	
111	^{183}Hf	(3/2)	$3/2^-$ 512	g
	^{185}W	3/2	$3/2^-$ 512	
	^{187}Os	1/2	$1/2^-$ 510	
113	^{187}W	3/2	$3/2^-$ 512	
	^{189}Os	3/2	$3/2^-$ 512	
115	^{189}W	(7/2)	$7/2^-$ 514	h
	^{191}Os	(9/2)	$9/2^-$	

[a] Measured ground-state spins are quoted from Fuller and Cohen (1969), unless otherwise noted. Values in parentheses have been inferred from spectroscopic data and are quoted from Lederer, Hollander, and Perlman (1967), or the references mentioned in Footnotes b, f, g, and h.

[b] Where no reference is given, the adopted assignments are from the Nuclear Data Group (1959–1965, 1966) or from Bunker and Reich (1971).

[c] Reference [70Li].
[d] Reference [69An19].
[e] Reference [69Ek01].
[f] Reference [68Ha39].
[g] Reference [69Mc08].
[h] Reference [70Ca].

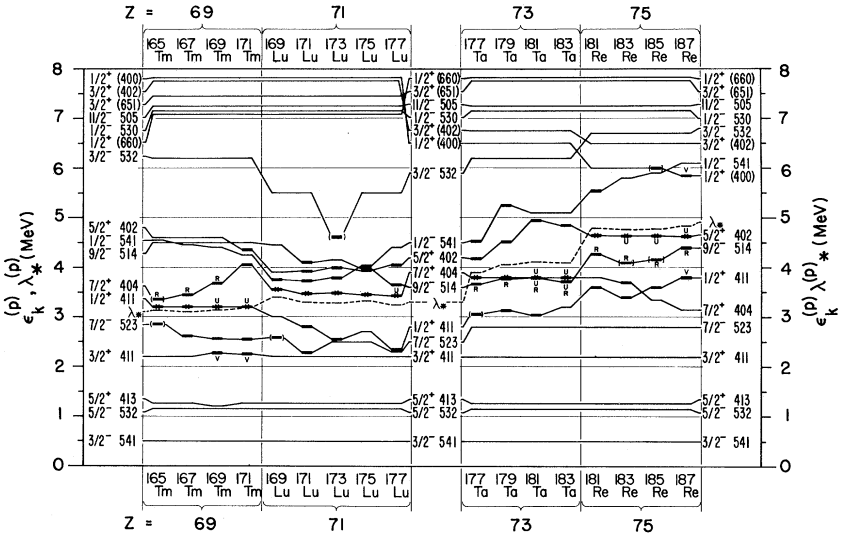

FIG. 8. The central portions of the single-proton level schemes, resulting from our analysis and BCS fit, for the region $69 \leq Z \leq 75$ (Version I analysis only). Values of the parameter[28] $\lambda_*^{(p)}$, resulting from the NBCS calculations are also included. (The zero for the energy scale[30] is the same as in Table I. Notations are explained in Sec. IV.B of the text.)

λ_* are made available in Figs. 5–11 (e.g., for estimates of the BCS amplitude parameters u_k and v_k; see Appendix C).[28] For most purposes, the accuracy obtainable from our figures or from Tables I and II should be adequate. We note that even the *fitted* levels[32] may not be determined to better than ± 100 keV relative to ϵ_F. To any potential user of our single-particle level schemes, it should furthermore be noted that we do not claim the *unfitted* single-particle levels to furnish a basis for quantitative predictions in general. Yet, we do anticipate that the qualitative picture is generally correct for the levels in the neighborhood of the Fermi surface. The proper use of the results requires that due care be taken, however. Specifically, the comparison between Version I and II shows this to be necessary.

For specific nuclides, detailed numerical information on our single-particle levels and the pairing parameters may be obtained upon request from either of the first two authors (W.O. or S.W.).

We can study the "compression" effect (Sec. III.A.1) by comparing the single-particle level spacings in Figs. 7–10 with the corresponding calculated quasiparticle excitation energies given in Column 5 of Tables III–VII. A drastic example is furnished by ^{159}Gd (Table V and Fig. 9). The spacing between the single-particle levels $5/2^-$ 523 and $3/2^-$ 521 (Fermi level) is 750 keV, compared with the quasiparticle energy which is only

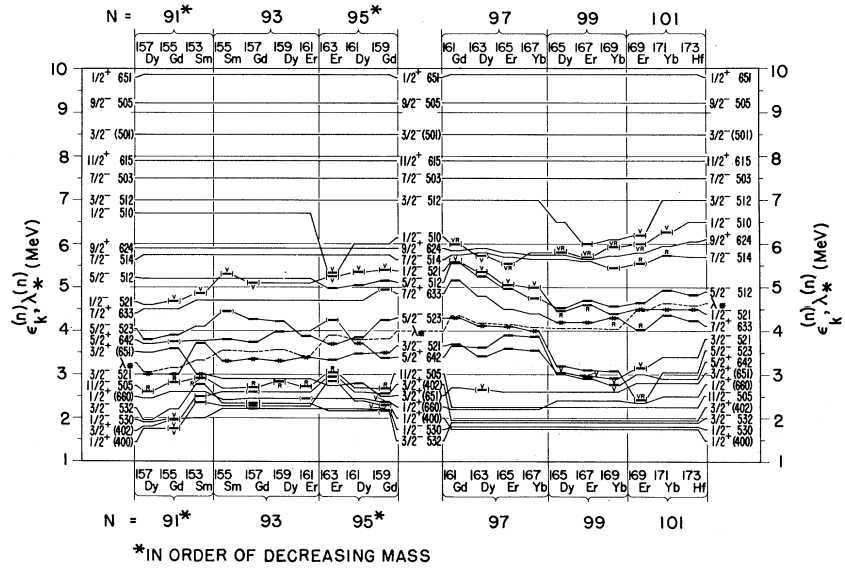

FIG. 9. The central portions of the single-neutron level schemes, resulting from our analysis and BCS fit, for the region $91 \leq N \leq 101$ (Version I analysis only). Values of the parameter[28] $\lambda_*^{(n)}$, resulting from the NBCS calculations are also included. The results for $N=91$, 93, and 95 should be considered essentially qualitative. (The zero for the energy scale[30] is the same as in Table II. Notations are explained in Sec. IV.B of the text. Isotones with $N=91$ and $N=95$ are arranged in order of decreasing A for clarity of presentation.) Note: there is no experimental evidence for the level $5/2^-$ 512 in ^{167}Yb.

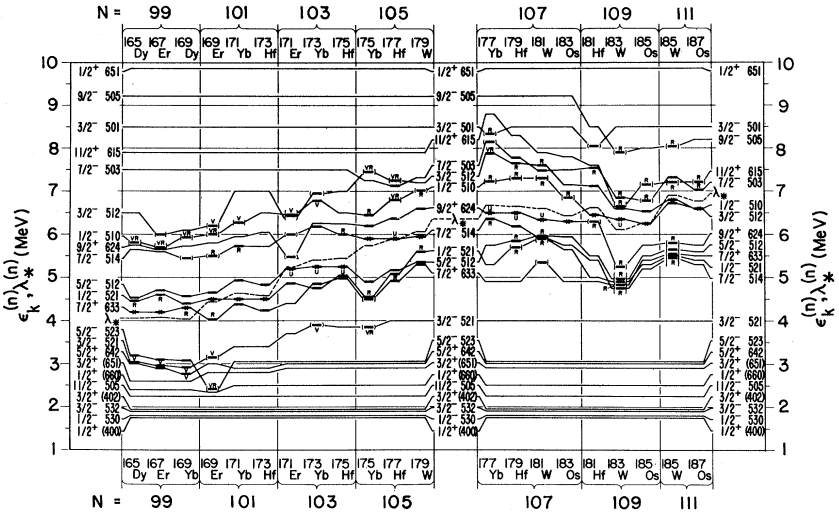

FIG. 10. The central portions of the single-neutron level schemes, resulting from our analysis and BCS fit, for the region $99 \leq N \leq 111$ (Version I analysis only). Values of the parameter[28] $\lambda_*^{(n)}$, resulting from the NBCS calculations are also included. (The zero for the energy scale[30] is the same as in Table II. Notations are explained in Sec. IV.B of the text.) Note: the level $7/2^-$ 514 in ^{175}Yb should be marked with a U.

152 keV. The other particle excitations are also strongly compressed, while the hole excitations are only slightly compressed. This skewness is related to the fact that $\lambda_* - \epsilon_F$ is here fairly large (317 keV). A similar example is furnished by ^{183}W in the Version II analysis, where, however, $\epsilon_F - \lambda_*$ is large (345 keV), and the compression is strong for the hole excitations but slight for particle excitations.

C. Comments on Data and Results

In the odd-proton case we have considered about 110 levels in 27 nuclides, and in the odd-neutron case about 220 levels in 35 nuclides. The larger average number of levels per nuclide in the neutron case is not only due to the larger level density (compare Figs. 9 and 10 with Figs. 7 and 8), but is also due to the early use of (d, p) reaction studies, which have given extensive information on quasiparticle[5] excitations in many odd-neutron nuclides.[25] However, owing to the larger level density in the neutron case, and also to the specific nature of the neutron levels encountered in the region $150 < A < 190$, the data are generally more difficult to analyze than for the odd-proton nuclides. This fact shows up here in the comparatively large number of symbols, brackets, and parentheses occurring in Tables V–VII, and Figs. 9–11, indicating uncertainties (see Secs. IV.A and B).[32]

Certain details concerning the data as well as our analysis and results for specific cases are discussed below. For further details the reader is referred to the review article by Bunker and Reich (1971). In this

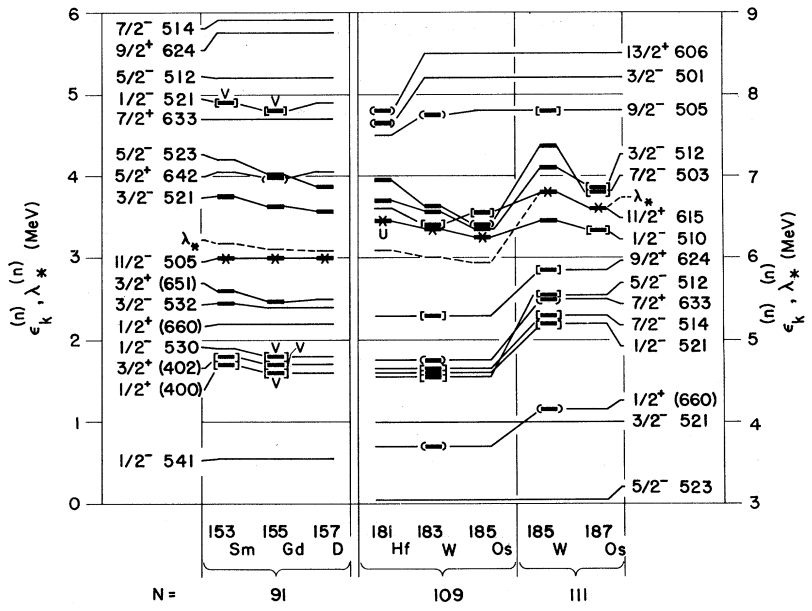

FIG. 11. Central parts of the single-neutron level schemes, resulting from our analysis and BCS fit with Version II, for $N = 91$, 109, and 111. Values of the parameter[28] $\lambda_*^{(n)}$, resulting from the NBCS calculations, are also included. The result should be considered highly tentative. (The zero for the energy scale[30] is the same as in Table II. Notations are explained in Sec. IV.B of the text.) Note: the $7/2^-$ 514 and $9/2^+$ 624 levels are reversed in the left part of the diagram.

Section, references are made to experimental work listed in our Bibliography for Level Data, Appendix D. For these we use the notations adopted in Appendix D, setting the reference in brackets.

1. The Odd-Proton Nuclides

The level data for the europium and terbium isotopes essentially covers a range of the spectrum different from that for the $Z \geq 67$ nuclides. In particular, there is little decisive information on the $1/2^+$ 411, and $7/2^-$ 523 states for these isotopes (cf. Bunker and Reich, 1971). On the other hand, for the holmium and thulium isotopes there are systematic data on the spacing between these two levels (this is why we include ^{159}Ho with only one excited quasiparticle state known). The absence of data for the $3/2^+$ 411 state in all holmium isotopes except for ^{165}Ho is noteworthy.

In ^{167}Tm, the $7/2^+$ 404 excitation has low enough energy (see Table III) that it might actually be the Fermi level [see Eqs. (3.13) and (3.14), and the discussion in Sec. III.B.1], despite the fact that $1/2^+$ 411 is the ground state. A similar statement can be made for ^{165}Tm, where the data are less certain, however. This possibility ties in very well with the systematics of measured ground-state spins for the thulium isotopes (Table VIII), in particular the recent results by Lindgren and collaborators [70Li] for ^{161}Tm and ^{159}Tm. It should be noted that the behavior of the unfitted $5/2^+$ 402 level for the thulium isotopes is probably somewhat misrepresented in our graphs (Figs. 7 and 8); a similar statement is true, e.g., about the $1/2^+$ 411 level in ^{175}Lu.

The plausible identification of the level $3/2^-$ 532 in ^{173}Lu is, to our knowledge, the only evidence for this state in the whole region (this single-particle level rises fairly steeply with decreasing deformation; see Fig. 2). From Table VIII, we see that the experimental ground-state assignment is $7/2^+$ 404 for all lutetium and tantalum isotopes for which information is available. This noteworthy feature may have alternative explanations. In Fig. 8, based on Version I, we have interpreted it as due to the crossing of the $9/2^-$ 514 and $7/2^+$ 404 levels, which is not incompatible with model expectations (see Fig. 2). However, the $9/2^-$ 514 excitation is so low in energy in all of the tantalum isotopes (see Table IV) that it might well be the actual Fermi level (see Sec. III.B.1)—in fact, this is likely to be the case for ^{181}Ta. This interpretation would give somewhat more satisfactory single-particle level systematics, considering the situation in the adjacent sequences of lutetium and rhenium isotopes.

The $1/2^+$ (400) level,[24] predicted to decrease in energy for decreasing deformation (Fig. 2), has actually been observed in ^{185}Re and ^{187}Re (see Table IV and Fig. 8). However, since $5/2^+$ 402 is the ground state, this $1/2^+$ excitation gets an appreciable γ-vibrational admixture, which makes the estimated quasiparticle energy somewhat uncertain.

2. The Odd-Neutron Nuclides

The density of single-neutron levels is particularly high in the lower central part of the spectrum (see Table II and Figs. 9–11), which is primarily of interest for the isotonic sequences $N=91$, 93, and 95. Furthermore, several $K=1/2$, 3/2, and 5/2 levels of both parities occur there, making the situation favorable for appreciable Coriolis coupling effects and vibrational admixtures. The coupling is even possibly enhanced by the presence of the interacting pairs of $N_0=4$ and 6 states,[20,22,24]

$$\begin{aligned} &1/2^+\,(400) \quad \text{and} \quad 1/2^+\,(660), \\ &3/2^+\,(402) \quad \text{and} \quad 3/2^+\,(651). \end{aligned} \tag{4.1}$$

In fact, it turns out that the experimental situation is quite complicated for the nuclides in this region, particularly for $N=91$ [see Bunker and Reich (1971)]. Our analysis for these cases is also rather tentative (cf. Table V), and the results presented for $N=91$, 93, and 95 in Fig. 9 and especially in Fig. 11 should be regarded as essentially qualitative.

It is of particular interest to compare the Version I (Fig. 9) and Version II (Fig. 11) results for $N=91$. In view of the low excitation energy of the $11/2^-$ 505 state (Table V) this might be the actual Fermi level (see discussion in Sec. III.B.1). Whether the ground state will be $3/2^+$ (651) or $3/2^-$ 521 then depends on the detailed properties and positions of these levels. We may in this way obtain an explanation of the change of ground-state assignments for $N=91$ (see Table IX) without invoking substantial level shifts (Fig. 9) (cf. the discussion in Sec. V). Furthermore, neutron-transfer reaction data for ^{155}Gd [67Tj01], indicate that $3/2^+$ (651), and possibly also $11/2^-$ 505, is mainly a hole excitation, which is compatible with the Version II result. It should also be noted that a somewhat less extreme evaluation of the precession term,[31] $\gamma(K)$, could here result in the near degeneracy of the three single-particle levels, $3/2^+$ (651), $3/2^-$ 521 and $11/2^-$ 505, the relative ordering in the experimental spectrum being then almost completely determined by the rotational contribution, E_K^{rot}.

The "partner" $3/2^+$ levels [Eq. (4.1)], identified both in ^{153}Sm and ^{155}Gd, seem to be the only instances as yet where two interacting $|\Delta N_0| = 2$ states have been well established.[22] The $1/2^+$ (400) state having been found in both nuclides, it is quite puzzling that the level $1/2^+$ (660) has not yet been observed. It is expected to have a lower excitation energy (cf. Fig. 3), estimated on the basis of Fig. 11 and Version II to be between 200 and 300 keV. The reason for its non-observation is not clear [although its (d, p) and (d, t) cross sections are expected to be small]; in fact, for ^{155}Gd the data [67Tj01 and 70Lø] seem to exclude the presence of another $1/2^+$ state below 500 keV. For the interpretation of the data for ^{155}Gd, including Coriolis coupling, we have utilized the analysis of Borggreen,

Løvhøiden, and Waddington (1969). A recent reanalysis of the neutron transfer data for ^{155}Gd, including Coriolis coupling [Kanestrøm and Tjøm (1970)], indicates that the $3/2^-$ 532 level may be at about the same energy as the $5/2^-$ 523 level at 321 keV, and mix strongly with this state.

No theoretical or experimental evidence exists for large vibrational effects in the observed hole states of ^{153}Sm. In ^{155}Gd the estimated shifts are large and also quite uncertain (see Table V).

For the $N=93$ and 95 nuclides, the information about the interacting states (4.1) is scarce, and in many cases uncertain. For $N=95$, the most noteworthy feature is the different ground-state assignments for all three isotones (Table IX). We interpret this as due to the relatively large variation of the $5/2^+$ 642 single-particle level (cf. Fig. 3) causing level crossings (Fig. 9). No contradiction with other data is found for this interpretation.

The isotonic sequences with $N=97$, 99, 101, 103, 105, and 107 are "well behaved," i.e., the interpretation of the available level data offers no appreciable difficulties, and the single-particle level schemes vary in a relatively smooth fashion (see Figs. 9 and 10, and Table IX). This region is also rich in data, particularly due to the extensive experimental investigations of the erbium and ytterbium isotopes.

The level $1/2^-$ 521, having a decreasing position with increasing A for the $N=97$ isotones (Table VI), has an appreciable vibrational admixture. For ^{167}Yb, there is little known about its structure, and the estimated value of E_{qp}^{emp} is therefore especially uncertain. We have not attempted to fit the four uncertain hole states in ^{165}Er. The $5/2^+$ 642 level in ^{165}Er and ^{167}Yb may have a relatively large Coriolis admixture, which we have, however, not taken into account. The position of the corresponding single-particle level is, therefore, perhaps more uncertain than indicated in Fig. 9.

In the $N=101$ nuclides, one of the two levels $7/2^+$ 633 or $5/2^-$ 512 has an excitation energy below, or at about, 100 keV (Table VI). It is, therefore, possible that $1/2^-$ 521 is not the Fermi level. However, our Version I interpretation leads to agreeable systematics (Figs. 9 and 10). We note also that the identification of the level $5/2^-$ 523 is quite tentative in ^{169}Er, which may be the reason for the slightly "anomalous" behavior of this single-particle level in Figs. 9 and 10.

The identification of the level $9/2^+$ 624, being established for the $N=105$ nuclides, is quite uncertain in ^{171}Er. We note the recent, still uncertain, evaluations for the position of the $1/2^-$ 510 level in ^{177}Hf (cf. Bunker and Reich, 1971) and ^{179}W [70Ca] from data. This level is well-established for the $N=107$ nuclides (we include ^{183}Os since it contributes to the systematics).

Extensive new data have recently been obtained from neutron transfer reactions for the tungsten isotopes [70Ca]. The experimental level information is included in Table VII. We have not been able to analyze in detail several of the previously unknown intrinsic states in ^{181}W, ^{183}W, and ^{185}W. As indicated in Table VII and Figs. 10 and 11, our results are tentative for many of these levels.

The situation for the isotones with $N=109$ and 111 is complicated due to the presence of the $11/2^+$ 615 state at low excitation energies. Some of the levels have been fitted only in Version II, as pointed out in Table VII. In ^{181}Hf, the identification of the levels $9/2^+$ 624 (not fitted in Version II) and $13/2^+$ 606 is uncertain, and their E_{qp}^{emp} values should be considered at most tentative.

It is again of interest to compare the Version I and II results (Figs. 10 and 11). In the $N=109$ nuclides it is possible that $1/2^-$ 510 remains the Fermi level, although it would seem possible to have $11/2^+$ 615 as the Fermi level for ^{183}W (the situation is inconclusive for ^{181}Hf). In the $N=111$ nuclides, we find an acceptable interpretation of the level systematics and ground state data (cf. Table IX) within Version II, taking $11/2^+$ 615 as the Fermi level (see Sec. III.B.1 and the above discussion of the $N=91$ nuclides). For ^{187}Os the Version II result leads to complete reordering of the single-particle levels for all four known states (see Figs. 10 and 11).

We have found that the results of the Version II analysis, although tentative and schematic, lead to a somewhat improved over-all interpretation of the data for the $N=91$, 109, and 111 isotones, if we consider both level systematics and ground state assignments. We do not claim that any of the versions, Eq. (3.15), should necessarily be correct. However, we take the result of our comparison as an empirical indication that there may, in fact, be a substantial variation of the zero-point rotational energy,[31] Eq. (3.13), in the band-head energy expression.

V. THE SINGLE-PARTICLE LEVEL SYSTEMATICS

If there are no appreciable residual effects in addition to those considered in our analysis (Sec. III), it should be appropriate to compare our resulting single-particle level schemes (Sec. IV) with results of single-particle model calculations (Sec. II).[1,7] Such a comparison should have a bearing on the validity of the model, as well as on the potential and shape parameters[6] entering into the model. In the systematics, we restrict ourselves entirely to the levels determined from a *fit* to the data. Furthermore, we confine ourselves to considering the spacings of the single-particle levels *relative* to a few well-established levels. We use the schemes presented in Figs. 7–11. For the $N=91$, 109, and 111 nuclides, we consider only the Version II results.

Single-particle level schemes calculated from potential models with varied assumptions are presented in Sec. V.A, and the systematics of semiempirical levels is presented in Sec. V.B. An over-all comparison is made in Sec. V.C, and a more detailed discussion of individual levels is given in Sec. V.D. We consider only gross

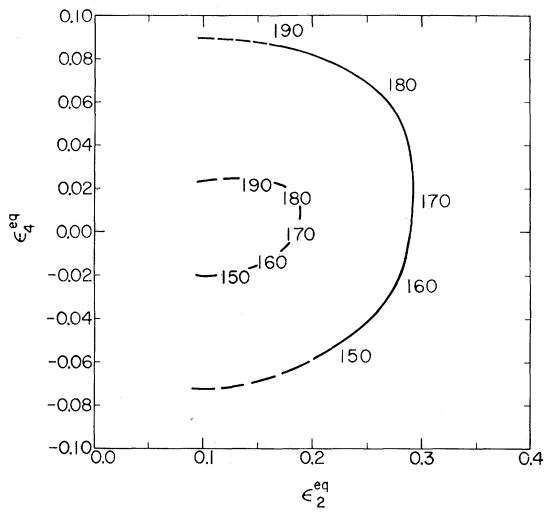

FIG. 12. Schematic graph showing the region of equilibrium spheroidal (ϵ_2^{eq}) and tetroidal (ϵ_4^{eq}) deformations[15,16] compatible with theoretical predictions and experimental evidence for nuclear shapes in the region $150<A<190$. The various nuclides are expected to be scattered between the curves as indicated roughly by the mass numbers.

features in the behavior of the single-particle levels, such as: average spacings estimated from theory and from experiment; trends in the relative positions of levels in terms of varying parameters and nucleon numbers; and level crossings (information from Tables VIII and IX may then be of interest).

For comparison with model calculations, it is relevant to know the expected equilibrium shapes[2] of the nuclear surface for nuclides in the region considered. Measurements of quadrupole moments and intraband $E2$ transition rates yield values of the "intrinsic" quadrupole moment (Q_0) which is primarily related to the quadrupole (β_2) or spheroidal (ϵ_2, η_2) deformation parameter.[15,16] A compilation of such data is given by Stelson and Grodzins (1965). Experiments with inelastic scattering of alpha particles have in addition given information about the hexadecapole (β_4) or tetroidal (ϵ_4, η_4) deformation parameter[15,16] (Hendrie *et al.*, 1968). Theoretical "equilibrium deformation" calculations, performed by various authors using varying assumptions, have in general led to good or fair agreement with the data. Both the Nilsson model and the Woods–Saxon potential (see Appendix B) have been utilized for calculating the single-particle energy contributions. The combined microscopic–macroscopic approach (according to the prescription by Strutinsky, 1967, 1968) is of particular interest, apparently being reasonably realistic and allowing moderate extrapolations along nucleon numbers. For current approaches with different schemes see Lamm (1969), Nilsson (1969), Gareev, Ivanova, and Pashkevitch (1969), and Nilsson *et al.* (1969). (An early approach was made by Bès and Szymanski, 1961).

We summarize schematically the various experimental and theoretical findings in Fig. 12. The equilibrium values of ϵ_2 and ϵ_4, compatible with data and predictions, are located between the inner and outer curves for various parts of the "rare-earth" region as roughly indicated by the mass numbers. Shapes of moderately eccentric spheroidal type (or quadrupole distortions) should predominate in the center of the region. Slightly "diamondlike" shapes are expected for lower-mass nuclides, and slightly "boxlike" shapes for higher-mass nuclides in the region (see Fig. 1).

A. Results of Potential Model Calculations

In Figs. 13 (proton) and 14 (neutron), we present the relevant parts of single-particle level schemes calculated with varied assumptions, appropriate for the region under consideration. In each figure, the graphs (a)–(c) have been computed with the current version of the Nilsson model (Gustafson *et al.*, 1967; Lamm, 1969; Nilsson, 1969; see also Appendix B),[33] while graph (d) has been obtained from the Dubna calculations with a Woods–Saxon potential (Gareev *et al.*, 1967; see also Appendix B). Furthermore, in each figure, graph (a) shows the level variation with ϵ_2 for $\epsilon_4=0$, graph (b) shows the level variation with ϵ_4 for $\epsilon_2=0.25$, graph (c) shows the possible changes of level positions for a combined variation of ϵ_2 and ϵ_4 (cf. Fig. 12), and graph (d) shows how the binding of the levels increases with mass number for $\beta_2=0.28$. Predicted effects of the ϵ_4 variation are associated primarily with the asymmetries which may be seen in Figs. 13(c) and 14(c).

In addition to the results displayed in Figs. 13 and 14, we have studied the level variations with potential and deformation parameters[6] from several other approaches (Gareev, Ivanova, and Pashkevitch, 1969; Gareev, Ivanova, and Shirikova, 1969; Bolsterli, Fiset, and Nix, 1969; Ford, Hoffman, and Rost, 1970; Ehrling and Wahlborn, 1970, 1971; cf. Figs. 2 and 3). We have found that the relative level variations with the parameters ϵ_2 and ϵ_4 (or β_2 and β_4),[15] within the restricted ranges considered (see Figs. 12–14), are generally very similar for all the various approaches. Due to the choice of potential parameters,[6] the binding energies of many levels may, however, be quite different in different schemes. This is particularly true of the relative positions of levels having different values of the quantum number N_0 [Eq. (2.25)], especially those which are sensitive to the spin–orbit coupling term (see Sec. II). A notable example is the $N_0=6$ levels[20] which originate in the $1i_{13/2}$ shell model state. Comparison of the results shown in the various graphs of Figs. 2, 3, 13, and 14 gives an idea of the possible variations involved. When a level spacing depends in a characteristic way on a

[33] The Nilsson model calculations (see Appendix B.3) utilized in the text of this review have been made with the computer program of Ehrling (1969).

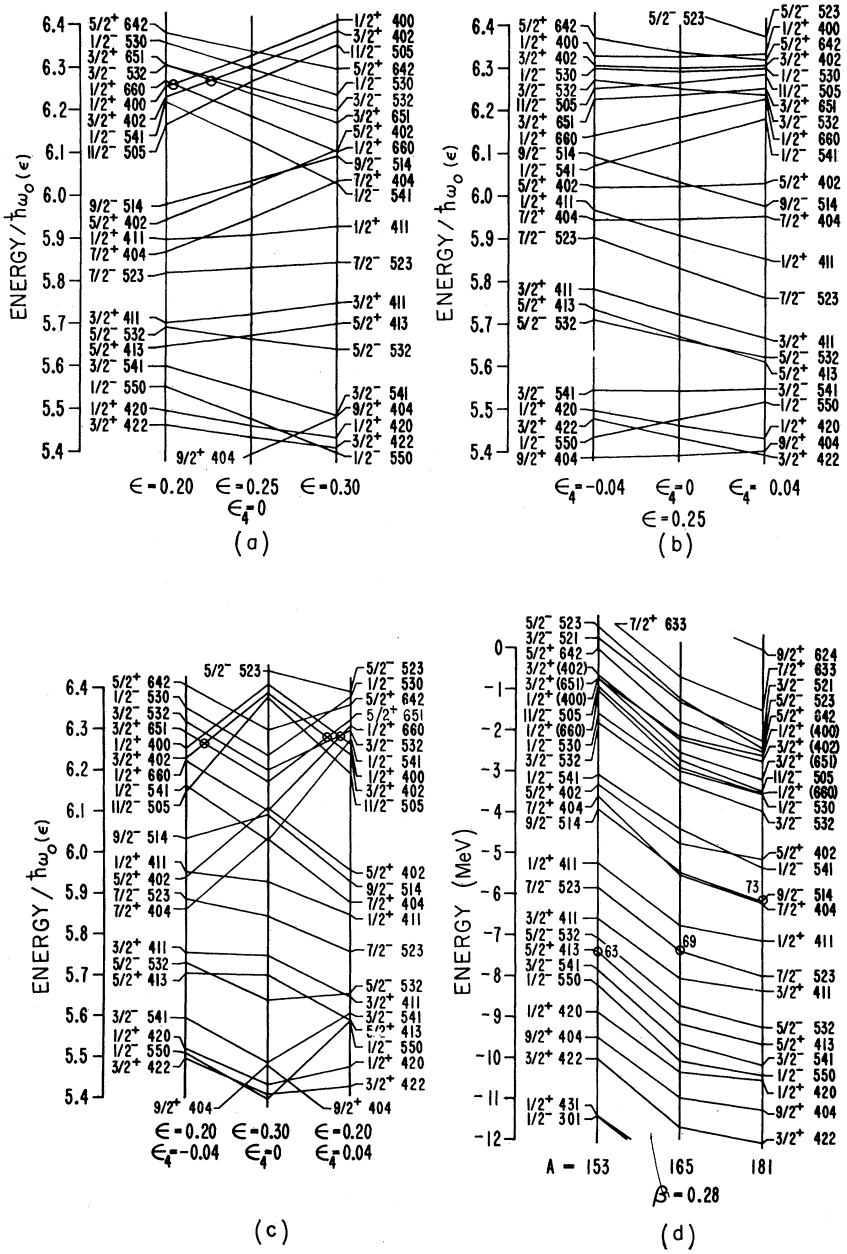

FIG. 13 (a) and (b). Results of Nilsson model calculations for single-proton levels, with varying spheroidal (ϵ_2) or tetroidal (ϵ_4) deformation.[16] (Rings indicate intersecting[21] $|\Delta N_0|=2$ levels having equal K^π. (c) and (d). Results of Nilsson model calculations with simultaneously varying ϵ_2 and ϵ_4 (c), and of deformed Woods-Saxon potential calculations (d), for single-proton levels. [In graph (c), the rings indicate intersection, as in graphs (a) and (b). In graph (d), the predicted position of the Fermi level is indicated for certain Z values.] See Sec. V.A for further comments. ($\epsilon \equiv \epsilon_2$, $\beta \equiv \beta_2$ here.)

potential or shape parameter, the data may furnish information on this parameter.

As the discussion will show, the set of parameters used appears sufficient to find a satisfactory interpretation of the available level systematics. No apparent need exists for considering deviation from axial symmetry or for introducing a nonlocal potential, e.g., in the effective-mass approximation.

B. Systematics of Relative Level Positions

From Figs. 7 and 8, we see that the single-proton levels $1/2^+$ 411 and $7/2^+$ 404 have been determined by fitting in a comparatively large number of cases. From Fig. 13, we see that these levels vary in quite different ways with the deformation parameters. It is, therefore, of interest to study the variations of other fitted single-proton levels relative to $1/2^+$ 411 and $7/2^+$ 404. These systematics are presented in Figs. 15 and 16, respectively.

For the single-neutron levels (Figs. 9–11), the situation is less clearcut. In the lower- and medium-mass part of the region, the levels $3/2^-$ 521 and $1/2^-$ 521 are frequently known, and their predicted deformation variations are roughly "parallel" (Fig. 14). In the

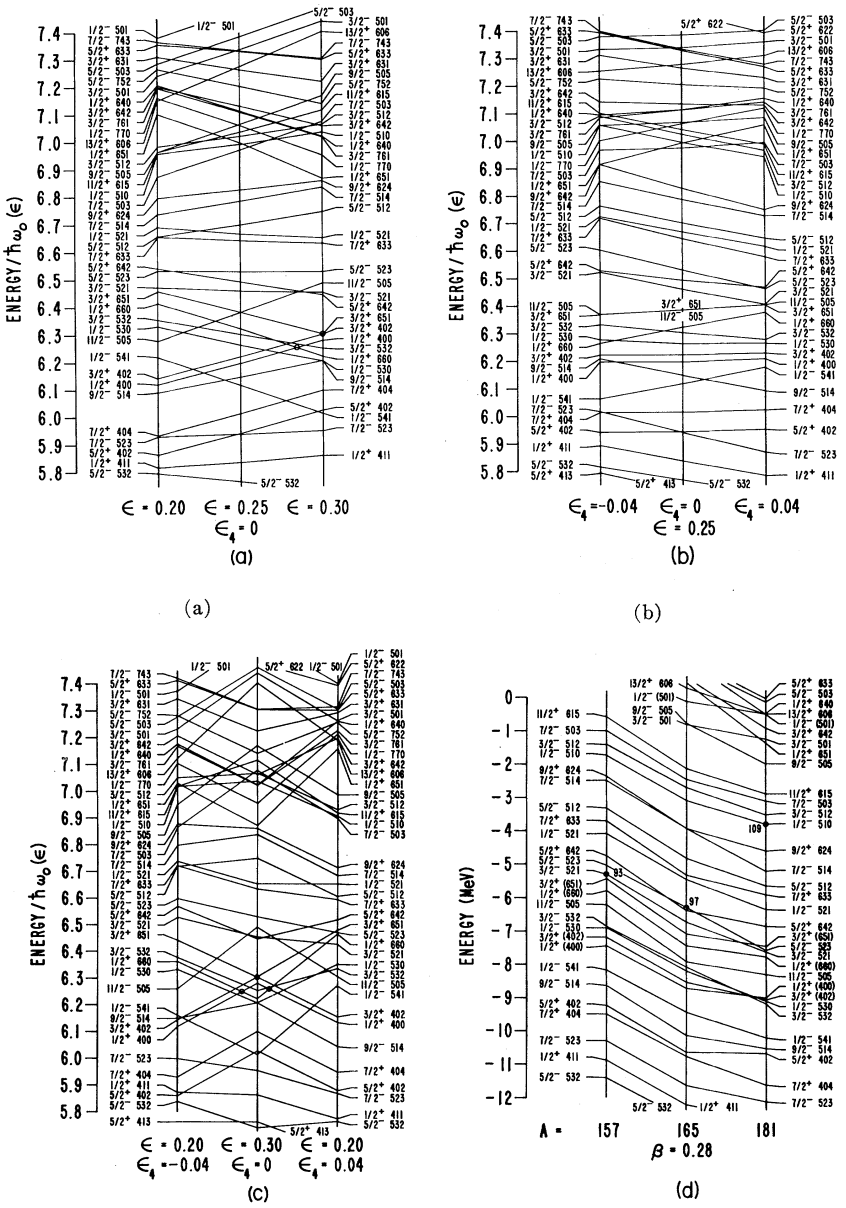

FIG. 14. (a) and (b). Results of Nilsson model calculations for single-neutron levels, with varying spheroidal (ϵ_2) or tetroidal (ϵ_4) deformation.[16] (Rings indicate intersecting[21] $|\Delta N_0|=2$ levels having equal K^π. Note: the $9/2^+$ level should read $9/2^+$ 624. (c) and (d). Results of Nilsson model calculations with simultaneously varying ϵ_2 and ϵ_4 (c) and of deformed Woods-Saxon potential calculations (d), for single-neutron levels. [In graph (c), the rings indicate intersection, as in graphs (a) and (b). In graph (d), the predicted position of the Fermi level is indicated for certain N values.] See Sec. V.A for further comments. ($\epsilon \equiv \epsilon_2$, $\beta \equiv \beta_2$ here.)

higher-mass part of the region, the levels $7/2^-$ 514 and $3/2^-$ 512 are relatively well-known, and their predicted variations with deformation are also roughly "parallel" (Fig. 14); they vary in a way different from those mentioned above, however. We have chosen to present the systematics of the fitted single-neutron levels in the following way: relative to $3/2^-$ 521 in Fig. 17, relative to $1/2^-$ 521 in Fig. 18, and relative to $7/2^-$ 514 and $3/2^-$ 512 (Version II) in Fig. 19.

In Figs. 15–19, we have only included those relative energies where at least one of the two single-particle levels involved is considered to be well-established, and determined within an uncertainty of less than 200 keV.[32] Parentheses around a point have the same meaning as in Tables III–VII, and Figs. 7–11 (identification of level uncertain). Brackets around a point indicate that the spacing may be uncertain by more than 200 keV. The definition of the symbols (R), R, (V), V, and U follows the same pattern as explained in Secs. IV.A and IV.B, with the modification that they are here applied to relative energies. In cases where the symbol U occurs, we have usually introduced "error bars" to indicate the estimated increase in uncertainty of the BCS blocking solution. We use dashed lines to connect points with the same classification if the odd nucleon number changes by more than two units.

We want to emphasize that care should be taken in interpreting the information displayed in Figs. 15–19. Each symbol introduced indicates a possible source of uncertainty.[32] However, features such as major trends in the relative positions of the levels can be considered significant.

C. Variations of Some Calculated and Empirical Level Spacings

We have plotted both theoretical and semiempirical single-particle levels relative to $1/2^+$ 411 for protons in Fig. 20, and relative to $1/2^-$ 521 for neutrons in Fig. 21. As indicated in the figures, connected points denote values of the spacings obtained from the calculations by Ford, Hoffman, and Rost (1970), and Gareev *et al.* (1967, 1969)—see brief descriptions in Appendix B.3. In the plotting, we have assumed values of the deformation parameters roughly according to the expected averages in different parts of the region (see Fig. 12).

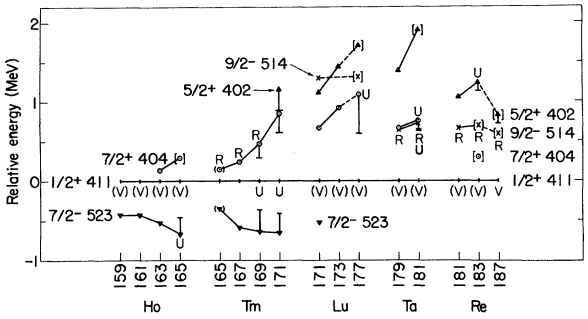

FIG. 15. Systematics of fitted single-proton levels, normalized with respect to the level $1/2^+$ 411. (Version I analysis only. Notations are explained in Sec. V.B.)

The values are given in Table X, where the mass numbers indicate approximately the centers of the five subregions considered. In plotting the circles, we have used the β_2 values of Table X, and taken $\beta_4=0$. The filled and open circles differ mainly in the treatment of the spin–orbit term. We have obtained the positions of the open squares from those of the open circles by adding the shifts estimated from the calculations by Gareev *et al.* (1969), using the β_4 values given in Table X. We have found that this procedure gives an adequate approximation for the "β_4 effect" on the single-particle levels considered here (cf. Figs. 13 and 14).

The fitted levels (from Figs. 7–11), in the cases where the reference level is known, are represented by plus signs for Version I, and x:s for Version II, in Figs. 20 and 21. Points where large uncertainties are expected are put within brackets (cf. Figs. 15–19 and comments in Sec. V.B),[32] although these uncertainties are usually negligible here considering the accuracy obtainable from the graphs.

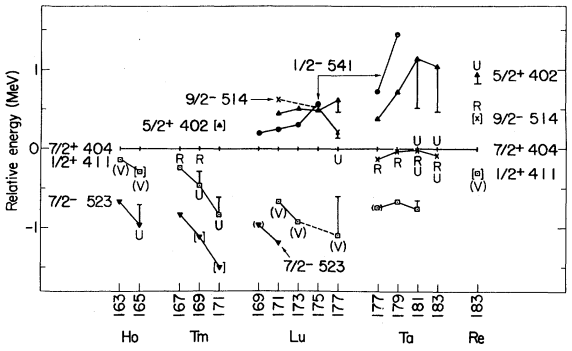

FIG. 16. Systematics of fitted single-proton levels, normalized with respect to the level $7/2^+$ 404. (Version I analysis only. Notations are explained in Sec. V.B.)

Although the diagrams in Figs. 20 and 21 are useful for orientation purposes, we should keep in mind the incomplete and schematic character of this presentation. Both the selection of data and the sets of potential and shape parameters[6] used are fairly restricted. The systematics presented in Figs. 15–19 are far more complete.

D. Discussion of Level Systematics and Potential Models

We have taken care to present both the systematics of fitted single-particle levels and the results of model calculations in an unbiased way. Neither of these two sides of the presentation has had any direct influence on the other; the fitting of levels to the data (Secs. III and IV) has no relation to the various sources of calculations we utilize throughout Sec. V. Consequently, we may hope to learn something from a comparison. To make this discussion also unbiased, we should leave it entirely to the reader. However, we believe that a few features should be pointed out here, and we do so below, commenting on the proton and neutron systematics in terms of the potential model calculations.

One type of bias is actually inherent in our analysis, although it has little effect on the fitted levels: we have assumed that the central part of the single-particle level schemes (cf. Tables I and II) should vary in a smooth way for *odd-Z isotopes* and for *odd-N isotones*.

TABLE X. Expected average deformation parameters ϵ_2 and ϵ_4 and the approximately equivalent[15] values of β_2 and β_4 (assumed for Figs. 20 and 21).

A	ϵ_2	ϵ_4	β_2	β_4
155	0.18	−0.04	0.21	0.06
163	0.24	−0.02	0.27	0.05
171	0.27	0	0.30	0.02
179	0.24	0.03	0.25	−0.03
187	0.18	0.05	0.18	−0.06

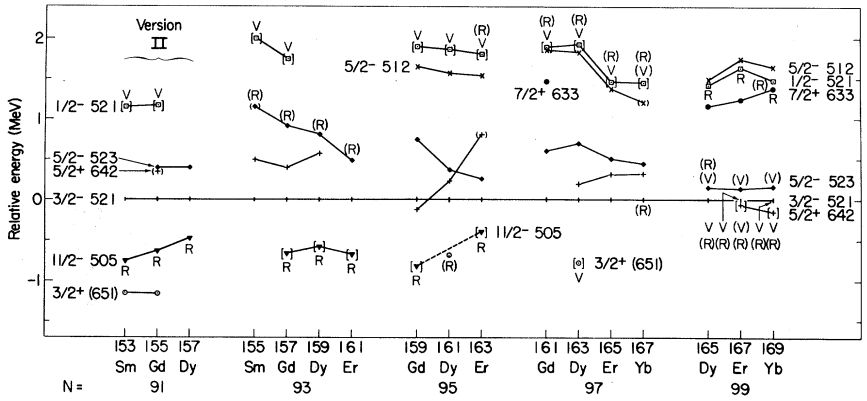

FIG. 17. Systematics of fitted single-neutron levels, normalized with respect to the level $3/2^-$ 521. (Version II analysis for the $N=91$ nuclides, and Version I analysis otherwise. Notations are explained in Sec. V.B.) Note: there is no experimental evidence for the level $5/2^-$ 512 in ^{167}Yb.

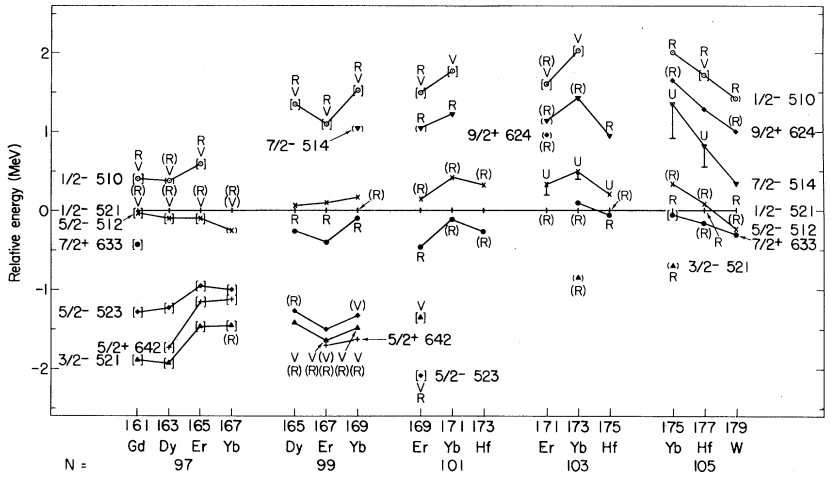

FIG. 18. Systematics of fitted single-neutron levels, normalized with respect to the level $1/2^-$ 521. (Version I analysis only. Notations are explained in Sec. V.B.) Note: there is no experimental evidence for the level $5/2^-$ 512 in ^{167}Yb.

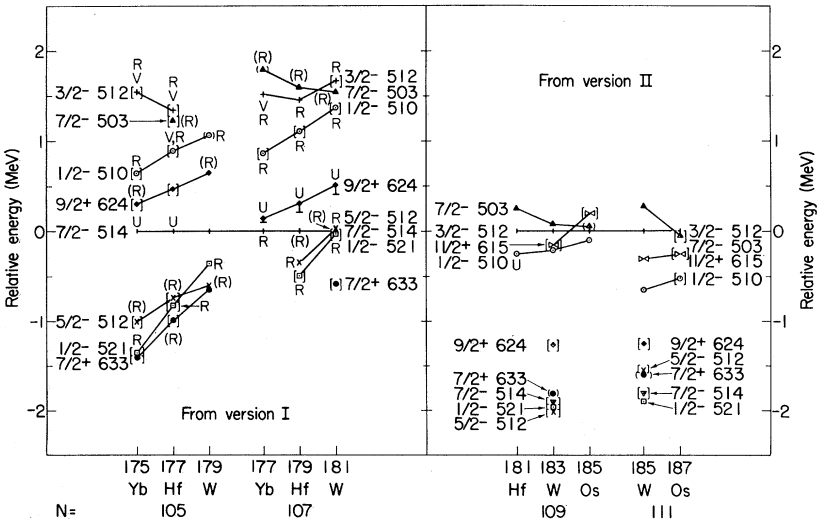

FIG. 19. Systematics of fitted single-neutron levels, normalized with respect to the level $7/2^-$ 514 for nuclides with $N=105$ and $N=107$ (Version I analysis) and with respect to the level $3/2^-$ 512 for nuclides with $N=109$ and $N=111$ (Version II analysis). (Notations are explained in Sec. V.B.)

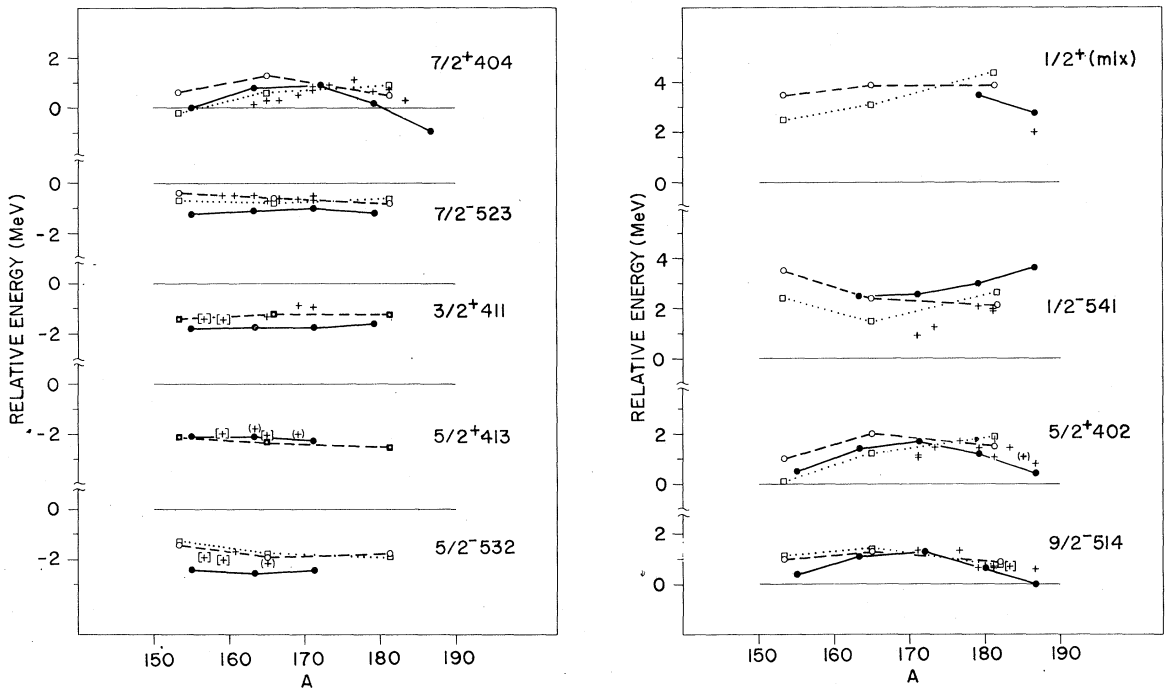

FIG. 20. Comparison between fitted (Version I) and theoretical single-proton level spacings relative to the level $1/2^+$ 411, *versus* mass number. (For further explanations, see Sec. V.C. and Table X.) Proton levels relative to $1/2^+$ 411. Notations: ●—●, theory (Ford, Hoffman, and Rost); ○- - -○, theory (Gareev *et al.*, $\beta_4=0$); □···□, theory (Gareev *et al.*, plus β_4-effect). + from present analysis of data.

However, one might alternatively impose the analogous requirement for sequences of *odd-Z isotones* and *odd-N isotopes*. This "orthogonal" procedure would be more difficult to pursue, since each sequence considered would involve a larger number of single-particle levels. We have chosen the well-examined odd-N ytterbium isotopes as a case study discussed in Appendix E. We find that the alternative presentation gives equally agreeable systematics in this case. The indication is, therefore, that the residual interaction effects which have not been explicitly accounted for in our analysis, and which would enter differently in the two kinds of systematics, are not important, and that consequently the single-particle[1] model should indeed be an appropriate basis for comparison with our type of systematics.

1. *The Single-Proton Levels*

For an orientation, we consider Fig. 20. The over-all qualitative agreement between systematics and predictions is apparent. The agreement is generally best for the Gareev calculations with the β_4-effect added, particularly if we consider the more sensitive levels (such as $7/2^+$ 404). The detailed trends are displayed in Figs. 15 and 16: see also Figs. 7 and 8 and Table VIII. These trends can be compared with the predictions presented in Fig. 13 (see also Fig. 2). We limit our discussion to a few significant features concerning the relative positions of levels within the following sets:

$1/2^+$ 411, $7/2^-$ 523, $3/2^+$ 411, and $5/2^+$ 413 (see Figs. 7, 15, and 20). The predictions for the relative positions of these four levels are quite stable in the region of interest and (except for minor differences in the spacings) agree well with each other. The agreement with the systematics is good, even quantitatively, and little can be learned about the potential and shape parameters from these levels alone.

$7/2^+$ 404 and $5/2^+$ 402 (Fig. 16). Most calculations predict a fairly constant spacing between these two levels. However, Fig. 2 shows that the levels as functions of η_2 may actually cross, and Fig. 13(d) indicates that they may approach each other for decreasing mass number. The systematics show such an approaching trend, and the variation of the spacing seems rather large. The order-of-magnitude agreement is fair.

$1/2^+$ 411 and $7/2^+$ 404 (Figs. 15, 16, and 20). The spacing is predicted to increase strongly with both ϵ_2 and ϵ_4, and the combined variation, therefore, should be quite pronounced across the region, particularly at the lower end [cf. Figs. 13(c) and 20]. The systematics show clearly this expected qualitative behavior. Moreover, good quantitative agreement could hardly be established with reasonable assumptions unless the

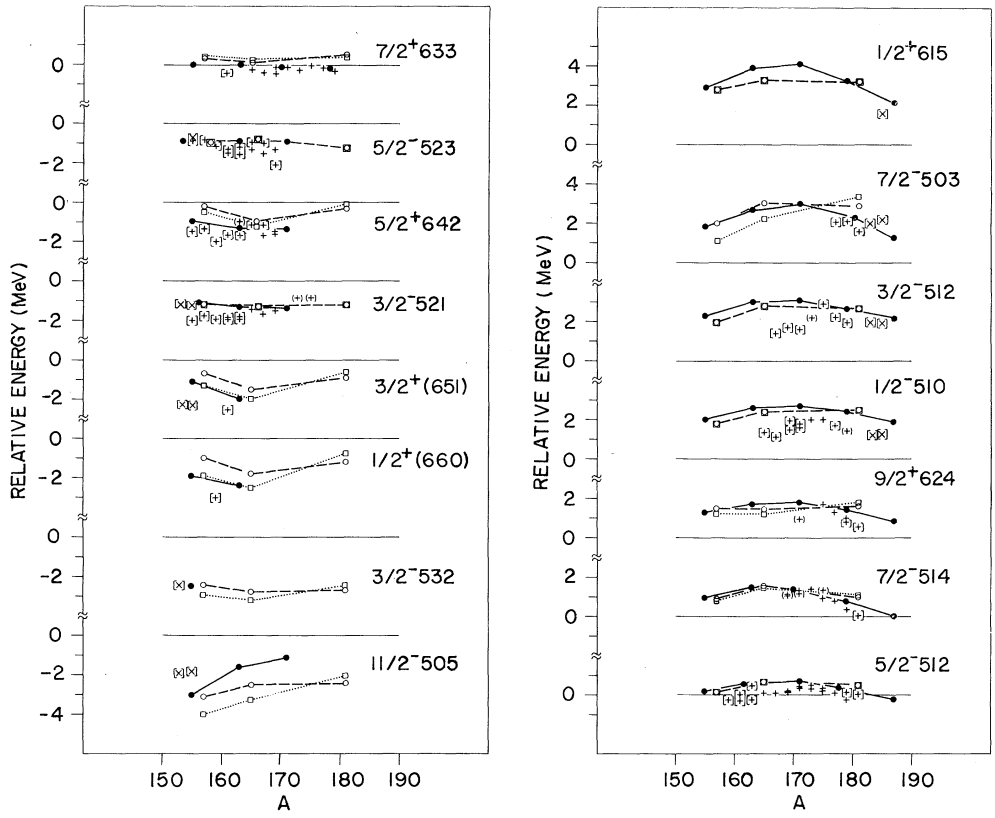

FIG. 21. Comparison between fitted (Version I or II) and theoretical single-neutron level spacings relative to the level $1/2^-$ 521, *versus* mass number. (For further explanations, see Sec. V.C and Table X.) Neutron levels relative to $1/2^-$ 521. Notations: ●—●, theory (Ford, Hoffman, and Rost); ○- - -○, theory (Gareev *et al.*, $\beta_4=0$); □···□, theory (Gareev *el al.*, plus β_4-effect). + or × from present analysis of data.

β_4 effect were included. This can readily be seen from Fig. 20, which also indicates that the β_2 deformation might be lower for odd-proton nuclides than we have assumed (Table X) for mass numbers below about 170.

$7/2^+$ 404, $9/2^-$ 514, and $1/2^-$ 541 (Fig. 16). According to the predictions, the first two levels strongly approach each other with increasing ϵ_4, and the same effect is accordingly expected with increasing A [cf. Fig. 13(c)]. The systematics clearly exhibit this trend. Since the decrease of ϵ_2 would actually counteract this trend (see e.g., Fig. 2), we again find fairly clear evidence for the ϵ_4 dependence in accordance with the expectations (Fig. 12). According to the models, the level $1/2^-$ 541 varies strongly relative to the others as a function of ϵ_2, and markedly relative to $9/2^-$ 514 as a function of ϵ_4. The predicted combined variation is rather drastic [cf. Fig. 13(c)], and agrees with the systematic trend.

$1/2^+$ 411, $5/2^+$ 402, $9/2^-$ 514, and $1/2^-$ 541 (Figs. 8, 15, and 20). The data are here restricted to the region $A>170$, and we can confine ourselves to considering Fig. 20. The predictions are seen to reproduce the qualitative trends of the systematics. However, assuming larger values than we have used (Table X) for β_2, and possibly also for $|\beta_4|$, in the region $170<A<180$ would improve the quantitative agreement.

It should be noted that the present discussion is based on data from Version I. In some cases, the Version II analysis might bring about changes (cf. discussion in Sec. IV.C.1), such as, e.g., shifting the order between the levels $1/2^+$ 411 and $7/2^+$ 404 for the lower-mass thulium isotopes. Such possible changes never appear large enough to invalidate any of the points in our present discussion—however, the zero-point rotational energies might be of importance for a more detailed comparison with potential models.

We find that the current potential model calculations can reproduce the single-proton level structure well. The relative positions of single-proton levels are somewhat less sensitive to the potential parameters[6] than are the single-neutron levels. This is possibly an effect of the Coulomb barrier (see comments at end of Sec. V.D.2). The shape parameters,[6] however, enter in a sensitive way into the variations of a few level spacings,

and a more detailed comparison should yield information about the values of ϵ_2 and ϵ_4 (or β_2 and β_4) in various parts of the region. Already the present comparison shows that deformation values in rough accordance with the expectations (Fig. 12), with an apparent maximum of ϵ_2 in the region $170<A<175$, are preferred by the systematics.

2. *The Single-Neutron Levels*

For an orientation, we may consider Fig. 21. The qualitative agreement between the systematics and any of the predictions is somewhat less apparent than for the proton levels. In particular, certain level spacings may show consistent deviations, which we discuss below. The more detailed trends are displayed in Figs. 17–19; see also Figs. 9–11, and Table IX. These trends can be compared with the predictions presented in Fig. 14 (see also Fig. 3). We limit our discussion to significant features in the relative positions of levels within the sets listed below (we use the Version II results for $N=91$, 109, and 111).

$3/2^-$ 521, $3/2^+$ (651), and $11/2^-$ 505 (Fig. 17).[24] Calculations for the lower-mass end of the region with $\epsilon_4=0$ tend to place the level $3/2^-$ 521 above $3/2^+$ (651), and the level $11/2^-$ 505 below both of them (cf. Figs. 3 and 14). An appropriate negative value of ϵ_4 brings the levels $3/2^+$ (651) and $11/2^-$ 505 close together and within 1 MeV below $3/2^-$ 521. This agrees with the systematics. Thus we seem to confirm both the negative value of ϵ_4 for the region $A<165$ (Fig. 12) and the preference for the Version II result for $N=91$ (cf. Sec. IV.C.2).

$3/2^-$ 521, $5/2^-$ 523, and $5/2^+$ 642 (Fig. 17). The predictions consistently place the level $5/2^-$ 523 less than 1 MeV above $3/2^-$ 521 (see Figs. 3 and 14). The level $5/2^+$ 642 is estimated from Woods–Saxon potential calculations [Figs. 3 and 14(d)] to be above $5/2^-$ 523 for $\epsilon_4=0$. However, negative ϵ_4 brings it down [Fig. 14(b), (c)], and for increasing ϵ_2 in the region $A<170$, $5/2^+$ 642 approaches $3/2^-$ 521. The trend of the systematics agrees with these expectations (it should be noted that the position of the level $5/2^+$ 642 in ^{163}Er is not established with certainty).

$1/2^-$ 521 and $3/2^-$ 521 (Figs. 17, 18, and 21). According to the predictions, this level spacing should be roughly 1.5 MeV, and insensitive to parameter variations. The systematics show a variation between 1 and 2 MeV with a possibly decreasing trend for increasing mass number below $A=175$. The level spacing is related to the relative position of the shell model states $3p_{3/2}$ and $1h_{9/2}$ (Fig. 3), which is strongly influenced by the spin–orbit term.

$1/2^-$ 521, $5/2^-$ 512, and $7/2^+$ 633 (Figs. 18 and 21). These spacings are not greatly influenced by ϵ_4; however, increasing ϵ_2 raises the level $5/2^-$ 512 relative to the two others. The spin–orbit term affects the positions appreciably, particularly the level $7/2^+$ 633 which originates in $1i_{13/2}$. The systematics show the three levels to lie in all cases within an interval of less than 1 MeV, and the position of $5/2^-$ 512 has a broad maximum at $A\approx173$ (cf. Appendix E).

$1/2^-$ 521, $7/2^-$ 514, and $9/2^+$ 624 (Figs. 18, 19, and 21). The levels $7/2^-$ 514 and $9/2^+$ 624 are predicted to lie above the level $1/2^-$ 521, the spacings increasing with ϵ_2, but being insensitive to ϵ_4. The relative position of $9/2^+$ 624 depends strongly on the spin–orbit term. The systematics agree with the expected trends and indicate a drop in the value of ϵ_2 compared to our assumption for $A\approx180$ (Table X).

$1/2^-$ 521 and $1/2^-$ 510 (Figs. 18 and 21; see also Fig. 19). The spacing is predicted to increase with ϵ_2, to be insensitive to ϵ_4, and to be on the average more than 2 MeV for the "rare-earth" region. The systematics show the expected variation with mass number (a maximum at $A=173$ or 175; see also Appendix E). However, they indicate an average spacing of around 1.5 MeV. This is a striking deviation in our comparison between predictions and systematics, as seen from Fig. 21. From Fig. 3 we see that the two levels approach the shell model states $3p_{3/2}$ and $2f_{5/2}$ in the spherical limit. The spacing of these states depends particularly on the surface diffuseness a_0, and the spin–orbit strength, λ_{so} [see Blomqvist and Wahlborn (1960)]. Yet, decreasing either parameter alone does not seem to reduce the spacing between the two $1/2^-$ states enough to account for the discrepancy. However, by simultaneously decreasing ϵ_2, one could reduce the average spacing by the required 0.5 MeV. It appears that suitable adjustments of all of the potential parameters[6] (Sec. II) and of ϵ_2 (deviations from Table X are allowed; cf. Fig. 12) might improve the agreement in this case without destroying the agreement found in any of the other cases discussed here.

$1/2^-$ 521 and $3/2^-$ 512 (Figs. 19 and 21). The level $3/2^-$ 512 is predicted to have a position a few hundred keV above $1/2^-$ 510, and to have practically the same dependence on ϵ_2 and ϵ_4 as this level. Therefore, the considerations made in the preceding paragraph should apply to the spacing between the levels $1/2^-$ 521 and $3/2^-$ 512 as well. The deviation between systematics and predictions is in this case somewhat less pronounced, however, and appears related to the possible drop of ϵ_2 at mass numbers below $A=170$ (cf. Sec. V.D.1). (We note that $1/2^-$ 521 and $3/2^-$ 512 both approach $3p_{3/2}$ in the spherical limit.)

$7/2^-$ 514, $3/2^-$ 512, and $7/2^-$ 503 (Fig. 19). The spacing between the levels $7/2^-$ 514 and $3/2^-$ 512 is predicted to be about 1.5 MeV, independent of ϵ_2 and ϵ_4, while the relative position of the level $7/2^-$ 503 depends fairly strongly on both ϵ_2 and ϵ_4. In the region $A\gtrsim170$, the levels $3/2^-$ 512 and $7/2^-$ 503 are expected to be nearly degenerate. All of these predictions are substantiated by the systematics, which are therefore compatible with the expectations for the ϵ_2 and ϵ_4 dependence in this case (Fig. 12).

3/2⁻ 512 and 11/2⁺ 615 (Fig. 19). The relative position of the level $11/2^+$ 615 is strongly affected by the spin–orbit term, and diverse potential model calculations give different results (cf. Figs. 3, 14, and 21). The spacing between the levels $11/2^+$ 615 and $3/2^-$ 512 increases with ϵ_2, but is not sensitive to ϵ_4. The near degeneracy of the two levels shown by the systematics is compatible with the model calculations for $A \gtrsim 180$ [cf. Fig. 14(c)].

It should be noted that the level systematics for $N=109$ and 111 from Version II (Figs. 11 and 19) is at least as convincing as the Version I result (Fig. 10), and is compatible with model predictions as discussed above. Considering also the $N=91$ case discussed earlier, we therefore find some preference for Version II. We again conclude, as in Sec. IV.C, that the variation of the zero-point rotational energy[31] appears important. For the odd-N nuclides with $93 \leq N \leq 107$, the differences between the Version I and II results are never large enough to invalidate any of the qualitative conclusions drawn from our discussion in this Section (the possible level shifts for $N=101$ are not important). More detailed analysis and more detailed calculations involving Eqs. (3.13) and (3.14), are required for further quantitative comparisons.

The single-neutron levels appear to be relatively sensitive to the potential parameters related to the surface-concentrated effects, i.e., the diffuseness, a_0, and the spin–orbit strength, λ_{so} (see Sec. II.B). This is at least partially due to the absence of a Coulomb barrier (wave functions with large tails may better "feel" the surface properties). In addition, several of the single-neutron states in the region of interest originate in the $1i_{13/2}$ shell-model state and, therefore, depend strongly on the spin–orbit term.

In conclusion, the systematics of the single-neutron levels seem to offer somewhat better possibilities of studying the potential parameters, such as the spin–orbit term, than do the single-proton levels. However, certain features of the systematics (e.g., the spacing between the levels $1/2^-$ 510 and $1/2^-$ 521) indicate that such a study is not quite straightforward in all cases. There appears to be a somewhat complicated relation between certain level spacings and both the potential and shape parameters.[6] The values preferred for ϵ_2 and ϵ_4 seem to follow the same pattern for both the single-proton and the single-neutron levels and to agree with the over-all expectations according to Fig. 12. The systematics seem to indicate a peaking of ϵ_2 for mass numbers in the interval $171 \lesssim A \lesssim 175$ and a somewhat larger drop outside of this interval compared to our average assumptions (Table X).

VI. SUMMARY AND CONCLUSIONS

As stated in the Introduction, this review has two main objectives, besides furnishing a general orientation on the subject, particularly on the single-particle[1] model for nonspherical[2] nuclei. These objectives are to derive semiempirical single-particle level schemes for various uses, and to discuss the systematics in terms of potential model calculations.

The first objective is accomplished as described in Secs. III and IV. The main results are presented graphically in Figs. 7–11. We emphasize that in using these level schemes one must exercise care and judgment; there are ambiguities and uncertainties involved in the analysis, as discussed in the text. However, we expect the relative positions of the actually fitted levels to be well-determined (within the acceptable tolerance of 100 keV, or else as indicated).[32] It is a noteworthy feature that the systematics indicate the presence of large variations in the zero-point rotational energy[31] contribution to the band heads.[6] This feature is illustrated by the comparison between the results of the "Version I" and the "Version II" analyses for the cases $N=91$, 109, and 111.

The second objective is represented by the discussion in Sec. V, dealing mainly with various gross features of the systematics, such as level crossings and trends in the relative positions of fitted levels. The conclusions that might be drawn are, therefore, fairly independent of the detailed level positions, and hence of the specific assumptions and approximations underlying our analysis. The single-particle model calculations, on which we base the discussion, are of the type described in Sec. II, i.e., we assume local potentials, having axial symmetry. The comparison with the systematics shows no departure which must necessarily be attributed to violation of these assumptions. Only major features of the model, represented by a few potential and shape parameters,[6] enter into the discussion. The relatively smooth variation of the semiempirical single-particle level schemes with the nucleon numbers N and Z shows that the interpretation along these lines is appropriate. The absence of significant discontinuities in the relative positions of fitted levels, as well as the comparison between alternative presentations of the schemes (cf. Appendix E), also shows that residual interactions, which have not been accounted for in our analysis, do not seem to have any important effects on the energy levels considered.

Given a reasonably realistic potential well, the details of the single-particle level structure are mainly related to the surface properties of the average field [Eq. (2.1)]. Therefore, besides the shape parameters, the surface diffuseness and the spin–orbit term, which is surface-concentrated, are the items of primary interest in the comparison of the model and the data. This is particularly true in the discussion of the single-neutron levels in the region considered here.

The values of the surface shape parameters preferred by the systematics are compatible with expectations based on other types of evidence, both experimental and theoretical (Fig. 12). The spheroidal deformation, ϵ_2, appears to be peaked in the interval $171 \lesssim A \lesssim 175$,

and usually to decrease rather markedly for adjacent mass numbers. The tetroidal deformation, ϵ_4, should change sign from negative ("diamondlike" shape) at $A\approx155$, to positive ("boxlike" shape) at $A\approx185$.

More data pertaining to the quasiproton and quasineutron excitations[5] are desirable for making feasible a more detailed quantitative analysis in terms of model parameters than done in this review. The most promising experiments are the one-nucleon transfer reactions,[25] which populate primarily these types of excitations and yield crucial information about the wave functions. The pace at which such data presently accumulate will certainly make more detailed model studies possible in the near future. Yet, as demonstrated in this review, the present energy level data already tell us that the single-particle model, with smoothly varying parameters, should furnish an appropriate basis for describing the intrinsic[4] excitations of the odd-mass nuclides in the region $150<A<190$.

ACKNOWLEDGMENTS

It is a pleasure for the authors to express their gratitude to Dr. Merle Bunker for his help in the selection of each individual level in our compilation of data, and to Dr. Gunnar Ehrling for his extensive computer programming of the single-particle model calculations. Besides rendering this indispensible assistance, both have generously made their unpublished results available to us. We want to thank sincerely Drs. Richard Chasman, George Ford, and Rayford Nix for their valuable help and suggestions. Enlightening discussions with Drs. Daniel Bès, Jan Blomqvist, Mark Bolsterli, Richard Casten, Edmund Fiset, Ole Hansen, Darleane Hoffman, Arthur Kerman, William Myers, Sven Gösta Nilsson, Charles Reich, Raymond Sheline, and Raymond Sorensen are acknowledged. We are also indebted to Drs. M. Bennett, R. Foucher, J. Gizon, I. Lindgren, and H. Ryde for furnishing us with recent experimental data prior to publication. The hospitality of the Los Alamos Scientific Laboratory, where two of us (W. O. and S. W.) have spent a year while completing this review, is greatly appreciated.

APPENDIX A: THE ROTOR-PLUS-PARTICLE MODEL

To bring out the main quantum-mechanical features of a rotating system with intrinsic[4] degrees of freedom, such as a nonspherical[2] nucleus, let us consider the following simplified model: The bulk part (core) of the rotor is assumed to create an average field, by which the particles interact with the rotor; we consider several fermions to move independently in orbitals fairly close to the Fermi energy. We assume the system to have axial symmetry[4] and an effective moment of inertia, $\Im=\Im_x=\Im_y$. The total angular momentum,[13] $\mathbf{I}=\mathbf{R}+\mathbf{J}$, consists of the rotational part, R, and the total intrinsic part, J. From symmetry considerations we realize that the relation $R_z=0$ or $I_z=J_z$ holds, and that I is a constant of motion, but J is not.

The Hamiltonian for this model is obtained by quantizing the classical expression for the rotational energy[34] and adding the contribution $H_{\rm ip}$ from the intrinsic motion of the independent particles. After elementary manipulations we find,

$$H_{\rm rpm}=H_{\rm adiab}+H_{\rm rpc}, \tag{A1}$$

where the "adiabatic"[26] part has the form

$$H_{\rm adiab}=(\hbar^2/2\Im)(\mathbf{I}^2+\mathbf{J}^2-2J_z^2)+H_{\rm ip}, \tag{A2}$$

and the "rotation-particle-coupling" (or "Coriolis") part has the form

$$H_{\rm rpc}=-(\hbar^2/2\Im)(I_+J_-+I_-J_+), \tag{A3}$$

the ladder operators being defined as usual ($I_\pm=I_x\pm iI_y$, $J_\pm=J_x\pm iJ_y$). The component J_z (but in general not $\mathbf{J}^2$) commutes with $H_{\rm adiab}$, and the corresponding eigenvalue, Ω, is therefore a good quantum number for that part of $H_{\rm rpm}$. Operating with $H_{\rm rpc}$ on a state with given Ω produces a linear combination of states with quantum numbers $|\,\Omega\pm1\,|$.

The general form of the eigenstates of $H_{\rm adiab}$ and their symmetry properties are discussed by several authors, e.g., Bohr and Mottelson (1953a), Nilsson (1955), Alder *et al.* (1956), Moszkowski (1957), Kerman (1959), Preston (1962, Chap. 10), Nathan and Nilsson (1965), Rogers (1965), and Davidson (1968, Chaps. 3 and 4). For half-integer Ω or integer $\Omega>0$, the normalized wave function can be written (we take here Ω to be positive, by definition)

$$\Phi_{M\Omega}{}^I=[(2I+1)/16\pi^2]^{1/2}\times[\Psi_\Omega D_{M\Omega}{}^I+(-1)^{I+\Omega}\Psi_{-\Omega}D_{M,-\Omega}{}^I]. \tag{A4}$$

Here, the intrinsic[4] wave function, Ψ_Ω, is an eigenstate of $H_{\rm ip}$ with eigenvalue $E_{\rm ip}(\Omega)$.[35] The rotation matrix,[36] $D_{M\Omega}{}^I$, is a simultaneous eigenstate of $\mathbf{I}^2$, with eigenvalue $I(I+1)$, of the component I_ξ ($\hat\xi$ is an arbitrary fixed

[34] If the core of the rotor has internal degrees of freedom, one may represent the effects of these in a simple way by adding higher powers of $\mathbf{R}^2$ to the basic rotational energy expression, $A_0\mathbf{R}^2+B_0\mathbf{R}^4+\cdots$, where $A_0\approx(\hbar^2/2\Im)$. The constant B_0 is empirically found to be small. For the purpose of the present review, this term can be ignored.

[35] The relation between the wave functions, Ψ_Ω and $\Psi_{-\Omega}$, is discussed in the literature. We assume the same phase conventions as Nathan and Nilsson (1965) paragraph 4.1, or Rogers (1965).

[36] The symbols $D_{M\Omega}{}^I$ are the elements of the transformation matrix of the $(2I+1)$-dimensional irreducible representation of the three-dimensional rotation group. They are functions of the Euler angles for the transformation between the (x, y, z) and (ξ, η, ζ) systems.[4] The following relations hold:

$$\mathbf{I}^2D_{M\Omega}{}^I=I(I+1)D_{M\Omega}{}^I,\quad I_\xi D_{M\Omega}{}^I=MD_{M\Omega}{}^I,\quad I_zD_{M\Omega}{}^I=\Omega D_{M\Omega}{}^I;$$

$$I_+D_{M\Omega}{}^I=[(I-\Omega+1)(I+\Omega)]^{1/2}D_{M,\Omega-1}{}^I,$$

$$I_-D_{M\Omega}{}^I=[(I-\Omega)(I+\Omega+1)]^{1/2}D_{M,\Omega+1}{}^I.$$

See further Rose (1957), Kerman (1959), Edmonds (1968), and Bohr and Mottelson (1969), paragraphs 1A-4 and 1A-6.

TABLE XI. Theoretical expectation values of $\mathbf{j}^2$ for single-particle states.

	State	$\langle \mathbf{j}^2\rangle_{\beta=0.28}$	$[j(j+1)]_{\text{def.}=0}$	K^2
p	$9/2^-$ 514	36.63	35.75	20.25
p	$7/2^-$ 523	35.68	35.75	12.25
p	$7/2^+$ 404	16.94	15.75	12.25
p	$5/2^-$ 532	34.55	35.75	6.25
p	$5/2^+$ 402	10.52	8.75	6.25
p	$3/2^+$ 411	11.73	8.75	2.25
p	$1/2^-$ 541	14.91	15.75	0.25
p	$1/2^+$ 411	7.69	3.75	0.25
n	$11/2^+$ 615	49.25	48.75	30.25
n	$11/2^-$ 505	36.03	35.75	30.25
n	$9/2^+$ 624	48.35	48.75	20.25
n	$7/2^+$ 633	47.05	48.75	12.25
n	$7/2^-$ 514	23.67	15.75	12.25
n	$5/2^+$ 642	45.62	48.75	6.25
n	$5/2^-$ 523	21.26	15.75	6.25
n	$3/2^+$ (651)	44.49	48.75	2.25
n	$3/2^-$ 521	19.31	24.75	2.25
n	$3/2^-$ 512	12.06	3.75	2.25
n	$3/2^+$ (402)	5.41	3.75	2.25
n	$1/2^+$ (660)	43.89	48.75	0.25
n	$1/2^-$ 510	10.89	8.75	0.25
n	$1/2^-$ 521	12.48	3.75	0.25
n	$1/2^+$ (400)	3.33	0.75	0.25

direction in space),[4] with eigenvalue M, and of $I_z=J_z$, with eigenvalue Ω. It is straightforward to derive the expectation value of H_{rpm}, Eq. (A1), for the adiabatic[26] eigenstate Eq. (A4). It reads

$$E(I,\Omega)=E_{\text{ip}}(\Omega)+(\hbar^2/2\Im)[I(I+1)+\langle\Omega\,|\,\mathbf{J}^2\,|\,\Omega\rangle-2\Omega^2+\delta_{\Omega,1/2}(-1)^{I+1/2}(I+\tfrac{1}{2})a_{\text{ip}}], \quad \text{(A5)}$$

where the "decoupling factor," a_{ip}, is given by the expression

$$a_{\text{ip}}=-\langle-\tfrac{1}{2}\,|\,J_-\,|\,\tfrac{1}{2}\rangle=-\langle\tfrac{1}{2}\,|\,J_+\,|\,-\tfrac{1}{2}\rangle. \quad \text{(A6)}$$

The matrix elements are taken with respect to the intrinsic wave function Ψ_Ω.

The contribution H_{rpc}, Eq. (A3), has nondiagonal matrix elements in the representation defined by Eq. (A4). For nonzero Ω and Ω' we derive the expression[36]

$$\langle IM\Omega'\,|\,H_{\text{rpc}}\,|\,IM\Omega\rangle=-(\hbar^2/2\Im)[(I-\Omega_<)(I+\Omega_>)]^{1/2}\langle\Omega'\,|\,J_\pm\,|\,\Omega\rangle, \quad \text{(A7)}$$

where $|\Omega'-\Omega|=1$, and where J_+ applies if $\Omega_>=\Omega'>\Omega=\Omega_<$, and J_- applies if $\Omega_>=\Omega>\Omega'=\Omega_<$ holds. The mixing of wave functions of the type (A4) introduced by these matrix elements is a nonadiabatic[26] effect, i.e., the particle and rotational degrees of freedom are not independent.

Considering an odd number of independent particles, one of which is unpaired ("seniority one"), we may set[18] (cf. Sec. II.C)

$$\mathbf{J}=\mathbf{j}=\mathbf{l}+\mathbf{s}, \qquad \Omega=K, \qquad E_{\text{ip}}(\Omega)=|\,\epsilon_K-\epsilon_F\,|, \quad \text{(A8)}$$

where ϵ_K is the single-particle eigenvalue [Eq. (2.14)], and ϵ_F is the Fermi level.[28] The other quantities appearing in Eq. (A5) can then be replaced by the following expressions:[27,31]

$$\langle\mathbf{J}^2\rangle\approx\langle K\,|\,\mathbf{j}^2\,|\,K\rangle_{\text{sp}}+2\sum_{k\neq K}(\langle k\,|\,\mathbf{j}^2\,|\,k\rangle_{\text{sp}}-M_k^2), \quad \text{(A9a)}$$

$$\langle K\,|\,\mathbf{j}^2\,|\,K\rangle_{\text{sp}}=\sum_{n,l,j}S_K(n,l,j)^2 j(j+1); \quad \text{(A9b)}$$

$$a_{\text{sp}}=-\sum_{n,l,j}S_K(n,l,j)^2(-1)^{j+1/2}(j+\tfrac{1}{2}). \quad \text{(A10)}$$

Here we assume any spherical representation, e.g., Eq. (2.15). Values of $\langle\mathbf{j}^2\rangle_{\text{sp}}$, Eq. (A9b), calculated from the wave functions by Gareev *et al.* (1967), are given in Table XI for some proton and neutron orbitals of interest in the region considered here. Values of the decoupling factor, a_{sp}, Eq. (A10), are tabulated, e.g., by Bunker and Reich (1971).

The presence of correlations modifies the description presented in this Appendix (see further Appendix C). If they may be considered to affect only the intrinsic motion,[4] the adiabatic part of the description, in particular Eq. (A4), is still valid, and Ω remains a good quantum number. Also Eq. (A5) is valid in principle, but $E_{\text{ip}}(\Omega)$ is replaced by a more general intrinsic energy expression, and the evaluation of the expectation value, $\langle\mathbf{J}^2\rangle$, and of the generalized decoupling factor, a, is complicated by the correlations. Even for such intrinsic states, which have predominantly one-quasiparticle[5] character, the deviations from the "single-particle" expressions, Eqs. (A8)–(A10), may be considerable [a similar statement is true of Eq. (A7)]. These questions enter into the discussion in Sec. III.

If axial symmetry is not assumed, the theory is considerably complicated. For a discussion of these matters, see Preston (1963, Chapt. 10), and the original papers on the subject by Davydov (1959) and Davydov and Filippov (1958). (See also Hecht and Satchler, 1962). With the methods of analysis pursued in this review, and the nuclides we have considered, no apparent need exists for discussing deviations from axial symmetry.

APPENDIX B: AXIALLY SYMMETRIC POTENTIALS AND MODELS

1. General Considerations

The general problem is formulated by Eqs. (2.1)–(2.3) and (2.14). We introduce the three dimensionless, nonnegative "form" functions $v(\mathbf{r})$, $u(\mathbf{r})$, and $w(\mathbf{r})$, defined by

$$V(\mathbf{r})=-V_0 v(\mathbf{r}), \quad U(\mathbf{r})=-U_0 u(\mathbf{r}), \quad \rho_c(\mathbf{r})=\rho_{c,0}w(\mathbf{r}). \quad \text{(B1)}$$

We assume that each of these form functions has its minimum value equal to zero, and its maximum value equal to one, in a finite region, $0<r\leq R'$ [this is approximately true of the Fermi function, Eq. (2.5)]. Furthermore the spatial extensions of the form functions are fixed by volume conservation requirements (the constant $\rho_{c,0}$ is then fixed by setting the total charge equal to Ze). All three functions, Eq. (B1), are expected to be of a similar form; in practice, their angular dependences should be compatible, but their average radius and surface diffuseness might be different. We restrict ourselves to axial symmetry and reflection symmetry[4] (one could readily relax the latter condition, however).

We represent implicitly the form function $v(\mathbf{r})$ in terms of the equipotential surfaces (EPS: s; this is suitable for general considerations and also for certain computational purposes) by an equation of the type

$$\rho^2=c^2f(v;z), \tag{B2}$$

where v enters as a parameter, and (ρ, z) are the cylindrical coordinates. The "characteristic," dimensionless function $f(v;z)$ is assumed to be a continuous function of v and z, and for each v value between 0 and 1 is required to be nonnegative in a *finite* domain of the z axis. The constant c is fixed by the volume conservation requirement, which we here assume to have the form[37]

$$c^2\int_{f\geq 0} f(\tfrac{1}{2};z)\,dz=4R_0^3/3, \tag{B3}$$

where R_0 equals the nuclear radius (see Sec. II).

The eigensolutions of the problem are briefly discussed in Sec. II. Different states with identical quantum numbers[18] K^π are in practice always nondegenerate.[21] In the absence of the spin–orbit term, the eigenvalues of l_z and s_z, i.e., Λ and Σ, respectively [Eq. (2.21)], would also be good quantum numbers. However, in the presence of a spin–orbit term, Λ and Σ remain approximately good quantum numbers, if the deformation is large enough to cause appreciable polarization of the spin along the z axis. Take the form function $u(\mathbf{r})$ [Eq. (B1)] to be defined by $\rho^2=c^2g(u;z)$ and consider prolate shapes.[16] Setting $\rho^2=x^2+y^2$, we find readily

$$\text{grad}\,u=[(2x/c^2)\hat{\mathbf{x}}+(2y/c^2)\hat{\mathbf{y}}-(\partial g/\partial z)\hat{\mathbf{z}}](\partial g/\partial u)^{-1}, \tag{B4}$$

from which we can show the identity[13]

$$c^2(\partial g/\partial u)\boldsymbol{\sigma}\cdot[\text{grad}\,u(\mathbf{r})\times\mathbf{p}] =2\hbar l_z\sigma_z+2(\boldsymbol{\sigma}\times\mathbf{r})_z p_z-c^2(\partial g/\partial z)(\mathbf{p}\times\boldsymbol{\sigma})_z \tag{B5}$$

(for spherical shapes[12] this expression becomes $2\hbar\mathbf{l}\cdot\boldsymbol{\sigma}$). With increasing deformation, the expectation value of each of the last two terms tends to zero [$(\boldsymbol{\sigma}\times\mathbf{r})_z$ and $\partial g/\partial z$ becomes small]. The first term of Eq. (B.5) is diagonal in Λ and Σ, having the eigenvalue $4\hbar\Lambda\Sigma$.

The tendency of one Λ and Σ component to dominate is a feature of the eigenstates of H_{sp} [Eq. (2.14)] found in actual calculations already at moderate deformations. Furthermore, from expansions in three-dimensional harmonic-oscillator components, we know that one value of the total oscillator number,[20] N_0 [Eqs. (2.22) and (2.23)] usually dominates, as expected (see Sec. II.C). The same is true, however to a lesser extent at moderate deformations, about the numbers $n_\perp$ and n_z, separately. We may more generally consider n_z as being the expectation value of the number of nodes a given wave function has along the z axis. For large prolate deformations, the potential can only accommodate a certain, relatively fixed number of such nodes, and n_z tends to become an approximately good quantum number.

For spherical or slightly deformed shapes, a spherical representation is clearly more efficient than the cylindrical one. However, for a definite shell-model substate, $M=K$ (or $-K$), the two possible (Λ, Σ) components are mixed according to the ratio of the appropriate Clebsch–Gordan coefficients.[19] In these cases, there is no great disadvantage in expanding the eigenstates in the cylindrical representation—only the relative purity in terms of (Λ, Σ) is lost. (See also Chasman and Wahlborn, 1967).

2. *The Harmonic-Oscillator Representations*

The three-dimensional harmonic oscillator wave functions considered are eigenstates of the Hamiltonian

$$H_{\text{hop}}=-(\hbar^2/2m)\Delta+(m\omega_\perp^2/2)(x^2+y^2)+(m\omega_z^2/2)z^2. \tag{B6}$$

The Schrödinger equation can readily be separated in Cartesian (x, y, z) or cylindrical (ρ, ϕ, z) coordinates. Using the latter alternative and excluding the spin eigenfunction, we find the normalized wave function [see Rassey (1958)]

$$\psi_{\text{cyl}}(\rho,\phi,z)=(2\pi b_z b_\perp^2)^{-1/2} \times\exp(i\Lambda\phi)\,p_{\mu\Lambda}(s)q_\nu(t)\exp[-(s^2+t^2)/2], \tag{B7}$$

and the energy eigenvalue

$$E(\mu,\nu,\Lambda)=(\mu+1)\hbar\omega_\perp+(\nu+\tfrac{1}{2})\hbar\omega_z. \tag{B8}$$

Here we define

$$s=\rho/b_\perp,\quad t=z/b_z,\quad b_\perp=(\hbar/m\omega_\perp)^{1/2},\quad b_z=(\hbar/m\omega_z)^{1/2}. \tag{B9}$$

The numbers μ and ν take values according to Eq. (2.19). The polynomials $p_{\mu\Lambda}(s)$ and $q_\nu(t)$, normalized

[37] Short of elaborate self-consistent calculations, there is no unique prescription for the volume conservation criterion. The present recommendation—to conserve the volume enclosed by the equipotential surface at 50% of the potential depth—is in rough accord with Fermi gas model considerations for the density of nucleons. (However, it is feasible to utilize Thomas–Fermi calculations for the nucleon density.)

with the Gaussian factor in Eq. (B7), have the following forms: $q_\nu(t)$ is just proportional to the Hermite polynomial, $H_\nu(t)$, and we find

$$p_{\mu\Lambda}(s)=\sum_{\alpha=0}^{\alpha_{\max}} a_{\mu\Lambda}(\alpha)s^{\mu-2\alpha}, \qquad \alpha_{\max}=(\mu-\Lambda)/2\geq 0, \tag{B10}$$

where

$$a_{\mu\Lambda}(\alpha)/a_{\mu\Lambda}(0) = \{\prod_{\beta=1}^{\alpha}[(\mu-2\beta+2)^2-\Lambda^2]\}[\alpha!4^\alpha(-1)^\alpha]^{-1} \tag{B11}$$

for $\alpha>0$, and (cf. Chasman and Wahlborn, 1967)

$$a_{\mu\Lambda}(0)=\sqrt{2}\{[(\mu+\Lambda)/2]![(\mu-\Lambda)/2]!\}^{-1/2}. \tag{B12}$$

Including the spin part, as we assume in the basis vector $|K^\pi;\mu,\nu,\Lambda\rangle_{\rm cyl}$ [Eq. (2.16)], amounts to multiplying the spatial wave function [Eq. (B7)] by the appropriate spin eigenstate χ_Σ, where $\Sigma=K-\Lambda=\pm\frac{1}{2}$.

Details concerning the calculations of the matrix elements of $H_{\rm sp}$ in the cylindrical representation and the diagonalization of the matrix are discussed by Damgaard *et al.* (1969) and Chasman (1970). Due to the possibility of choosing both the oscillator constants $b_\perp$ and b_z [Eq. (B9)] in an optimal way, the convergence of the cylindrical expansion, Eq. (2.16), can be made fast enough to give accurate eigensolutions with moderate computing efforts, even for complicated nonspherical potentials.[38]

If the frequencies are equal, $\omega_\perp=\omega_z=\omega_0$, in Eq. (B6), the Schrödinger equation can be separated in spherical coordinates. The eigenvalues are found to equal $(N_0+3/2)\hbar\omega_0$ [cf. Eq. (2.22)]. The radial equation has the eigenfunctions $R_{nl}(r)$, each of which is proportional to an associated Laguerre polynomial in r/b_0, times the product $(r/b_0)^l\exp(-r^2/2b_0^2)$ [see de-Shalit and Talmi (1963)]. The radial quantum number, n [Eq. (2.18)], is the number of nodes of the function $rR_{nl}(r)$ in the interval $0\leq r<\infty$. The oscillator constant is $b_0=(\hbar/m\omega_0)^{1/2}$. The angular and spin part of the wave function has the well-known form for a spin-$\frac{1}{2}$ particle in a central potential[19]; it can be given the "uncoupled" form $Y_{l\Lambda}(\hat{\mathbf{r}})\chi_\Sigma$ (with $\Sigma=K-\Lambda$) or the "vector coupled" form $X_{ljK}(\hat{\mathbf{r}};\text{spin})$ (see, e.g., Chi, 1966). For diffuse nonspherical potentials, such as those discussed in Sec. II, the spherical expansion, Eq. (2.15), with the oscillator basis states as given here, has not been very extensively used for diagonalization of $H_{\rm sp}$. The convergence is slow, except for small deformations. Generally, a better method is to first diagonalize $H_{\rm sp}$ in the cylindrical representation, giving the components $C_K(\mu,\nu,\Lambda)$ [Eq. (2.16)], and then to compute spherical components, $S_K(n,l,j)$ [Eq. (2.15)], as needed, e.g., according to the expression

$$S_K(n,l,j) = \sum_{\mu,\nu,\Lambda}[(l,\Lambda,\tfrac{1}{2},K-\Lambda\,|\,j,K)I_\Lambda(\mu,\nu;n,l)C_K(\mu,\nu,\Lambda)]. \tag{B13}$$

Here, the first factor in the bracket is a Clebsch–Gordan coefficient,[19] and the factor I_Λ is an overlap integral, performed in cylindrical coordinates, between the spatial parts of the cylindrical and the (conjugated) spherical basis functions.

The use of harmonic-oscillator wave functions in general as a basis set for expanding bound-state, single-particle nuclear wave functions offers several advantages. In particular, if one knows the expansion coefficients, one can easily reproduce the wave functions for various applications. One can also make use of general rules for transforming the component states (Talman, 1970).

In the spherical limit, it is found that a small number of harmonic-oscillator components can describe the radial wave function quite well out to a distance considerably larger than the nuclear radius. Expansions along n (l and j are fixed) show that the purity of a Woods–Saxon wave function in terms of one spherical oscillator component is rarely less than 80%, and usually larger than 90%. As a rule, only one of the admixed oscillator components has a considerable amplitude.

3. *Some Specific Potential Models*

We list below, with brief descriptions, the models utilized in various parts of the present review.

The Nilsson Model. Detailed accounts of the current formulation have recently been given in the literature (Gustafson *et al.*, 1967; Lamm, 1969; Nilsson, 1969; and Nilsson *et al.*, 1969). The model, which is based on the anisotropic harmonic oscillator, is suitably formulated with the use of the "stretched coordinates," i.e., x and y are expressed in units of $b_\perp$, and z in units of b_z [Eq. (B9)]. After this transformation is performed in Eq. (B6), the following terms are added to the Hamiltonian:

$$H_\kappa=-\kappa_0\hbar\bar{\omega}_0[2\mathbf{l}\cdot\mathbf{s}+\mu_0(\mathbf{l}^2-\langle\mathbf{l}^2\rangle_{\rm shell})]; \tag{B14}$$

$$H_4=\epsilon_4\hbar\omega_0 r_{\rm sc}^2 P_4(\hat{\mathbf{r}}_{\rm sc}). \tag{B15}$$

Not only $\mathbf{r}_{\rm sc}$, but also $\mathbf{l}$, is referred to the stretched

[38] It is possible, at least for moderate, finite deformations, to assign the appropriate cylindrical quantum numbers to a set of single-particle orbitals, without analyzing the wavefunctions, by simply considering the order of the energy eigenvalues. Assuming given K^π, and disregarding quasi-intersections, the energy, apart from a constant, is approximately given by an expression of the type

$$E(\bar{N}_0,\bar{n}_z,\bar{\Lambda})\approx(\bar{N}_0-\bar{n}_z)v_\perp(\epsilon)+\bar{n}_z v_z(\epsilon)-\bar{\Lambda}(K-\bar{\Lambda})u_0(\epsilon),$$

where $v_\perp(\epsilon)$, $v_z(\epsilon)$, and $u_0(\epsilon)$ are positive quantities, depending on the deformation, which we symbolically denote by ϵ; $v_\perp>v_z$ holds for prolate deformations (cf. the Nilsson model, Appendix B.3). In practice, then, the order of levels with the same $\bar{N}_0$ value is determined by $\bar{n}_z$.

coordinates. The quantities $\bar{\omega}_0$, κ_0, and μ_0 are constants. The parameter ϵ_4 determines the tetroidal[16] deformation, and the spheroidal deformation, ϵ_2, is defined by the relations

$$\omega_\perp=\omega_0(\epsilon_2,\epsilon_4)(1+\epsilon_2/3),\qquad \omega_z=\omega_0(\epsilon_2,\epsilon_4)(1-2\epsilon_2/3). \tag{B16}$$

The ratio $\omega_0(\epsilon_2,\epsilon_4)/\bar{\omega}_0$ is determined by the volume conservation condition (for $\epsilon_4=0$ this reduces to setting $\omega_\perp^2\omega_z=\bar{\omega}_0^3=$ const.). The Hamiltonian is diagonalized for each N_0 space[20] at a time, which is a reasonably good approximation when stretched coordinates are used (the $|\Delta N_0|=2$ couplings are then mainly provided by H_4). The energies are obtained in units of $\hbar\omega_0(\epsilon_2,\epsilon_4)$; the constant $\hbar\bar{\omega}_0$ has roughly the value $41A^{-1/3}$ MeV. We have used the following parameter values for the calculations discussed in the text (Lamm, 1969):

$$\kappa_0^p=\kappa_0^n=0.0637;\qquad \mu_0^p=0.60,\qquad \mu_0^n=0.42. \tag{B17}$$

The model by Gareev et al. Several articles on this approach have been published by Gareev *et al.* (1967, 1968, 1969) in Dubna (see also Nemirovskiĭ and Chepurnov, 1966). The model is formulated by Eqs. (2.1)–(2.3), and the potential used is of the Woods–Saxon type [Eqs. (2.4) and (2.5)] with the generalization according to Eq. (2.6). The spin–orbit and Coulomb terms are defined by the form functions, Eq. (B1), being equal, $v(\mathbf{r})=u(\mathbf{r})=w(\mathbf{r})$. The representation used for diagonalizing $H_{\rm sp}$ is of the "coupled" spherical type.[19] Instead of harmonic-oscillator wave functions, however, a set of generalized radial functions are used to make the expansion for bound states converge relatively fast (for details, see the above-mentioned articles). For the calculations quoted in this review, the potential parameters used are roughly in accordance with Sec. II.B, including Eq. (2.8), the values being[17] $V_1=53$ MeV, $V_2=33.5$ MeV, $r_0=1.24$ fm (for $\beta_4=0$), and $a_0=0.63$ fm [cf. Eqs. (2.9) and (2.10)]. For the spin–orbit strength [cf. Eq. (2.12)] the expression $\kappa_{\rm so}=0.263[1+2(N-Z)/A]$fm^2 is used [with Eq. (2.11)].

Ford, Hoffman, and Rost (1970) also use a model defined essentially by Eqs. (2.1)–(2.3) with the Woods–Saxon potential [Eqs. (2.4) and (2.5)] generalized according to Eq. (2.6). However, they choose a spherically symmetric spin–orbit term,[12] setting $U(\mathbf{r})=V(r)$, and take the charge distribution to be uniform [Eq. (2.13)] inside the actual nuclear surface. Only quadrupole (β_2) deformations[16] are considered. The matrix of the Hamiltonian is diagonalized in a "coupled" spherical representation.[19] The radial factors, $R_{nlj}(r)$, are taken to be the radial wave functions obtained in the spherical limit of the potential used. This choice leads to certain problems concerning convergence and component states belonging to the continuum. The following potential parameters (cf. Sec. II.B) have been used in the calculations quoted in the text[17]: $V_0=45.3$ MeV for neutrons, $V_0=49.2+50(N-Z)/A$ MeV for protons, $r_0=1.26$ fm, $a_0=0.60$ fm, $\lambda_{\rm so}=39.5$.

Ehrling and Wahlborn (1970, 1971) have used a model defined by Eqs. (2.1)–(2.3) with a Woods–Saxon type of potential [Eqs. (2.4) and (2.5)] generalized by the substitution according to Eq. (2.7), including spheroidal and tetroidal deformations.[16] The form functions [Eq. (B1)] have been chosen equal, $v(\mathbf{r})=u(\mathbf{r})=w(\mathbf{r})$, but other choices are possible. This common form function is defined implicitly by the equation for the EPS:s [cf. Eq. (B2)]. We can, e.g., choose this equation to have the form

$$\begin{aligned}\rho^2\{R_\perp+a_\perp\ln[(1/v)-1]\}^{-2}&\\ +z^2\{R_z+a_z\ln[(1/v)-1]\}^{-2}&\\ =1+(35/8)(\eta_4/R_*^2)\rho^2z^2/(\rho^2+z^2),&\end{aligned} \tag{B18}$$

where one sets

$$\begin{aligned}R_\perp&=R_*(1+\eta_2/2+3\eta_4/8)^{-1/2},\\ R_z&=R_*(1-\eta_2+\eta_4)^{-1/2},\end{aligned} \tag{B19}$$

and determines R_* by the volume conservation condition, Eq. (B3). With $v(\mathbf{r})$ defined by Eq. (B18), it is possible to vary the surface thickness by choosing $a_\perp$ and a_z suitably. Examples of EPS:s from Eq. (B18) with $a_\perp=a_z=a_0$ are shown in Fig. 1. The matrix of $H_{\rm sp}$ is diagonalized in the cylindrical harmonic-oscillator representation [Eq. (2.16)]; see Appendix B2. The matrix is limited by the choice of the maximum value of N_0 for the oscillator shells[20] included (typically, $N_{0,\max}\approx 15$). The potential parameters for the illustrative cases shown in Figs. 2 and 3 are given by Eq. (2.27). (The equilibrium spheroidal deformation evaluated in this example is $\eta_2\approx 0.3$.)

4. *Other Approaches. Comparative Studies*

We first list some additional references and then comment briefly on a comparison between different approaches.

The Nilsson (1955) model has been extended to shapes deviating from axial symmetry by Newton (1960), and to a nonstatic potential (in the effective-mass[11] approximation) by Lemmer (1960), and Lemmer and Green (1960). An account of these approaches is given by Preston (1963), Sec. 10.6.

Early calculations with nonspherical Woods–Saxon potentials were made by Chepurnov and Nemirovskiĭ (1963). Further work was made by Nemirovskiĭ and Chepurnov (1966), and Faessler and Sheline (1966). Rost (1967) introduced the method of coupled channels to this problem.

Calculations with energy-dependent, nonspherical Woods–Saxon potentials were made by Röper (1966), and Bennewitz and Haug (1968). In the latter article, generalizations are discussed for the use of single-

particle calculations in fission theory. This line is further developed for static potentials by Pashkevitch and Strutinsky (1969), and Damgaard *et al.* (1969), who make use of the cylindrical harmonic-oscillator representation for diagonalization. This method is also used by Chasman (1970).

Another approach, appropriate for fission theory, is made by Bolsterli, Fiset, and Nix (1969). The class of potentials used is obtained by folding a uniform pseudo-density of prescribed shape with a Yukawa interaction. The eigensolutions are obtained by a method of finite differences.

It is of interest to make a comparison between different approaches with respect to the formulation of the potential as well as the method of solution. We have, specifically, compared results of calculations obtained from the different but fairly general schemes formulated by Bolsterli, Fiset, and Nix (1969), and by Ehrling and Wahlborn (1970, 1971). As an extreme test case, we have considered the potential generated by two tangent spheres (each radius appropriate to $A\approx 120$), folded with a Yukawa interaction, for the problem of single-neutron eigenstates, Eqs. (2.1), (2.2), and (2.14). The solutions are then derived by the numerical method of finite differences, and by diagonalization in cylindrical harmonic-oscillator representation, respectively. The results for the eigenvalues of all bound states from the two methods agree, to within the expected accuracy. The accuracy is found to be quite high (error less than 50 keV) in the diagonalization method with, e.g., $N_{0,\max}=17$. To obtain a comparable accuracy with the finite-difference method, a computing time at least one order of magnitude longer is required. A direct comparison has also been made for the eigenvalues of the spheroidal[16] potential presented in Figs. 2 and 3. Except for the most loosely bound states, the different schemes are compatible. With suitably adjusted potential depths, the individual curves for $\epsilon_K(\eta_2)$ agree to within a fraction of one MeV for $0\leq\eta_2\leq 0.7$.

In conclusion, a direct geometrical characterization of the nuclear surface, as utilized by Bolsterli, Fiset, and Nix (1969), appears preferable to multipole expansions of one type or the other [Eqs. (2.6) and (2.7)]. In solving for the eigenstates, the diagonalization in cylindrical representation (see, e.g., Damgaard *et al.*, 1969) is equivalent or superior to other possible methods. The construction of the Hamiltonian matrix is a nontrivial problem and various techniques are necessary to make it feasible on available computers. The diagonalization usually then takes the major part of the computing time.

APPENDIX C: QUASIPARTICLES AND THEIR INTERACTIONS

In principle, at least part of the nucleon–nucleon interactions in a nucleus can be accounted for, on the average, by a self-consistent field. In the single-particle model,[1] this field can be represented, in a phenomenological way,[7] by the potential well plus spin–orbit and Coulomb terms, as described in Sec. II. Here we consider essentially only those residual forces which are not accounted for in a single-particle description, and which lead to important correlations in the motion of the nucleons.

The Hamiltonian for the nucleus in the framework of the model for the intrinsic motion considered here can be written in the form,

$$H_{\text{intrinsic}}=\sum_{sk}\epsilon_k a_{sk}^{\dagger}a_{sk}$$
$$-(\tfrac{1}{2})\sum_{s'k'\cdots\sigma\kappa}\sum\langle s'k',\sigma'\kappa'\,|\,\hat{G}\,|\,sk,\sigma\kappa\rangle a_{\sigma'\kappa'}{}^{\dagger}a_{s'k'}{}^{\dagger}a_{sk}a_{\sigma\kappa},\quad\text{(C1)}$$

where the indices (sk), etc., denote all relevant quantum numbers, including τ_3, for a nucleon orbital.[14,27] The fermion creation $(a_{sk}^{\dagger})$ and annihilation (a_{sk}) operators fulfill the anticommutation relations

$$[a_{sk},a_{s'k'}]_+=[a_{sk}^{\dagger},a_{s'k'}^{\dagger}]_+=0,\qquad[a_{sk}^{\dagger},a_{s'k'}]_+=\delta_{sk,s'k'},\quad\text{(C2)}$$

if (sk) and $(s'k')$ refer to identical nucleons, but are assumed to commute if the labels refer to nonidentical nucleons. The sums in Eq. (C1) extend over the single-particle orbitals, with energy ϵ_k, of both proton and neutron potential wells. The operator $\hat{G}$ represents the residual nucleon–nucleon interaction.

The following references contain discussions of approaches based on the phenomenological Hamiltonian, Eq. (C1), or on some version of the more general Hartree–Fock–Bogoliubov theory: Mottelson (1959, 1962), Belyaev (1959), Baranger (1960, 1963), Baranger and Kumar (1968a, b), Kumar and Baranger (1968). See also the books by Lane (1964) and Brown (1967). The book by Thouless (1961) contains basic theory of many-fermion systems and deals with the methods discussed in this Appendix.

The presentation we have chosen is especially adapted to the intrinsic[4] motion of nonspherical nuclei. However, most of the considerations are, with some modifications, applicable to spherical nuclei as well. In that case, the degeneracies of the shell model orbitals and the angular momentum coupling have to be taken into account.

1. Quasiparticles and the BCS Theory

A treatment of the pairing correlations in a many-fermion system, appropriate to the theory of superconductivity, was presented by Bardeen, Cooper, and Schrieffer (1957a, b). Its applicability as an approximation in nuclear physics was suggested by Bohr, Mottelson, and Pines (1958). The theory was further developed for use in nuclear structure by Soloviev (1958/59), and by Belyaev (1959), who also discussed the application to collective properties. Other discussions have been presented by Mottelson (1959, 1962)

and Nathan and Nilsson (1965), and in the books by Lane (1964) and by Brown (1967).

For nuclei of medium and large mass numbers, there are negligible pairing correlations between neutrons and protons in states at low excitation energies (cf. Soloviev, 1963). The neutron and proton systems may therefore be considered separately for that part of the intrinsic[4] model Hamiltonian which represents the single-particle motion and the pairing correlations. We restrict ourselves here to discussion of one of the systems. Pairing correlations mean that the interaction considered takes place between particles only when they occupy pairs of time-reversed orbitals ($\pm sk$). In Eq. (C1), therefore, we select the matrix elements of $\hat{G}$ between pairs of identical particles, setting $\sigma\kappa=-sk$, $\sigma'\kappa'=-s'k'$.

Consider the ground state of the system with an even number of fermions. In the BCS approximation, the wave function is written[27]

$$|\Psi_0^{\rm BCS}\rangle=\prod_k (u_k+sv_k a_{sk}^\dagger a_{-sk}^\dagger)\,|0\rangle, \qquad \text{(C3)}$$

where normalization implies

$$u_k^2+v_k^2=1. \qquad \text{(C4)}$$

We determine the (nonnegative) amplitude parameters (u_k, v_k) by requiring the expectation value of the Hamiltonian for independent particles plus pairing interactions to be stationary, with the subsidiary condition

$$\langle\mathfrak{N}\rangle=n_0, \qquad \mathfrak{N}=\sum_{sk} a_{sk}^\dagger a_{sk}, \qquad \text{(C5)}$$

where $\mathfrak{N}$ is the number operator, and n_0 is the number of particles. This condition is necessary to assure a correct location of the Fermi energy. The wave function, Eq. (C3), contains a mixture of components with different particle numbers. The physical meaning of u_k and v_k can be read from Eqs. (C3) and (C4): v_k^2 means the probability that the pair of time-reversed single-particle orbitals ($\pm sk$) is occupied by a pair of particles, and *vice versa* for u_k^2.

We consider the solution of the problem under simplifying assumptions. First, we represent the attractive pairing-force matrix element in Eq. (C1) by a positive constant, G, being an average independent of (k, k') and defined in a symmetrized way,

$$(\tfrac{1}{2})\sum_{s,s'} ss'\langle s'k', -s'k'\,|\,\hat{G}\,|\,sk, -sk\rangle\approx G. \qquad \text{(C6)}$$

The expectation value of the Hamiltonian considered $-\lambda\mathfrak{N}$, where λ is a Lagrangian parameter, then reads

$$E_0'\approx 2\sum_k (\epsilon_k-\tilde{\lambda})v_k^2-G(\sum_k u_k v_k)^2. \qquad \text{(C7)}$$

Here we have made the further approximation of replacing $\lambda-(Gv_k^2/2)$ by a constant $\tilde{\lambda}$ (the "chemical potential"). In solving this problem it is suitable to introduce the "correlation parameter," Δ, defined by

$$\Delta=G\sum_k u_k v_k. \qquad \text{(C8)}$$

The solution gives the famous BCS equations for $(\tilde{\lambda}, \Delta)$,

$$n_0=\sum_k [1-(\epsilon_k-\tilde{\lambda})/e_k(\tilde{\lambda}, \Delta)], \qquad \text{(C9)}$$

$$(2/G)=\sum_k [1/e_k(\tilde{\lambda}, \Delta)], \qquad \text{(C10)}$$

and for the quantities (u_k, v_k),

$$\left.\begin{matrix} u_k \\ v_k \end{matrix}\right\} = 2^{-1/2}[1\pm(\epsilon_k-\tilde{\lambda})/e_k(\tilde{\lambda}, \Delta)]^{1/2}. \qquad \text{(C11)}$$

Here we define [cf. Eq. (3.5)]

$$e_k(\tilde{\lambda}, \Delta)=[(\epsilon_k-\tilde{\lambda})^2+\Delta^2]^{1/2}. \qquad \text{(C12)}$$

We now return to a more complete model Hamiltonian (not restricting ourselves to one kind of particle). We substitute for the fermion operators a_{sk}, $a_{sk}^\dagger$ the "quasiparticle" operators α_{sk}, $\alpha_{sk}^\dagger$ according to the canonical transformation (Bogoliubov, 1958a, b; Valatin, 1958),

$$\alpha_{sk}^\dagger=u_k a_{sk}^\dagger-sv_k a_{-sk}, \qquad \alpha_{sk}=u_k a_{sk}-sv_k a_{-sk}^\dagger, \qquad \text{(C13)}$$

which preserves the anticommutation relations, Eq. (C2). The Hamiltonian can then be split into different parts,

$$H=H_0+H_{11}+H_{20}+H_{\rm int}^{\rm qp}, \qquad \text{(C14)}$$

where H_0 is a constant term, representing the energy of the "core." In the simplified description, Eqs. (C6)–(C12), H_{11} has the form [cf. Eq. (3.4)]

$$H_{11}=\sum_{sk} e_k\alpha_{sk}^\dagger\alpha_{sk}\,(=H_{\rm qp}), \qquad \text{(C15)}$$

i.e., a Hamiltonian for independent "quasiparticles." The operator H_{20} would contain terms of the type $\alpha\alpha$ and $\alpha^\dagger\alpha^\dagger$, which break pairs; however, our treatment as described above leads to $H_{20}\equiv 0$. The remaining term, $H_{\rm int}^{\rm qp}$, being biquadratic in the operators α and $\alpha^\dagger$, represents the true quasiparticle interactions, an important aspect of which will be discussed in Appendix C2.

The particle and quasiparticle number operators [cf. Eqs. (C5) and (C13)] do not commute with each other. Therefore, a particle number fluctuation is inherent in the description, as mentioned earlier [see also Eq. (C3)]. This is an important feature of the BCS theory. The diffuse Fermi surface allows us to consider the "quasiparticle", Eq. (C13), as being a "hybrid" of a particle excitation (with probability u_k^2) and a hole excitation (with probability v_k^2).

If we neglect $H_{\rm int}^{\rm qp}$, the Hamiltonian is H_0+H_{11}, where H_0 has the (approximate) eigenstate $|\Psi_0^{\rm BCS}\rangle$, Eq. (C3), which is therefore denoted as the "quasiparticle" vacuum, and where H_{11} has the form given by Eq. (C15). For the odd system, where the orbital (sk)

is occupied by the odd particle, the wave function has approximately the form

$$|\Psi_{sk}{}^{\mathrm{BCS}}\rangle \approx \alpha_{sk}{}^{\dagger}|\Psi_0{}^{\mathrm{BCS}}\rangle, \tag{C16}$$

which we denote as a "one-quasiparticle" state.[5] This description is somewhat deficient—in particular, the effect of "blocking" (Sec. III) has not been properly taken into account. For a more complete discussion of the odd system and blocking, see Secs. III.A and III.C.

2. Vibrations and the RPA Theory

The theory of nuclear vibrations originated within the framework of the collective model by Bohr (1952) and Bohr and Mottelson (1953a) (see also Alder *et al.*, 1956). Microscopic descriptions in terms of the quasiparticle picture were given by Arvieu and Vénéroni (1960), Marumori (1960), and Baranger (1960), utilizing the random phase approximation (RPA), also called the "method of linearization of the equations of motion." Extensive applications of these schemes have been made to quasiparticle motion and surface vibrations in spherical nuclei (Kisslinger and Sorensen, 1963) and in nonspherical nuclei (Bès *et al.*, 1965; Bès and Cho, 1966; Soloviev and Vogel, 1967; Soloviev, Vogel, and Jungklaussen, 1967). Reviews of these subjects and related matters have been given by Green (1965), and by Bès and Sorensen (1969). The vibrational phenomena in nuclei are reviewed by Nathan (1964) and by Nathan and Nilsson (1965). For accounts of theory and comparisons with experiment, see also the books by Preston (1963, Chap. 10), Lane (1964), Brown (1967), and Davidson (1968).

We briefly outline here the microscopic description of harmonic surface vibrations in nuclei. We present schematically the RPA method, using the quasiparticle approximation (Appendix C1) and disregarding blocking effects. In $H_{\mathrm{intrinsic}}$ [Eq. (C1)], we consider only the long-range quasiparticle interactions, $H_{\mathrm{int}}{}^{\mathrm{qp}}$ [cf. Eq. (C14)], including the neutron–proton interaction, which lead to collective oscillations.

The relevant Hamiltonian is here simply denoted by H. We consider first the even system (even Z, and even N) and assume, in principle, that the ground-state wave function, $\tilde{\Psi}_0$, is known (this is distinguished from the quasiparticle vacuum, Ψ_0, which is an eigenstate of the pairing Hamiltonian only). The equations of motion of a harmonic vibrational mode (L, M) then read, generally,

$$[H, O_{LM}]=-\hbar\omega_{LM}O_{LM}, \qquad [H, O_{LM}{}^{\dagger}]=\hbar\omega_{LM}O_{LM}{}^{\dagger}. \tag{C17}$$

Assuming $\omega_{LM}>0$ and setting $H|\tilde{\Psi}_0\rangle=0$, one can show the relations

$$O_{LM}|\tilde{\Psi}_0\rangle=0, \tag{C18}$$

$$H|\Psi_{LM}\rangle=\hbar\omega_{LM}|\Psi_{LM}\rangle, \tag{C19}$$

where we define

$$|\Psi_{LM}\rangle=O_{LM}{}^{\dagger}|\tilde{\Psi}_0\rangle. \tag{C20}$$

Thus, the operator $O_{LM}{}^{\dagger}(O_{LM})$ creates (annihilates) a "phonon", i.e., a vibrational quantum, of energy $\hbar\omega_{LM}$, and Ψ_{LM} is the wave function of the "one-phonon" vibrational state. We require $O_{LM}{}^{\dagger}(O_{LM})$ to be a boson operator.

We now introduce the "double-quasiparticle" creation operators, defined by

$$A_{kk'}{}^{LM\dagger}=[\alpha_{sk}{}^{\dagger}\alpha_{s'k'}{}^{\dagger}]_{LM}, \tag{C21}$$

where the orbitals involved are combined to form the proper coupling,[27]

$$|M_k \pm M_{k'}|=L, \qquad M_k+M_{k'}=M \tag{C22}$$

(in the spherical case, a tensor operator of rank L is formed). We consider here only modes with $L>1$. The commutator with the Hamiltonian can be written in the form

$$[A_{kk'}{}^{LM\dagger}, H]=\sum_{\kappa\kappa'}[P_{kk',\kappa\kappa'}{}^{LM}A_{\kappa\kappa'}{}^{LM\dagger}+R_{kk',\kappa\kappa'}{}^{LM}A_{\kappa\kappa'}{}^{LM}] + \text{terms in } \alpha^{\dagger}\alpha + \text{biquadratic terms.} \tag{C23}$$

An analogous equation holds for the corresponding annihilation operator, $A_{kk'}{}^{LM}$. The coefficients $P_{kk',\kappa\kappa'}{}^{LM}$ and $R_{kk',\kappa\kappa'}{}^{LM}$ are the matrix elements of the quasiparticle interaction considered $(H_{\mathrm{int}}{}^{\mathrm{qp}})$ between two-quasiparticle states, and between $|\tilde{\Psi}_0\rangle$ and four-quasiparticle states, respectively.

The basic approximation in RPA is the following: for the description of collective motion, only the linear terms in $A_{kk'}{}^{LM\dagger}$ and $A_{kk'}{}^{LM}$ are important in Eq. (C23), and the "phonon" operator, $O_{LM}{}^{\dagger}$, is a linear combination of these operators; in keeping with this assumption one also treats the "double-quasiparticle" operators as if they were boson operators ("quasiboson" approximation). A suitable choice of this linear combination transforms Eq. (C23) to the form, Eq. (C17), which describes harmonic vibrations. Finding this transformation is, therefore, equivalent to solving the linearized equations of motion for the collective oscillations created by the part of $H_{\mathrm{int}}{}^{\mathrm{qp}}$ considered.

We set

$$O_{LM}{}^{\dagger}=\sum_{kk'}[X_{kk'}{}^{LM}A_{kk'}{}^{LM\dagger}-Y_{kk'}{}^{LM}A_{kk'}{}^{LM}], \tag{C24}$$

where the terms are compatible with the coupling, Eq. (C22), and where the coefficients $X_{kk'}{}^{LM}$ and $Y_{kk'}{}^{LM}$ are to be determined.[39] The conditions discussed above give

[39] Normalization of the phonon state, Ψ_{LM}, requires

$$\sum_{kk'}[(X_{kk'}{}^{LM})^2-(Y_{kk'}{}^{LM})^2]=1.$$

equations of the form

$$\sum_{\kappa\kappa'}[P_{kk',\kappa\kappa'}{}^{LM}X_{\kappa\kappa'}{}^{LM}+R_{kk',\kappa\kappa'}{}^{LM}Y_{\kappa\kappa'}{}^{LM}]=WX_{kk'}{}^{LM}, \quad (C25)$$

$$\sum_{\kappa\kappa'}[P_{kk',\kappa\kappa'}{}^{LM}Y_{\kappa\kappa'}{}^{LM}+R_{kk',\kappa\kappa'}{}^{LM}X_{\kappa\kappa'}{}^{LM}]=-WY_{kk'}{}^{LM}, \quad (C26)$$

which we refer to as the "RPA equations". These equations define an eigenvalue problem with an asymmetric matrix, the eigenvalue denoted by W. For the nuclear surface vibrations considered here, the solution of interest[40] is the one with the lowest positive eigenvalue, $W=\hbar\omega_{LM}$. The Hamiltonian for the relevant collective contribution of the quasiparticle interactions (in the even system) may then be written

$$(H_{\text{int}}{}^{\text{qp}})_{\text{coll}}=\sum_{LM}\hbar\omega_{LM}O_{LM}{}^{\dagger}O_{LM}(=H_{\text{vibr}}) \quad (C27)$$

[cf. Eq. (3.4)]. (We consider here only $L\geq 2$.)

If one approximates the ground state by the quasiparticle vacuum, Ψ_0,—the "Tamm–Dancoff" approximation—one can see that only the X terms [Eq. (C24)] will be effective. This is known to be a poor representation for nuclear vibrations (see, e.g., Lane, 1964). It is an important characteristic feature of RPA, therefore, that $\tilde{\Psi}_0$ contains the so-called ground-state correlations, i.e., admixtures of two particle–two hole, four particle–four hole, etc., excitations. Both types of terms in Eq. (C24) are then of significance. The "one-phonon" state, Ψ_{LM} [Eq. (C20)], contains corresponding components with 2, 4, 6, $\cdots$ quasiparticles.

It is of interest to consider the schematic case of a separable interaction, i.e., one where the elements of the matrices P and R [Eq. (C23)] are factorable with respect to (kk') and $(\kappa\kappa')$. This is, e.g., true of the quadrupole or octapole models for surface vibrations frequently used (see Bès and Sorensen, 1969), if the exchange effects are neglected. If the unperturbed two-quasiparticle energies are denoted by $E_{kk'}$ and the two-body matrix elements are written as $-\chi_{LM}q_{LM}(kk')q_{LM}(\kappa\kappa')$, the RPA equations give simply for the neutron or proton system

$$2\chi_{LM}\sum_{kk'}[q_{LM}(kk')^2E_{kk'}(E_{kk'}{}^2-W^2)^{-1}]=1, \quad (C28)$$

the X and Y coefficients being proportional to $q_{LM}(kk')(E_{kk'}\pm W)^{-1}$. A graphical presentation of a quadratic dispersion equation like Eq. (C28) is instructive[40] [see Nathan and Nilsson (1965) and Bès and Sorensen (1969)]. The description is complicated slightly if the neutron-proton Y_{LM} interaction is included.

When an odd particle is present in the system, we have to take into account the particle–vibration coupling. The terms in $\alpha^{\dagger}\alpha$ of Eq. (C23) are then no longer negligible, since they can cause scattering of the odd quasiparticle. We assume that the phonon [Eq. (C24)] has only a small amplitude for any particular orbital, and that, hence, the commutation relations,

$$[\alpha_{sk}{}^{\dagger},O_{LM}{}^{\dagger}]=0, \qquad [\alpha_{sk},O_{LM}{}^{\dagger}]=0, \quad (C29)$$

are approximately fulfilled. If only vibrational and quasiparticle degrees of freedom are considered, the relevant coupling part of the quasiparticle interactions can generally be written in the following form ($L\geq 2$ assumed):

$$(H_{\text{int}}{}^{\text{qp}})_{\text{coupl}}=-\sum_{LM}\sum_{sk,s'k'}\mathcal{K}_{s'k',sk}{}^{LM}\times[O_{LM}{}^{\dagger}+(-1)^{M}O_{L,-M}]\alpha_{sk}{}^{\dagger}\alpha_{s'k'}(=H_{\text{pvc}}) \quad (C30)$$

[cf. Eq. (3.4)]. The coefficients $\mathcal{K}_{s'k',sk}{}^{LM}$, which are evaluated from two-body matrix elements, characterize the particle-surface coupling. If we consider only one quasiparticle and zero or one phonon present in the odd system with the coupling, Eq. (C30), included, the wave functions are in general linear combinations of components of the type

$$\alpha_{sk}{}^{\dagger}\,|\,\tilde{\Psi}_0\rangle \quad \text{and} \quad O_{LM}{}^{\dagger}\alpha_{s'k'}{}^{\dagger}\,|\,\tilde{\Psi}_0\rangle=\alpha_{s'k'}{}^{\dagger}\,|\,\Psi_{LM}\rangle,$$

(cf. Sec. III.B.2). Each of these components has a highly complex structure, due to the ground-state correlations. However, the X and Y coefficients [Eq. (C24)] are sufficient for the evaluation of the collective properties of the components.

After all the approximations made in Parts 1 and 2 of this Appendix, the resulting Hamiltonian consists of the three terms, Eqs. (C15), (C27), and (C30), for the types of applications discussed here (see Sec. III.A.2). Frequently, the approximation of taking a spin-independent quadrupole or octupole force has been used in actual calculations. The evaluation of $\hbar\omega$, as well as of the X and Y coefficients, is then highly simplified [cf. Eq. (C28)], and the results are found to lead to at least qualitative agreement with experiment. In Eq. (C30), the coupling coefficient in this case has schematically the form

$$\mathcal{K}_{s'k',sk}{}^{LM}=N_{LM}(u_ku_{k'}-v_kv_{k'})\langle s'k'\,|\,r^LY_{LM}\,|\,sk\rangle, \quad (C31)$$

where u_k, v_k are the BCS amplitudes (see Appendix C.1), and N_{LM} is a constant determined by the strengths assumed for the L-multipole parts of the nucleon–nucleon forces.

APPENDIX D: BIBLIOGRAPHY FOR LEVEL DATA

The experimental energy level data presented in Tables III–VII, as well as our comments in the text

[40] For a stable solution of the RPA equations to exist, corresponding to a vibrational mode LM, the strength of the relevant part of the quasiparticle interaction must not exceed a certain critical value. On the other hand, if the interaction is too weak, the lowest eigensolution with $W>0$ ceases to describe a collective mode. (See Bès and Sorensen, 1969).

pertaining to these data, are essentially based on information that was available to us when we closed our search of the literature around March 1, 1970. (Some recent references were added later.) In quoting specific references, we set in brackets the abbreviated notation listed below. Here the first two numerals denote the year of publication or of receipt of information, and the following two letters are the first letters of the first author's surname. The last two numerals agree in most cases with the numeration given to these references by the Nuclear Data Journal. These numerals are omitted for the most recent references, except where duplicate notations would result.

In the text we occasionally omit the reference notation in referring to early, frequently quoted data. In these cases—as well as, of course, for other specific information—the reader is referred to the review article by Bunker and Reich (1971), to the Table of Isotopes (Lederer *et al.*, 1967), and to the publications by the Nuclear Data Group (1959–1965, 1966).

APPENDIX E: A CASE STUDY: THE YTTERBIUM ISOTOPES

Throughout this work, we have considered the behavior of the single-particle levels in sequences of odd-proton isotopes and odd-neutron isotones. It is of interest, however, to study the "orthogonal" sequences of odd-neutron isotopes and odd-proton isotones (cf. Sec. V.D). We have not systematically studied this alternative presentation, but have limited ourselves to a discussion of the ytterbium isotopes. Due to the extensive (d, p) and (d, t) work by Burke *et al.* (1966), these form one of the best studied sets of nuclides in the region. Generally, sequences of odd-neutron isotopes are advantageous for this kind of study, since several levels may be known in a long sequence of nuclides and the effect of a varying Coulomb field is not present.

Part of the "central group" of single-particle levels for the ytterbium isotopes are presented in Fig. 22, normalized to the $1/2^-$ 521 state. These levels are taken directly from the result of our analysis, presented in Figs. 9 and 10, and have only been rearranged for the purpose of the present discussion. The notations used for the single-particle levels and for the uncertainties in their determinations[32] are the same as in Figs. 9 and 10 and are explained in Sec. IV.B. Comments on some individual nuclides are given in Sec. IV.C.2.

We consider for the discussion the ten levels in Fig. 22, each of which has been fitted to the data in at least two isotopes. Although no rules of smooth behavior have been applied to this sequence, we see that the relative variations of the individual fitted levels are no larger than those found in the schemes shown in Figs. 9 and 10. This indicates that the possible residual interaction effects, which we have not taken into account, should be relatively unimportant. The result also seems to verify our basic assumption of the stability of the single-particle[1] model.

We see that the best established features of Fig. 22 are the near degeneracy of the levels $1/2^-$ 521 and $7/2^+$ 633, and the parallel variations of the levels $5/2^-$ 512, $7/2^-$ 514, and $1/2^-$ 510, which have maximum spacing relative to $1/2^-$ 521 in ^{173}Yb. These features are compatible with the model calculations (Figs. 14 and 21) and support the conclusion (Sec. V.D) that the spheroidal[16] deformation parameter, ϵ_2, has a maximum between $A=171$ and $A=175$. Equilibrium deformation calculations (cf. Sec. V) by Lamm (1969) and Nilsson *et al.* (1969) give, for the ytterbium isotopes, a maximum deformation, $\epsilon_2^{eq}\approx 0.27$, for $A=171$, 172, or 173. The calculations by Gareev, Ivanova, and Pashkevitch (1969) give a maximum deformation, for even–even ytterbium isotopes, of $\beta_2^{eq}\approx 0.27$ for the region $172\leq A\leq 176$. We expect here also that $\epsilon_4\approx 0$ (cf. Fig. 12).

Comparison between the theoretically predicted equilibrium deformations and the interpreted deformation dependence of the empirically found level variations presents a critical test of the model used. The evidence of agreement in the ytterbium isotopes is partial proof that the close relationship between the level structure at the Fermi surface and the "total energy," predicted by the use of the single-particle model, has an empirical basis in nuclear structure. Further proof must await further theoretical results.

The question of uniqueness in the determination of the single-particle level schemes may also be discussed in connection with this case study, where we can compare with the work of Chasman (1966). He has fitted eleven single-particle levels to the known level data for

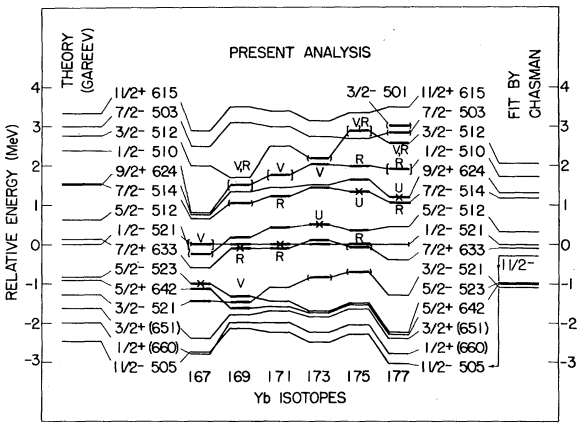

FIG. 22. Central parts of the single-neutron level schemes for the odd-mass ytterbium isotopes with $167\leq A\leq 177$ from the present analysis (Figs. 9 and 10). On the left is presented an appropriate theoretical single-neutron level scheme from a deformed Woods-Saxon potential. The result of the analysis by Chasman (1966) is presented on the right. (Notations are the same as in Figs. 9 and 10 and in Sec. IV.B of the text.) Note: there is no experimental evidence for the level $5/2^-$ 512 in ^{167}Yb.

all the odd-A ytterbium isotopes simultaneously. He has chosen the remainder of a total of 30 levels according to the Nilsson (1955) model and made an essentially exact solution of the pairing model with a constant G value. Corrections due to collective effects are not applied. Such contributions can be considered relatively unimportant for most ytterbium isotopes (note, however, the comments in Sec. IV.C.2, specifically for ^{167}Yb). The result of the fit is shown to the right in Fig. 22. We see that it agrees quite well with the average empirical situation for the six ytterbium isotopes [Chasman (1966) also presents an alternative, but similar, spectrum with the $11/2^-$ 505 level depressed].

To the left in Fig. 22, we also show a Woods–Saxon scheme (Gareev *et al.*, 1967), appropriate to the average situation for the ytterbium isotopes. We find good average agreement between this scheme and Chasman's scheme (excluding $11/2^-$ 505), as well as our systematics, with the exception of the spacings of the $1/2^-$ 510 and $3/2^-$ 512 levels relative to $1/2^-$ 521. As discussed in Sec. V.D.2 and illustrated in Fig. 21, the current predictions overestimate these spacings. For $1/2^-$ 510 in Fig. 22, the average deviation is about 0.7 MeV.

However, no important qualitative differences appear in the results of these apparently quite different approaches to the level data analysis, and both approaches agree reasonably well with the approximate model predictions. This indicates that the effect of the ambiguities (Sec. III.D) in the semiempirical determination of the levels is less than might be suspected.

The experience of this case study strengthens our confidence in the conclusions drawn from the behavior of the semiempirical single-particle levels, and in the validity of the single-particle model.

REFERENCES

Alaga, G., 1955, Phys. Rev. **100,** 432.
——, 1957, Nucl. Phys. **4,** 625.
Alder, K., A. Bohr, T. Huus, B. Mottelson, and A. Winther, 1956, Rev. Mod. Phys. **28,** 432.
Arvieu, R., and M. Véneroni, 1960, Compt. Rend. **250,** 992, 2155.
Bang, J., J. Krumlinde, and S. G. Nilsson, 1965, Phys. Letters **15,** 55.
Baranger, M., 1960, Phys. Rev. **120,** 957.
——, 1963, Phys. Rev. **130,** 1244.
——, and K. Kumar, 1968a, Nucl. Phys. **A110,** 490.
——, and K. Kumar, 1968b, Nucl. Phys. **A122,** 241.
Bardeen, J., L. N. Cooper, and J. R. Schrieffer, 1957a, Phys. Rev. **106,** 162.
——, L. N. Cooper, and J. R. Schrieffer, 1957b, Phys. Rev. **108,** 1175.
Belyaev, S. T., 1959, Kgl. Danske Videnskab. Selskab, Mat.-Fys. Medd. **31,** No. 11.
Bennewitz, J., and P. K. Haug, 1968, Z. Physik **212,** 295.
Bès, D. R., 1963, Nucl. Phys. **49,** 544.
——, and Y. C. Cho, 1966, Nucl. Phys. **86,** 581.
——, P. Federman, E. Maqueda, and A. Zuker, 1965, Nucl. Phys. **65,** 1.
——, and R. Sorensen, 1969, Advances in Nuclear Physics, edited by M. Baranger and E. Vogt (Plenum Press, New York and London, Vol. 2, p. 129.
——, and Z. Szymanski, 1961, Nucl. Phys. **28,** 42.
Blomqvist, J., and S. Wahlborn, 1960, Arkiv Fysik **16,** 545.
Bogoliubov, N. N., 1958a, Nuovo Cimento **7,** 794.
——, 1958b, Zh. Eksp. Teor. Fiz. **34,** 58, 73 [Soviet Phys. JETP **7,** 41, 51].
Bohr, A. 1952, Kgl. Danske Videnskab. Selskab, Mat.-Fys. Medd. **26,** No. 14.
——, and B. R. Mottelson, 1953a, Kgl. Danske Videnskab. Selskab, Mat.-Fys. Medd. **27,** No. 16 [2nd Edition 1957].
——, and B. R. Mottelson, 1953b, Phys. Rev. **90,** 717.
——, and B. R. Mottelson, 1969, *Nuclear Structure*, Vol. I: Single-Particle Motion (W. A. Benjamin, Inc., New York and Amsterdam).
——, B. R. Mottelson, and D. Pines, 1958, Phys. Rev. **110,** 936.
Bolsterli, M., E. O. Fiset, and J. R. Nix, 1969, *Physics and Chemistry of Fission* (IAEA, Vienna), p. 183.
Borggreen, J., G. Løvhøiden, and J. C. Waddington, 1969, Nucl. Phys. **A131,** 241.
Brockmeier, R. T., S. Wahlborn, E. J. Seppi, and F. Boehm, 1965, Nucl. Phys. **63,** 102.
Brown, G. E., 1967, *Unified Theory of Nuclear Models and Forces* (North-Holland Publishing Co., Amsterdam, 2nd Ed.).
Bunker, M. E., and C. W. Reich, 1971, Rev. Mod. Phys. **43,** 348.
Burke, D. G., B. Zeidman, B. Elbek, B. Herskind, and M. Olesen, 1966, Kgl. Danske Videnskab. Selskab, Mat.-Fys. Medd. **35,** No. 2.
Chasman, R. R., 1966, Nucl. Phys. **89,** 11.
——, 1970, Phys. Rev. **C1,** 2144.
——, and J. O. Rasmussen, 1956, Report UCRL-3629, Berkeley.
——, and S. Wahlborn, 1967, Nucl. Phys. **A90,** 401.
Chepurnov, V. A., and P. E. Nemirovskiĭ, 1963, Nucl. Phys. **49,** 90.
Chi, B. E., 1966, Nucl. Phys. **83,** 97.
Collard, H. R., L. R. B. Elton, and R. Hofstadter, 1967, *Nuclear Radii*, Vol. 2, Group 1, Landolt-Börnstein, Numerical Data and Functional Relationships in Science and Technology (Springer-Verlag, Berlin, Heidelberg, and New York).
Damgaard, J., H. C. Pauli, V. V. Pashkevitch, and V. M. Strutinsky, 1969, Nucl. Phys. **A135,** 432.
Davidson, J. P., 1968, *Collective Models of the Nucleus* (Academic, New York and London).
Davydov, A. S., 1959, Zh. Eksp. Teor. Fiz. **9,** 1555 [Sov. Phys. JETP **36,** 1103].
——, and G. F. Filippov, 1958, Nucl. Phys. **8,** 237.
de-Shalit, A., and I. Talmi, 1963, *Nuclear Shell Theory* (Academic New York).
Edmonds, A. R., 1968, *Angular Momentum in Quantum Mechanics* (Princeton U. P., revised printing).
Ehrling, G., 1969 ALGOL computer program for the Nilsson model, Research Institute for Physics, Stockholm (unpublished).
——, and S. Wahlborn, 1970, "A general scheme for the calculation of single-particle eigenstates," Annual Report, Research Institute for Physics, Stockholm.
——, and S. Wahlborn, 1971, Phys. Letters **34B,** 369.
Elbek, B., and P. O. Tjøm, 1969, Advances in Nuclear Physics, edited by M. Baranger and E. Vogt (Plenum Press, New York and London), Vol. 3, p. 259.
Elton, L. R. B., 1961, *Nuclear Sizes* (Oxford U. P., London).
Faessler, A., and R. K. Sheline, 1966, Phys. Rev. **148,** 1003.
Ford, G. P., D. C. Hoffman, and E. Rost, 1970, "Calculations of Single-Particle Levels in a Deformed Diffuse Well," LASL Report LA-4329, Los Alamos.
Fredriksson, S., 1969, "Empiriskt Enpartikelnivåschema i Deformerade Atomkärnor," KTH Examination work in Theoretical Physics, Royal Institute of Technology, Stockholm (unpublished).
Fuller, G. H., and V. W. Cohen, 1969, Nucl. Data **A5,** 433.
Gareev, F. A., S. P. Ivanova, and B. N. Kalinkin, 1967, "On the Accuracy of Calculation of the One-Particle States of Deformed Nuclei," JINR Preprint P4-3326, Dubna.
——, S. P. Ivanova, and B. N. Kalinkin, 1968, Izv. Akad. Nauk SSSR Ser. Fiz. **32,** 1690 [Bull. Acad. Sci. USSR Phys. Ser. **32,** 1559].
——, S. P. Ivanova, B. N. Kalinkin, S. K. Slepnev, and M. G. Ginsburg, 1967, "Tables of Wave Functions of One-Particle States of Deformed Nuclei of the Rare-Earth Region for a Finite Diffused Potential," JINR Preprint P4-3607, Dubna.

——, S. P. Ivanova, and V. V. Pashkevitch, 1969, "Equilibrium Deformations β_{20} and β_{40} of Nuclei in Rare-Earth and Transuranium Regions and β_{40}-Dependence of Single-Particle Characteristics," JINR Preprint E4-4704, Dubna.
——, S. P. Ivanova, and N. Yu. Shirikova, 1969, "Effect of the Hexadecapole Deformation on the Properties of the One-Quasiparticle States of the Rare-Earth Nuclei," JINR Preprint P4-4259, Dubna.
——, L. I. Vinokurov, and B. N. Kalinkin, 1967, One-Particle States of Deformed Nonaxial Nuclei," JINR Preprint E4-3453, Dubna.
Green, A. M., 1965, Rept. Prog. Phys. **28,** 113.
Gustafson, C., I.-L. Lamm, B. Nilsson, and S. G. Nilsson, 1967, Arkiv Fysik **36,** 613.
Hecht, K. T., and G. R. Satchler, 1962, Nucl. Phys. **32,** 286.
Hendrie, D. L., N. K. Glendenning, B. G. Harvey, O. N. Jarvis, H. H. Duhm, J. Saudinos, and J. Mahoney, 1968, Phys. Letters **26B,** 127.
Kalpazhiu, M. K., and P. Vogel, 1966, "Calculations of Properties of Collective States in Deformed Nuclei in the Region $176 \leq A \leq 190$," JINR Preprint E-2579, Dubna.
Kanestrøm, I., and P. O. Tjøm, 1969, Nucl. Phys. **A138,** 177.
——, and P. O. Tjøm, 1970, Nucl. Phys. **A145,** 461.
Kerman, A. K., 1956, Kgl. Danske Videnskab. Selskab, Mat.-Fys. Medd, **30,** No. 15.
——, 1959, Nuclear Reactions, edited by P. M. Endt and M. Demeur (North-Holland Publ. Co., Amsterdam), Vol. 1, p. 427.
Kisslinger, L. S., and R. A. Sorensen, 1963, Rev. Mod. Phys. **35,** 853.
Kumar, K., and M. Baranger, 1968, Nucl. Phys. **A110,** 529.
Lamm, I.-L., 1969, Nucl. Phys. **A125,** 504.
Lane, A. M., 1964, *Nuclear Theory* (W. A. Benjamin, Inc., New York).
Lederer, C. M., J. M. Hollander, and I. Perlman, 1967, *Table of Isotopes* (Wiley, New York), 6th ed.
Lemmer, R. H., 1960, Phys. Rev. **117,** 1551.
——, and A. E. S. Green, 1960, Phys. Rev. **119,** 1043.
Malov, L. A., V. G. Soloviev, and U. M. Fainer, 1968, "Non-rotational States of Deformed Odd-Z Nuclei in the Region $177 \leq A \leq 187$," JINR Preprint E4-4224, Dubna.
Marumori, T., 1960, Prog. Theoret. Phys. (Kyoto) **24,** 331.
Monsonego, G., and R. Piepenbring, 1966, Nucl. Phys. **78,** 265.
——, and R. Piepenbring, 1968, J. Phys. (France) **29,** Supplément No. 1, 42.
Moszkowski, S. A., 1957, Handbuch der Physik, edited by S. Flügge, (Springer-Verlag, Berlin), Vol. 39, p. 411.
Mottelson, B. R., 1959, *The Body Problem* (Le Problème à N Corps), (Methuen, London; Wiley, New York), p. 283.
——, 1962, *Rendiconti della Scuola Internazionale di Fisica, Varenna, 1960* (Zanichelli, Bologna), p. 44.
——, and S. G. Nilsson, 1959, Kgl. Danske Videnskab. Selskab, Mat.-Fys. Skrifter **1,** No. 8.
Myers, W. D., 1970, Nucl. Phys. **A145,** 387.
Nathan, O., 1964, "Studies of Nuclear Quadrupole and Octople Vibrations," Thesis (Ejnar Munksgaards Forlag, Copenhagen).
——, and S. G. Nilsson, 1965, *Alpha-, Beta, and Gamma-Ray Spectroscopy*, edited by K. Siegbahn (North-Holland Publ. Co., Amsterdam), Vol. 1, p. 601.
Nemirovskiĭ, P. E., 1960, *Sovremennye Modeli Atomnogo Yadra* (Atomizdat, Moscow) [*Contemporary Models of the Atomic Nucleus* (Pergamon Press, Oxford, 1963)].
——, and V. A. Chepurnov, 1966, Yad. Fiz. **3,** 998 [Sov. J. Nucl. Phys. **3,** 730].
Newton, T. D., 1960, Can. J. Phys. **38,** 700.
Nilsson, B., 1969, Nucl. Phys. **A129,** 445.
Nilsson, S. G., 1955, Kgl. Danske Videnskab. Selskab, Mat.-Fys. Medd. **29,** No. 16.
——, C. Fu Tsang, A. Sobiczewski, Z. Szymanski, S. Wycech, C. Gustafson, I.-L. Lamm, P. Möller, and B. Nilsson, 1969, Nucl. Phys. **A131,** 1.
——, and O. Prior, 1961 Kgl. Danske Videnskab. Selskab, Mat.-Fys. Medd. **32,** No. 16.
Nuclear Data Group, 1959-65, Nucl. Data Sheets (National Academy of Sciences—National Research Council).
——, 1966, Nucl. Data **B1,** Nos. 1-3.
Ogle, W., and S. Wahlborn, 1969, ALGOL and FORTRAN-IV Computer Programs for BCS calculations, Research Institute for Physics, Stockholm, and LASL, Los Alamos, (unpublished).
Pashkevitch, V. V., and V. M. Strutinsky, 1969, Yad. Fiz. **9,** 56 [Sov. J. Nucl. Phys. **9,** 35].
Piepenbring, R., 1966, "Contribution à l'étude des transitions dipolaires électriques dans les noyaux déformés de masse impaire de la région des terres rares," Thesis, University of Strasbourg, France.
Preston, M. A., 1963, *Physics of the Nucleus* (Addison-Wesley, Reading, Mass., 2nd printing.
Prior, O., F. Boehm, and S. G. Nilsson, 1968, Nucl. Phys. **A110,** 257.
Rassey, A. J., 1958, Phys. Rev. **109,** 949.
Rogers, J. D., 1965, Ann. Rev. Nucl. Sci. **15,** 241.
Röper, P., 1966, Z. Physik **195,** 316.
Rose, M. E., 1957, *Elementary Theory of Angular Momentum* Wiley, New York).
Rost, E., 1967, Phys. Rev. **154,** 994.
Rowe, D. J. 1965, Nucl. Phys. **61,** 1.
Satchler, G. R., 1958, Ann. Phys. (N.Y.) **3,** 275.
Soloviev, V. G., 1958/9, Nucl. Phys. **9,** 655.
——, 1963, *Selected Topics in Nuclear Theory* (IAEA, Vienna), p. 233.
——, and P. Vogel, 1967, Nucl. Phys. **A92,** 449.
——, P. Vogel, and G. Jungklaussen, 1967, Izv. Akad. Nauk SSSR Ser. Fiz. **31,** 518 [Bull. Acad. Sci. USSR Phys. Ser. **31,** 515].
Stelson, P. H., and L. Grodzins, 1965, Nucl. Data **A1,** 21.
Strutinsky, V. M., 1967, Nucl. Phys. **A95,** 420.
——, 1968, Nucl. Phys. **A122,** 1.
Talman, J. D., 1970, Nucl. Phys. **A141,** 273.
Thouless, D. J., 1961, *The Quantum Mechanics of Many Body Systems* (Academic, New York).
Tobocman, W., 1961, *Theory of Direct Nuclear Reactions* (Oxford U. P., London).
Valatin, J. G., 1958, Nuovo Cimento **7,** 843.
Wahlborn, S., 1962, Nucl. Phys. **37,** 554.
——, 1966, Arkiv Fysik **31,** 33.
Woods, R. D., and D. S. Saxon, 1954, Phys. Rev. **95,** 577.

59Bi11 K. W. Bichard, J. W. Mihelich, and B. Harmatz, Phys. Rev. **116,** 720 (1969).
60Ha18 B. Harmatz, T. H. Handley, and J. W. Mihelich, Phys. Rev. **119,** 1345 (1960).
60Ne2 J. O. Newton, Phys. Rev. **117,** 1520 (1960).
61Me5 E. R. Merz and A. A. Caretto, Jr., Phys. Rev. **122,** 1558 (1961).
61We11 H. I. West, Jr., L. G. Mann, and R. J. Nagle, Phys. Rev. **124,** 527 (1961).
62Ba32 E. Bashandy and M. S. El-Nesr, Arkiv Fysik **21,** 65 (1962).
62Ha24 B. Harmatz, T. H. Handley, and J. W. Mihelich, Phys. Rev. **128,** 1186 (1962).
62Va6 J. Valentin, D. J. Horen, and J. M. Hollander, Nucl. Phys. **31,** 353 (1962).
63Di09 R. M. Diamond, B. Elbek, and F. S. Stephens, Nucl. Phys. **43,** 560 (1963).
63Va28 J. Valentin and A. Santoni, J. Phys. (France) **24,** 648 (1963).
63Ve09 M. N. Vergnes and R. K. Sheline, Phys. Rev. **132,** 1736 (1963).
64Ab03 A. A. Abdumalikov, A. A. Abdurazakov, K. Y. Gromov, F. N. Mukhtasimov, and G. Y. Umerov, Izv. Akad Uz. SSR, Ser Fiz. Mat. Nauk **8,** No. **2,** 42 (1964); Chem. Abstr. **61,** 7885b (1964).
64Al04 P. Alexander, F. Boehm, and E. Kankeleit, Phys. Rev. **133,** B284 (1964).
64Lö04 K. E. G. Löbner, Phys. Letters **12,** 33 (1964).
64Pe13 L. Persson and H. Ryde, Arkiv Fysik **25,** 397 (1964).
65Bi07 K. M. Bisgård, L. J. Nielsen, E. Stabell, and P. Østergård, Nucl. Phys. **71,** 192 (1965).
65Bj01 S. Bjørnholm, J. Borggreen, H. J. Frahm, and N. J. S. Hansen, Nucl. Phys. **73,** 593 (1965).
65Bo08 J. D. Bowman, J. de Boer, and F. Boehm, Nucl. Phys. **61,** 682 (1965).
65De05 J. de Boer, Nucl. Phys. **61,** 675 (1965).
65Er03 J. R. Erskine, Phys. Rev. **138,** B66 (1965).
65Gr20 K. Y. Gromov, A. S. Danagulyan, A. T. Strigachev,

and V. S. Shpinel, Yad. Fiz. **1,** 389 (1965) [Sov. J. Nucl. Phys. **1,** 276 (1965)].

65Gr35 K. Y. Gromov, Z. T. Zhelev, V. Zvolska, and V. G. Kalinnikov, Yad. Fiz. **2,** 783 (1965); Sov. J. Nucl. Phys. **2,** 559 (1966).

65He06 C. Heiser and K. F. Alexander, Nucl. Phys. **70,** 415 (1965).

65Ke09 R. A. Kenefick and R. K. Sheline, Phys. Rev. **139,** B1479 (1965).

65Ko13 H. R. Koch, Z. Physik **187,** 450 (1965).

65Ma18 B. P. K. Maier, Z. Physik **184,** 153 (1965).

66Al05 P. Alexander, H. Ryde, and E. Seltzer, Nucl. Phys. **76,** 167 (1966).

66Bl06 P. H. Blichert-Toft, G. E. Funk, and J. W. Mihelich, Nucl. Phys. **79,** 12 (1966).

66Bo02 J. Borggreen, H. J. Frahm, N. J. S. Hansen, and S. Bjørnholm, Nucl. Phys. **77,** 619 (1966).

66Bu16 D. G. Burke, B. Zeidman, B. Elbek, B. Herskind, and M. Olesen, Kgl. Danske Videnskab. Selskab., Mat.-Fys. Medd. **35,** No. 2 (1966).

66Fu04 L. Funke, H. Graber, K.-H. Kaun, H. Sodan, and J. Frána, Nucl. Phys. **84,** 471 (1966).

66Fu06 ——, H. Graber, K.-H. Kaun, H. Sodan, L. Werner, and J. Frána, Nucl. Phys. **84,** 449 (1966).

66Fu07 ——, H. Graber, K.-H. Kaun, J. Römer, H. Sodan, and J. Frána, Nucl. Phys. **84,** 443 (1966).

66Fu11 ——, H. Graber, K.-H. Kaun, H. Sodan, and J. Frána, Nucl. Phys. **88,** 641 (1966).

66Gn V. Gnatovich K. Ya. Gromov, and F. N. Mukhtasimov, "New data on the conversion electron spectra of Dy-153, Dy-155, and Dy-157," Preprint JINR P-2729, Dubna (1966).

66Gr25 K. Y. Gromov and F. N. Mukhtasimov, Yad. Fiz. **4,** 1102 (1966) [Sov. J. Nucl. Phys. **4,** 793 (1967)].

66Ha23 B. Harmatz and T. H. Handley, Nucl. Phys. **81,** 481 (1966).

66Zy02 J. Zylicz, P. G. Hansen, H. L. Nielsen, and K. Wilsky, Nucl. Phys. **84,** 13 (1966).

67Be M. J. Bennett, "Nuclear Structure of ^{161}Dy, ^{159}Dy, and ^{157}Dy,". Thesis, Florida State University (1967), and private communication.

67Bi10 K. M. Bisgård and E. Veje, Nucl. Phys. **A103,** 545 (1967).

67Bl12 P. H. Blichert-Toft, E. G. Funk, and J. W. Mihelich, Nucl. Phys. **A100,** 369 (1967).

67Bo19 W. Bondarenko, N. Kramer, P. Prokofjew, P. Manfrass, A. Andreeff, and R. Kästner, Nucl. Phys. **A102,** 577 (1967).

67Bo31 ——, and P. T. Prokof'ev, Izv. Akad. Nauk SSSR, Ser. Fiz. **31,** 596 (1967); Bull. Acad. Sci. USSR, Phys. Ser. **31,** 591 (1968).

67Du05 B. C. Dutta, T. V. Egidy, T. W. Elze, and W. Kaiser, Z. Physik **207,** 153 (1967).

67Ma24 P. Manfrass, A. Andreeff, R. Kästner, W. Bondarenko, N. Kramer, and P. Prokofjew, Nucl. Phys. **A102,** 563 (1967).

67Ma25 G. Markus, W. Michaelis, H. Schmidt, and C. Weitkamp, Z. Physik **206,** 84 (1967).

67Ma28 S. G. Malmskog, Arkiv Fysik **33,** 317 (1967).

67Mo13 Y. Motavalledi-Nobar, J. Barthier, J. Blachot, and R. Henck, Nucl. Phys. **A100,** 45 (1967).

67Sc05 O. W. B. Schult, M. E. Bunker, D. W. Hafemeister, E. G. Shera, E. T. Jurney, J. W. Starner, A. Bäcklin, B. Fogelberg, U. Gruber, B. P. K. Maier, H. R. Kock, W. N. Shelton, M. Minor, and R. K. Sheline, Phys. Rev. **154,** 1146 (1967).

67Tj01 P. O. Tjøm and B. Elbek, Kgl. Danske Videnskab. Selskab., Mat.-Fys. Medd. **36,** No. 8 (1967).

68Al W. P. Alford and M. T. Lu, Bull. Am. Phys. Soc. **13,** 895 (1968), and private communication quoted by Bunker and Reich (1971); their Ref. 70Lu.

68Bo18 J. Borggreen and J. P. Gjaldbaek, Nucl. Phys. **A113,** 659 (1968).

68Bu M. E. Bunker, G. Berzins, and J. W. Starner, "State Maxing in ^{165}Ho," in *Contributions to the International Symposium on Nuclear Structure* (Dubna, 1968, p. 35), and private communication (1970).

68Ek01 C. Ekström, I. Lindgren, H. Nyqvist, A. Rosén, and K. E. Adelroth, Phys. Letters **26B,** 146 (1968); Erratum: Phys. Letters **26B,** 387 (1968).

68Gr R. L. Graham, J. S. Geiger, and M. W. Jones, *Proceedings International Symposium on Nuclear Structure,* Dubna, p. 135 (IAEA, Vienna, 1968).

68Ha10 R. A. Harlan and R. K. Sheline, Phys. Rev. **168,** 1373 (1968).

68Ha39 B. Harmatz and T. H. Handley, Nucl. Phys. **A121,** 481 (1968).

68Ke P. Kemnitz, L. Funke, H. Graber, K.-H. Kaun, H. Sodan, and G. Winter, "Untersuchung des γ-Spektrums von Zerfall des ^{155}Sm mit einem hochauflösenden Anti-Compton-Spektrometer," Zentralinstitut für Kernforschung, Rossendorf bei Dresden, Preprint ZFK-138 (1968).

68Ku02 W. Kurcewicz, Z. Moroz, Z. Preibisz, and B. Schmidt Nielsen, Nucl. Phys. **A108,** 434 (1968).

68Ku14 T. Kutsarova, V. Zvol'ska, and M. Weis, Izv. Akad. Nauk SSSR, Ser. Fiz. **32,** 126 (1968) [Bull. Acad. Sci. USSR, Phys. Ser. **32,** 121 (1968)].

68Me02 D. G. Megli, G. P. Agin, V. R. Potnis, and C. E. Mandeville, Nucl. Phys. **A107,** 217 (1968).

68Ri07 F. A. Rickey, Jr., and R. K. Sheline, Phys. Rev. **170,** 1157 (1968).

68Sh12 E. B. Shera, M. E. Bunker, R. K. Sheline, and S. H. Vegors, Jr., Phys. Rev. **170,** 1108 (1968).

68Sh R. K. Sheline, *Proceedings International Symposium on Nuclear Structure,* Dubna, (IAEA, Vienna, 1968, p. 71).

68Sk B. Skånberg, H. Ryde, and S. A. Hjorth, "Rotational Bands in Odd Ta and Lu Isotopes," Annual Report, Research Institute for Physics, Stockholm, (1968), p. 29; and private communication.

69Ad B. Ader, "Etude de la désintégration par capture électronique des isotopes 175 et 177 du tungstène. Schémas de niveaux de isotopes 175 et 177 du tantale, interprêtés dans le cadre du modèle de Nilsson," Thesis, University of Paris, Orsay (1969).

69An19 W. Andrejtscheff, W. Mailing, and F. Stary, Nucl. Phys. **A137,** 474 (1969).

69Ar23 P. Arlt, Z. Malek, G. Musiol, G. Pfrepper, and H. Strusny, Izv. Acad. Nauk SSSR, Ser. Fiz. **33,** 1218 (1969); [Bull. Acad. Sci. USSR, Phys. Ser. **33,** 1133 (1970)].

69Ba38 D. Barnéoud, J. Boutet, J. Gizon, and J. Valentin, Nucl. Phys. **A138,** 33 (1969).

69Co16 W. B. Cook and M. W. Johns, Can. J. Phys. **47,** 1899 (1969).

69Da01 P. J. Daly, P. Kleinheinz, and R. F. Casten, Nucl. Phys. **A123,** 186 (1969).

69Ek01 C. Ekström, T. Noreland, M. Olsmats, and B. Wannberg, Nucl. Phys. **A135,** 289 (1969).

69Fo R. Foucher, R. Henck, J. P. Husson, J. Jastrzebski, A. Johnson, J. M. Kuchly, P. Siffert, G. Astner, E. Hagebö, I. Kjelberg, P. Patzelt, private communication (1969).

69Gr T. Grotdal, K. Nybø, and B. Elbek, Kgl. Danske Videnskab. Selskab., Mat.-Fys. Medd. **37,** No. 12 (1969); quoted by Kanestrøm and Tjøm (1969).

69Ha10 P. G. Hansen, P. Hornshøj, and K. H. Johansen, Nucl. Phys. **A126,** 464 (1969).

69Ha12 K. A. Hagemann, S. A. Hjorth, H. Ryde, and H. Olsson, Phys. Letters **28B,** 661 (1969).

69Hj01 S. A. Hjorth, H. Ryde, and B. Skånberg, Arkiv Fysik **38,** 537 (1969).

69Jo16 K. H. Johansen, B. Bengtson, P. G. Hansen, and P. Hornshøj, Nucl. Phys. **A133,** 213 (1969).

69Ke10 P. Kemnitz, L. Funke, K.-H. Kaun, H. Sodan, and G. Winter, Nucl. Phys. **A137,** 679 (1969).

69Ko18 J. Konijn, B. J. Meijer, B. Klank, R. A. Ristinen, Nucl. Phys. **A137,** 593 (1969).

69Ku03 E. Kuhlman and K. E. G. Löbner, Z. Physik **222,** 144 (1969).

69Ku07 T. Kuroyanagi and T. Tamura, Nucl. Phys. **A133,** 554 (1969).

69Mc08 L. D. McIsaac, R. G. Helmer, and C. W. Reich, Nucl. Phys. **A132,** 28 (1969).

69Me R. A. Meyer, private communication to M. E. Bunker (1969).

69Sm04 R. K. Smither, E. Bieber, T. von Egidy, W. Kaiser, and K. Wien, Phys. Rev. **187,** 1632 (1969).

69So H. Sodan, L. Funke, K.-H. Kaun, P. Kemnitz, and G. Winter, "Niveaus im ^{185}W von Zerfall des ^{185}Ta," Preprint, Zentralinstitut für Kernforschung, Rossendorf bei Dresden (1969).

69Tj P. O. Tjøm, "Single Particle States in the Rare Earth Mass Region Studied by Means of (d, p) and (d, t) Reactions," Preprint (1969), and private communication quoted by Bunker and Reich (1971).

69Tj01 P. O. Tjøm and B. Elbek, Kgl. Danske Videnskab. Selskab., Mat.-Fys. Medd. **37,** No. 7 (1969).

69Un04 J. Ungrin, D. G. Burke, M. W. Johns, and W. P. Alford, Nucl. Phys. **A132,** 322 (1969).

70Ba46 D. Barnéoud, C. Foin, A. Baudry, A. Gizon, and J. Valentin, Nucl. Phys. **A154,** 653 (1970).

70Bo02 J. Borggreen and G. Sletten, Nucl. Phys. **A143,** 255 (1970).

70Ca R. F. Casten, P. Kleinheinz, P. J. Daly, and B. Elbek, "A Study of Energy Levels and Coriolis Coupling in Odd-Mass Tungsten Isotopes by Use of (d, p), (d, t), and (^{3}He, α) Reactions," Preprint (1970), to be published in Kgl. Danske Videnskab. Selskab., Mat.-Fys. Medd.

70Gi J. Gizon, D. Barnéoud, and J. Valentin, Nucl. Phys. **A148,** 561 (1970).

70Hj S. A. Hjorth, H. Ryde, K. A. Hagemann, G. Løvhøiden, and J. C. Waddington, Nucl Phys. **A144,** 513 (1970).

70Li I. Lindgren, private communication (1970).

70Lø G. Løvhøiden, J. C. Waddington, K. A. Hagemann, S. A. Hjorth, and H. Ryde, Nucl. Phys. **A148,** 657 (1970).

70Mi01 W. Michaelis, F. Weller, U. Fanger, R. Gaeta, G. Markus, H. Ottmar, and H. Schmidt, Nucl. Phys. **A143,** 225 (1970).

70Mu T. J. Mulligan, R. K. Sheline, M. E. Bunker, and E. T. Jurney, Phys. Rev. **C2,** 655 (1970).

70Ro V. C. Rogers, L. E. Beghian, F. M. Clikeman, F. S. Mehoney, Nucl. Phys. **A144,** 81 (1970).

70Sk04 B. Skånberg, S. A. Hjorth, and H. Ryde, Nucl. Phys. **A154,** 641 (1970).

70Wi09 G. Winter, L. Funke, K. Hohmuth, K. H. Kaun, P. Kemnitz, H. Sodan, Nucl. Phys. **A151,** 337 (1970).